Thesis

Depositional environments during the Messinian in the Rifian corridor, Morocco

Menno van Oorschot

May 8, 2016

Abstract

Before closure during the late Messinian, the Atlantic ocean was connected with the Mediterranean via two major corridors: a northern corridor through present-day Spain and a southern corridor (henceforth referred to as the Rifian corridor) through present-day northern Morocco. The aim of this paper is to investigate a) the dominant depositional environment in the Southern Rifian corridor and b) to get more insight in its development: when did it close? The Saiss basin in Northern Morocco is formed by a fore-deep basin related to the formation of the Riff mountain range. And is, therefore, subject to tectonically driven sediment supplies. Additionally, the fact that the basin was an active conduit for water transport between the Atlantic ocean and the Mediterranean sea implies that bottom currents could have dominated depositional processes. This thesis presents the sedimentological and bio-stratigraphical results and interpretations of two composite sections in the Saiss Basin. One at Jebel Haricha near Sidi Kacem and one at Oued Mahdouma in between Fes and Meknes. Field descriptions enabled the division of both section into facies associations. The Jebel Haricha is chronologically composed of a distal turbidite stage, a quiet marine stage, again a distal marine stage and a proximal tubidite lobe stage. The Oued Mahdouma section is composed of a quiet marine stage with a gradual increase of turbiditic influence near the top. And, after a sharp erosive transition, of a lacustrine stage. Bio-stratigraphic analysis of Foraminafera indicates a depositional window in between ± 6.37 and 6.29 ma for the Jebel Haricha section. The age of the Oued Mahdouma section is not determined. The sections exemplarily show that the depostional mechanisms in the Southern marine corridor are dominated by gravitational driven turbidite systems rather than bottom current driven contourites. Although the influence of bottom currents cannot be excluded. These sections do not give more insight in the closure of the marine corridor, they give no indication whether the

corridor was open or closed. The Jebel Haricha section shows, however, that just before or during closure of the corridor in the east the western area of the corridor was marked by active sedimentation in an open marine environment. Which is dominated by flysch deposits and not particularly bottom currents.

Contents

List of Figures

Chapter 1

Introduction

The Saiss basin in northern Morocco has been the scene of an ongoing discussion related to the closing of the Mediterranean Sea from the Atlantic Ocean. The Mediterranean sea was connected to the Atlantic Ocean through several corridors. The Saiss Basin reflects a remnant of the Rifian Corridor, the most southern connection between the Atlantic Ocean and the Mediterranean Sea. It is situated in the external fore-deep system of the Rifian mountain range. The basin is bordered by the Gharb basin in the west, the Mid-Atlas mountain range in the south and the west, and the Rifian mountain range in the north (figure 1.1).

Several stratigraphic studies have been conducted on the subject but publications on the processes controlling sedimentation remain sparse. Insights in sedimentation are of utmost importance to link stratigraphic events. To get an understanding of the processes controlling sedimentation in marine corridors and specifically the Southern Rifian corridor; the Saiss basin was chosen to take two high definition sedimentary logs. The Saiss basin was marked by active sedimentation during the time when the Southern marine corridor was open.

The deposition in the Rifian corridor was probably controlled by both the evolution of a fore-deep basin and the in- and out-flow of vast amounts of water through the marine corridor.

The fore-deep basin stretched from the Mediterranean to the Atlantic ocean and therefore formed the conduit for the Rifian corridor. Like all typical fore-land basins the Rifian foreland basin exists of: (1)

wedge top basins, formed on top of the accretionary wedge and consists of alluvial and deltaic deposits; (2) a foredeep basin, where the sections of this thesis are situated, fore-deep deposits are mostly characterized by deep pelagic and turbidite deposits; and (3) a shallow ramp near the hinge of the underlying plate (Flinch, 1993; Mutti et al., 2003).

The evolution of the fore-deep started with subsidence due to loading which resulted in turn in the drowning of the underlying Moroccan Meseta. The second part is marked by the onset of turbidite deposits and the last stage is characterized by fluvio-deltaic and alluvial deposits (Flinch, 1993; Mutti et al., 2003; Covey, 1986).

The focus in this thesis lies at the turbidite system stage. Typical fore-deep basins are filled by turbiditc systems with palaeo current directions parallel to the axis of the basin (Mutti et al., 1999).

The Rifian fore-deep is of major influence on the formation of the Rifian corridor. The Rifian corridor consists of a northern arm and a southern arm with a thrust nappe in between (Flinch, 1993). The northern corridor consists of connected intra-montane basins; the southern corridor is formed by the fore-deep. The establishment of the main southern Rifian corridor is estimated at ± 8 ma or younger (Krijgsman et al., 1999). This was determined due the fact that metamorphic rock, resulting from the collision of the Alboran plate with Iberia and Africa, was unroofed during extension in the internal domain (Comas et al., 1999). The unroofing of the metamorphic rocks could be radiometrically dated at ± 8 ma (Monie et al., 1984). Loading and subsidence due to the formation of thrusts was the ultimate result of this collision as will further be explained in the geologic setting.

The marine corridors allowed the influx of surface sea water into the Mediterranean to replete evaporated water. In turn, a thick saline current moved moved from the Mediterenean towards the Atlantic ocean; the Paleo-Mediterenean Overflow Water (PNOW). Around ± 6.3 ma the inflow of water increased in the direction of the Mediterranean through the Rifian corridor (Benson et al., 1991). This resulted in cold oceanic bottom water entering the Rifian corridor. This enhanced inflow lasted until approximately 5.5 ma (Benson et al., 1991).

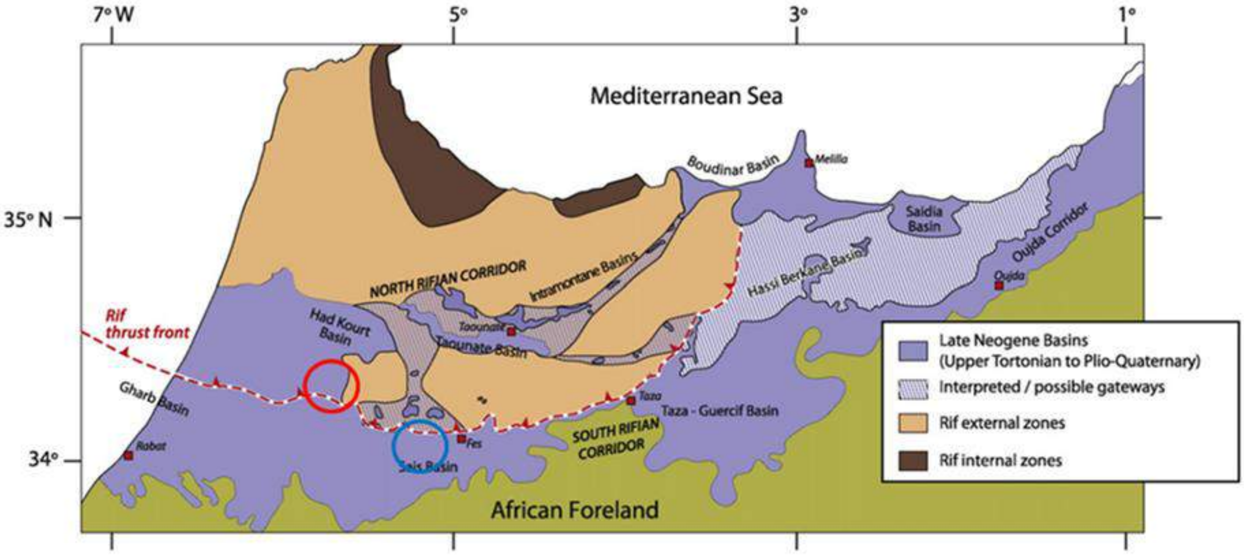

Figure 1.1: An overview of the Rifian corridors by Flecker et al. (2015). The Jebel Haricha section (red circle) and the Oued Madhouma section (blue circle) are located on the map.

It was much debated whether the Rifian Corridors closed due to glacio-eustatic sea level fall or tectonics. When the beginning and end of the Messinian Salinity Crisis (henceforth referred to as MSC) were dated, they could be linked to benthic delta-O-18 values (Krijgsman et al., 1999). This showed that the onset of the MSC is not coeval with the fall of the glacio-eustatic sea level. A paleodepth reconstruction indicated a sealevel drop of ± 400 m, whilst delta-O-18 values of benthic foraminifera at Bou Regreg point to a maximal eustatic sea level drop of ± 40 m around this time (Krijgsman et al., 1999). The closure of the Rifian corridors, which is linked to the MSC, is thus probably due to active tectonics.

This thesis presents the sedimentological and bio-stratigraphical results and interpretations of two sections in the Saiss Basin. Its aim is to investigate a) the dominant depositional environment in the Southern Riffian corridor and b) to get more insight in its development: when did it close?

Chapter 2

Geologic framework

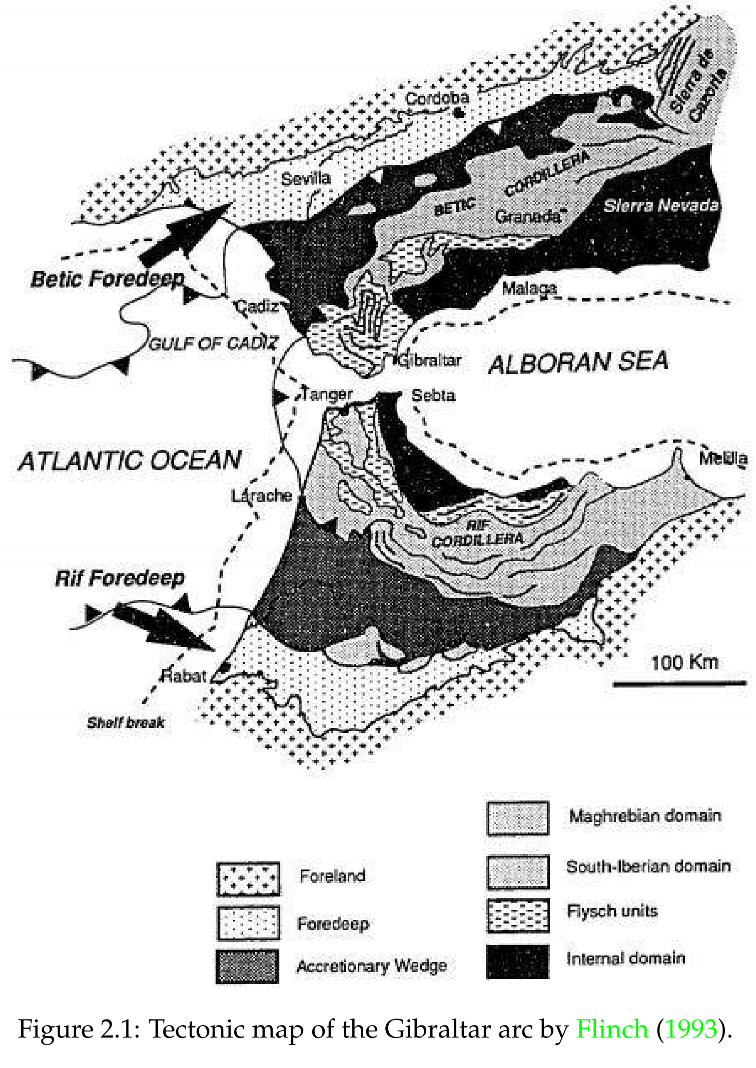

Figure 2.1: Tectonic map of the Gibraltar arc by Flinch (1993).

The southern Rifian corridor was located in the fore-deep of the Rifian mountain range, which is part of the Gibraltar Arc. When Africa collided with Europe the Atlas mountains were formed. The exact onset of the African and Iberian convergence zone with the European plate is still debated, but it is assumed that it started during early Paleogene. During late Neogene the convergence evolved into a plate boundary zone. An interaction of the Alboran ”domain” with the African, European and Atlantic plates had great effect on the morphology of Morocco. Due to westward movement the Alboran plate collided with the Iberian and African passive margins. This resulted in thrusting and the formation of an accretionary wedge during the Aquitanian-Burdigalian times (Balanya and Garcia-Duenas, 1987). Since Paleaogene times tectonic units of the half circular Gibraltar arc have thrusted outwards onto the late Palazeaozoic basement (Platt and Vissers, 1989). The thrust belts are formed in multiple phases, due to the complexity of the Alpine orogenesis (Sissingh, 2008). In front of the frontal thrust belts, foredeep basins developed, which deepen towards the orogenic belt (e.g. post-Burdigalian Gharb and Saiss basins). In these basins, thick Neogene deposits have accumulated, characterized as thick turbidite sequences. The extensional collapse of the back-arc (Alboran domain) was coeval with the collapse of the frontal accretionary wedge during Early Miocene times and uplift of the internal domain. The frontal extensional collapse is accommodated by frontal compression resulting in the emplacement of an accretionary complex with thrusting and imbrication (figure 2.2) (Morel et al., 1983; Flinch, 1993). The formations belonging to the accretionary wedge are known as the Perifaine Nappe. The area, mainly that of the Jebel Haricha section, underwent two major tectonic phases. During the Late Tortonian NW-SE compression, parallel to Mesozoic grabens, which gave rise to frontal structures. And since Pliocene times a N-S compression which reactivated fault systems in the basement, which resulted in strike-slip movement (Sani et al., 2007).

Furthermore, the Gibraltar arc is divided in an internal and an external domain. The internal domain consists of metamorphic rocks originating from the Alboran micro-plate. The external domain consists of rocks originating from the African and the European plate (Andrieux, 1971; Flinch et al., 1996). The external domain is marked by

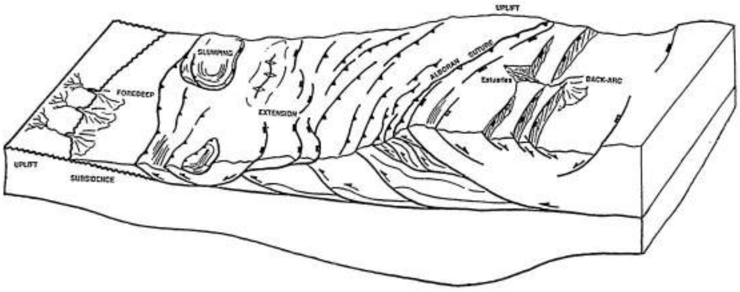

Figure 2.2: A tectonic overview of the Gibraltar Arc. Uplift in the internal zone, extension in the back-arc, extensional collapse of the frontal accretionary complex and its associated compression. And the formation of a foredeep and the flexural response of uplift in the foreland. Image from Flinch (1993).

thin-skinned tectonics (Flinch and Bally, 1991).

The folded Palaeozoic basement consists mainly of phyllites and quartzites (Faugeres, 1978). Into the folded Palaeozoic basement half-grabens related to Triassic rifting were formed. The half-grabens were filled with red beds. On top of the red beds and the remaining exposed basement marls and sands were deposited (Michard, 1976). Furthermore, the area was, until Lutetian times, covered mostly with marine limestones and marls. Neogene deposits unconformably superpose the Palaeozoic basement and its Mesozoic cover (Michard, 1976). These Neogene deposits are deposited in the fore-deep of the Gibraltar arc. They consist mainly of Miocene clastics originating from the Palaeozoic basement.

Within the fore-deep basins two transgressive-regressive cycles are recognized (Flinch, 1993). The first one occurring during the Upper Tortonian to Lower Messinian and the second one occurring during the Upper Messinian to the Lower Pliocene. The deposits characteristic of these cycles are interpreted as of prograding deltaic to turbiditic and pelagic origin (Flinch, 1993). An accretionary complex (known as the Prerifaine nappe) was emplaced onto the Moroccan meseta during the Tortonian. The accretionary wedge collapses, creating accommodation space for the supra-nappe deposits in the foredeep basins (Flinch et al., 1996). Thus, The stratigraphy in the Saiss basin, and partly the Gharb basin, can be divided in a pre-nappe series from Langhian to Tortonian times and a post-nappe series during late Tortonian to Plio-Quarternary

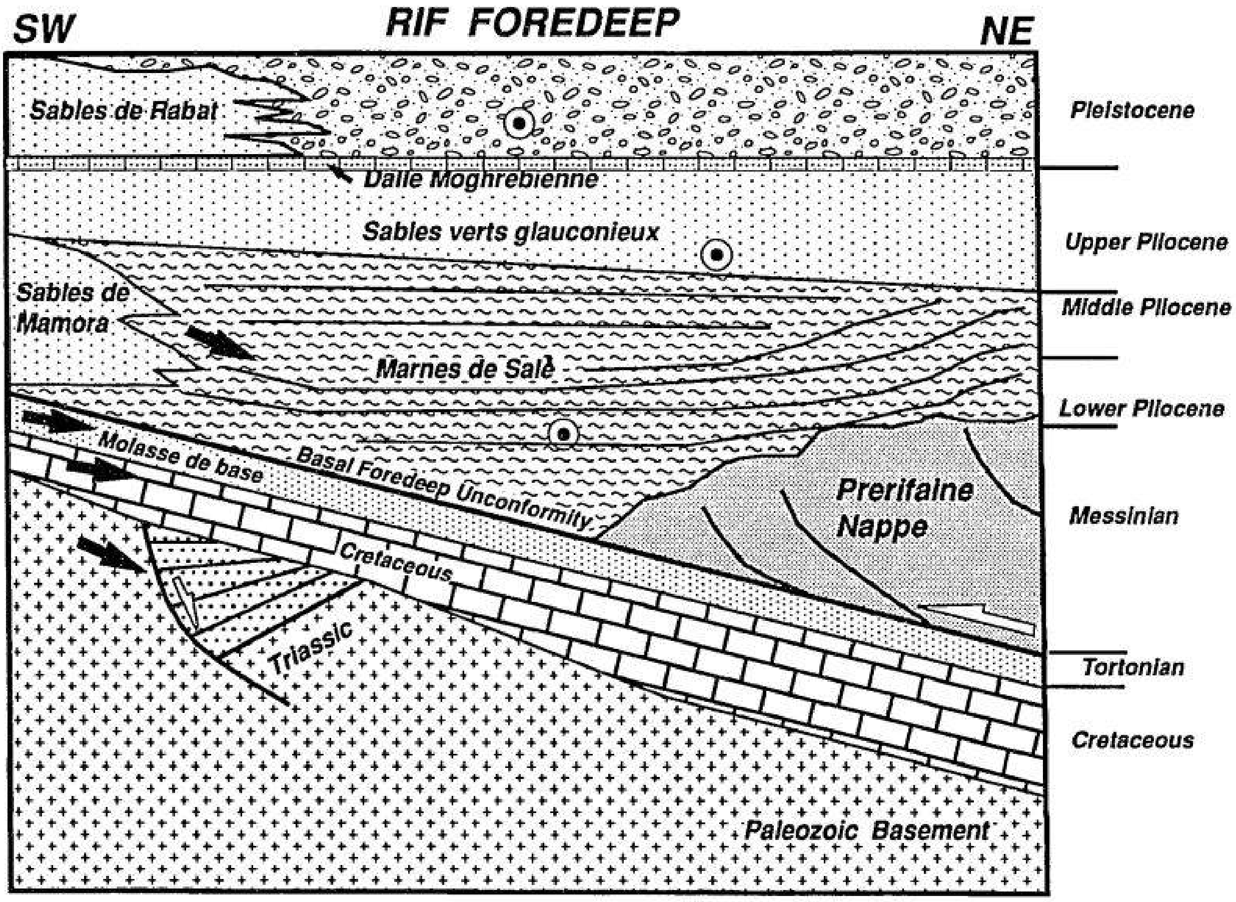

Figure 2.3: An impression of the Rifian foredeep and its deposits by Flinch (1993). Circles indicate paleaocurrent directions towards the reader and the circles resemble sediment influx.

times (Brahim and Chotin, 1984). Wells drilled in the Gharb basin show that the supra-nappe is marked by an transgression followed by an regression at the top throughout the entire basin (Flinch et al., 1996).

The closure of the Tethys, extensive orogenic activity and a decline in temperature (figure 2.4) resulted in aridification of the African continent (SINGH, 1988). Sea level fluctuations during the Messinian are shown in figure **??**. A gradual rise of the fluctuations cycles is observed.

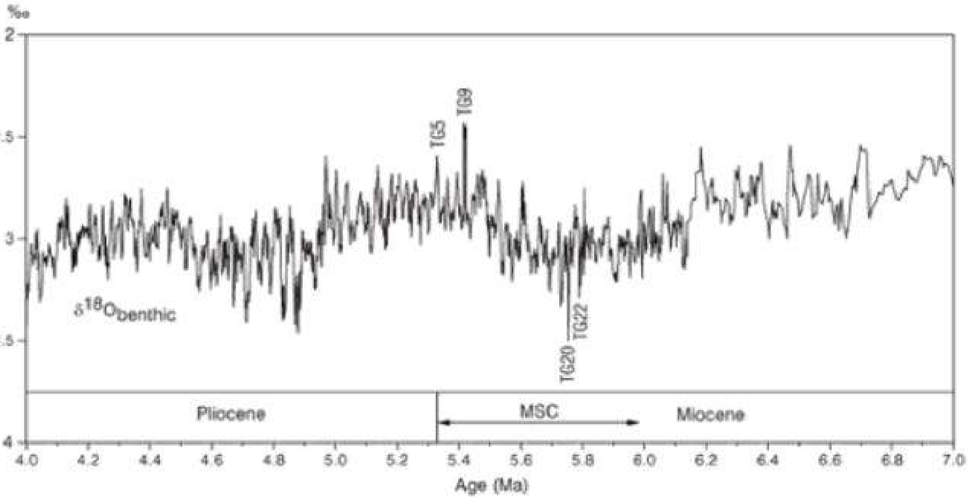

Figure 2.4: Section of the oxygen isotope record modified from Zachos et al. (2001). It shows a decline in temperature towards the end of the Miocene.

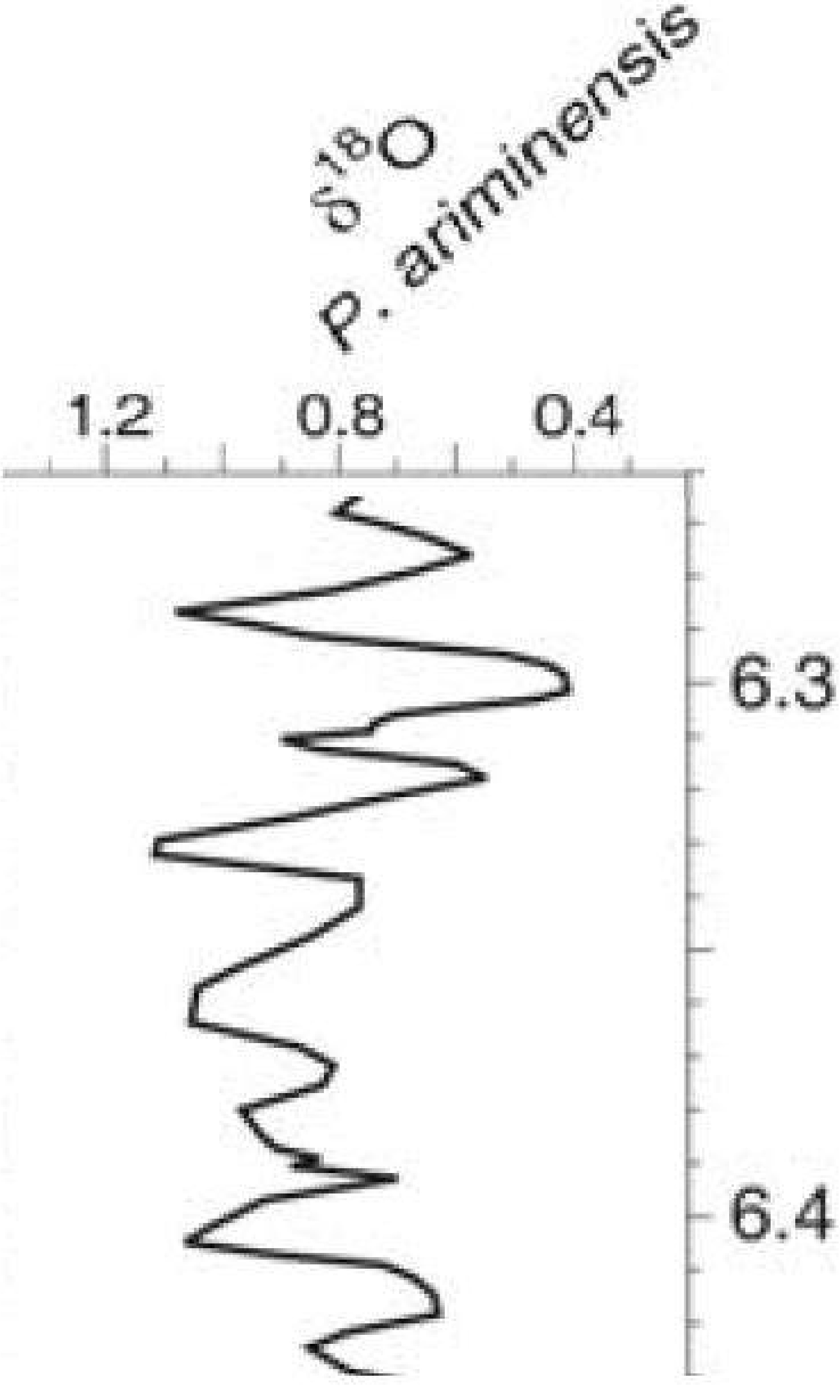

Figure 2.5: No major sea level fluctuations in the interval 6.37 to 6.29 ma. A gradual sea level rise is observed, which means the environmental shallowing in the upper part of the section must be caused by other mechanisms.

Chapter 3

Methods

3.1 Overview sections

In this section the locations of the two high resolution sections will be reviewed.

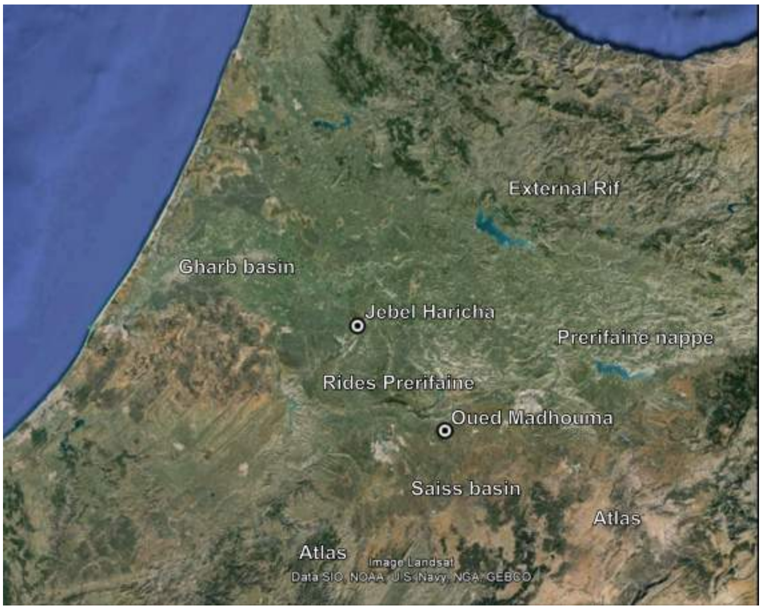

Figure 3.1: Satellite image of Morocco giving an overview of the locations of the two sections. The Jebel Haricha section is located close or on a lateral ramp of the Rides Prerifaine. West of this section lies the Gharb basin. Together with the Saiss basin in the south, it forms the fore-deep basin of the Rifian mountain belt. The Oued Madhouma section is located in the Saiss basin. Southern border of the Saiss basin is formed by the Middle Atlas mountains.

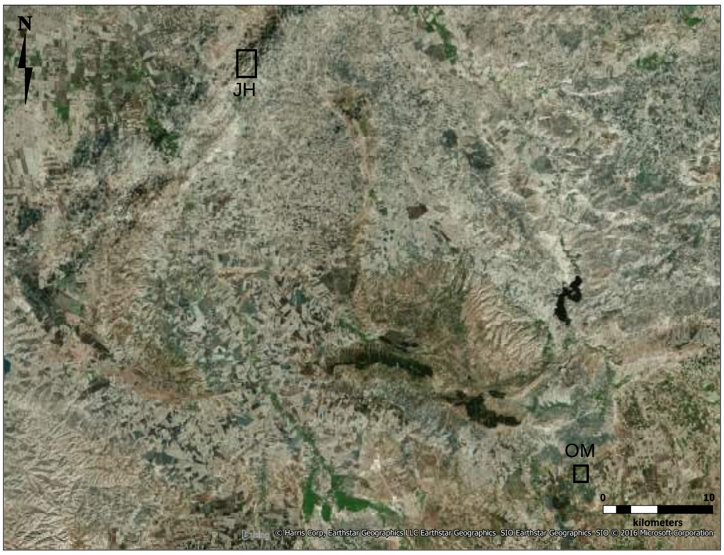

Figure 3.2: Satellite image of Morocco giving an overview of the locations of the Jebel Haricha (JH) and the Oued Madhouma (OM) sections.

Table 3.1: Location Jebel Haricha section

Coordinates of the base of the sections	latitude in dec. degrees	longitude in dec. degrees
Gulley section	34.270452°	-5.651026°
Road section	34.286015°	-5.642543°

3.1.1 The Jebel Haricha section

The section can be reached through the small village of Legrinatt Lahericha, east of Sidi Kacem. Enter the village from the south, follow the road around the village and turn left in a northward direction. Go right on a three-way junction north of the village. Take the first road right, one must walk from this point onwards. Follow the relief on the northern side of the valley for a few hundred meter to reach the upper half of the section. The road on the south side of the valley makes an easy descend towards the bottom of the section.

The Jebel Haricha composite section consists of two sections. One section is exposed in a gulley (gulley section) and the other is exposed at the side of a road (road section). The sections partly overlap. The lateral continuity of the deposits makes it possible to link the two section based on the first exposure of indurated sandstone beds since the marl interval.

© 2016 DigitalGlobe © 2016 GeoEye Earthstar Geographics SIO © 2016 Microsoft Corporation

Figure 3.3: Satellite image and overview of the Jebel Haricha composite section. Sections A, B and C are located in the south, sections R and S in the north. There is two kilometers in between sections ABC and RS (yellow line).

Figure 3.4: Satellite image and overview of the ABC section in the southern area of the Jebel Haricha composite section. The outcrop is exposed due to the incision of meteoric water. The red dotted lines represent the different components of the section.

Figure 3.5: Satellite image and overview of the RS section in the northern area of the Jebel Haricha composite section. It is uncertain if the road-section has an natural of human origin. The red dotted lines represent the different components of the section.

Figure 3.6: The Jebel Haricha section probably lies on top of a transform fault associated to the Rides Perifaine (see geologic setting and Sani et al. (2007). On the picture the transform fault is marked with a red dotted line ((Sani et al., 2007)).

Table 3.2: Location Oued Madhouma section

Coordinates of the section	latitude in dec. degrees	longitude in dec. degrees
Middle of the valley	33.940929°	-5.319037°

3.1.2 The Oued Madhouma section

Take the northern road from Mekness to Fez, the N6. When crossing a bridge at the village of Douar Oued Mahdouma; turn left.

The Oued Madhouma section consists of six more or less overlapping section, all taken in and around a river valley. The overlap gives a good represtation of the paleo-processes active in the area so that a model could be made.

Figure 3.7: Satellite image and overview of the five Oued Madhouma sections. The sections are located in the valley of a small river.

Figure 3.8: An overview of section A of the Oued Madhouma sections.

Figure 3.9: An overview of section B of the Oued Madhouma sections.

3.2 Grain size analysis

Samples for grain size analysis were taken every ± 10 m from fresh rock. The samples were stored in plastic bags and transported to the Netherlands. In the laboratory of the University of Utrecht, the samples were resized into the advised size of ± 1-3 cm in diameter. A acetic acid solution of 3 molar was added to the samples to dissolve the carbonates in the matrix and possibly to remove the carbonate coating around the individual grains. The samples were further disintegrated into the loose sediments required. A pH tape was used to check the rate of carbonate dissolution. The acid was then removed with a centrifuge (2200 RPM, 15 minutes) in three rounds and replaced with deionized water. The samples are analyzed in the Malvern Mastersizer 2000, a laser diffraction based particle size measuring machine. Each sample was measured three times to optimize measuring results. The results were then processed with excel.

3.3 Biostratigraphy

A semiquantitative analysis of potential marker species was carried out on the larger than 125 mm fraction of the washed residue for 56 samples from the sections HA, HR, HS. The analysis was done by Maria Tulbure, University of Utrecht. In normal tray marker species were counted in 15 squares. The distribution of the marker species was divided in the following groups: trace(0-5), common (5-15), abundant (15-35), acme (larger than 35). In addition, the coiling direction of the neoglobo-quadrinids was determined. The distribution of these six species is based on surveying a standard number of fields (15 out of 45) on a rectangular picking tray and specified in qualitative terms (presence, absence) for Haricha section.

Chapter 4

Results

4.1 Facies descriptions

4.1.1 Section Jebel Haricha

Facies association A

This facies association consists of an alternation of sandstones and siltstones in a fining upward trend towards the top. The sandstone/siltstone ratio decreases towards the top, with sandstone layers every ± 3-8 meters at the top. Roughly, all the beds have the same angle of deposition. There is no lower boundary of this facies association described, the bottom part is faulted and folded making it hard to recognize features.. The facies association is probably deposited on top of fine grained material (see under and superposed section).

The bottom part of the section is badly exposed, it is nearly impossible to distinguish structures and fossils. It is unclear what the lateral extent of these deposits is. Although, when looking at figure 4.2, the units seem to be laterally continuous for at least a few hundred meters. Then again, due to faulting the extent of the lateral continuity remains uncertain.

The bottom part is marked by the abundance of sand layers. The sandstones can be described as very fine, slightly coarsening upwards, well sorted, purple and orange sandstones (figure 4.8). The sandstones are intercalated with gray siltstones. The colour of the siltstones varies between gray and dark gray, caused by intervals of more biogenic input. Noteworthy is that thinner silt layers are darker in colour. The sandstone layers are approximately 20-40 cm thick. The bed thickness of the siltstones are much more variable than of the sandstone beds, ranging from ± 0.2 m to ± 5 m. An overall increase towards the top is observed. During a small interval in the middle, the siltstone layers become thicker (± 2.5 m) and more uniform. The contact between the siltstones and sandstones appears to be sharp. However, there are some layers in which the siltstone seems to be a continuous follow-up of the sandstone.

The average grainsize and sorting of the sandstone facies decreases towards the upper boundary of the facies association (figure 4.57). The grainsize decreases from 4 to 4.5 phi, the sorting decreases from poorly to very poorly sorted. The average grainsize and sorting of the siltstones is slightly decreasing towards the top. The sorting is and remains very poorly. Grading in individual sandstone beds could hardly be recognized in the field, but particle size analysis indicates a slightly fining upward trend. It is unclear if individual siltstone bed contain grading. The skewness increases from ± 0.45 to ± 0.6 indicating an increased ratio of silt in the sandstones towards the top. The siltstones are positively skewed, indicating the presence of finer material. The thin sections also show an increase in fine material towards the top. Figure 4.17 and 4.18 respectively represent sandstone beds from the bottom and the top of this facies association.

The grains mainly exist of orange coated grains. The sandstones also contain black heavy minerals and quartz grains larger than the average grainsize. There are intervals with an increased abundance of heavy minerals. Besides fine silt, the siltstone layers contain heavy minerals. Also in the siltstones variations in heavy mineral content have been observed. The heavy mineral content varies throughout the section. Near the top of the facies association the carbonate content increases, the siltstones become more marly. Purple/red circular accretions with a diameter of ± 4 cm and a hole in the middle are visible. They are situated at the surfaces of the sandstone layers. It is the entrance of a burrow, this feature indicates vertical burrowers. Near the top bioturbation is still present in the form of tubes with a diameter of ± 1 cm. The middle and top part of the section are marked by iron concretions. The purple coloured parts of the layers are more indurated than the orange parts. The indurated purple characteristics are probably originate from diagenisis; ferro-manganese concretions?. Furthermore, pyrite raspberries are observed.

The sandstones contain the following fossils: white shell fragments (± 1 mm, figure 4.12), complete unidentified bivalve shells (figure 4.13) and complete Pectinidae (figure 4.10). Near the top a Bryozoan related piece was found (figure 4.16). The siltstones are filled with small complete shells (± 0.5 cm, figure 4.12), these are insitu and are present throughout the entire facies association. The surfaces of most of the layers are marked with bioturbation. Sedimentary structures are only visible near the bottom or not visible at all. The main burrowers are the genus Rhizocorallium (figure 4.11) and an unidentified species of vertical burrowers. The rate of bioturbation decreases towards the top. Rhyzocorallium is no longer present at the top. The siltstones are bioturbated by multiple species, although the burrowing species are unknown (figure 4.4 and 4.5, and figure 4.6). First, white circular forms in the shape of tunnels with a diameter of ± 1 cm in the silt layers indicate bioturbation, although the material within the circle corresponds to the silt. Secondly, an ± 18 cm long tube with a diameter of ± 2 cm is observed within the silt layer. The tube seems to be disconnected on both ends. The tube is coated with an orange/red, oxidized layer of a few mm thick. Within this tubes the material differs slightly from the surrounding silt in that it is finer. Clearly these originated from burrowing species. However, the species remains unknown. Also in the siltstones the rate of bioturbation decreases towards the top.

Sedimentary structures are not abundant or not easily recognized, less than 20% of the sandstone layers contain sedimentary structures. In the middle of this facies association the structures are most abundant. Most of the recognized structures appear to be cross (figure 4.9) and horizontal lamination. At some locations there are structures visible within the silt layers. They can be marked as cross-bedding (figure 4.9).

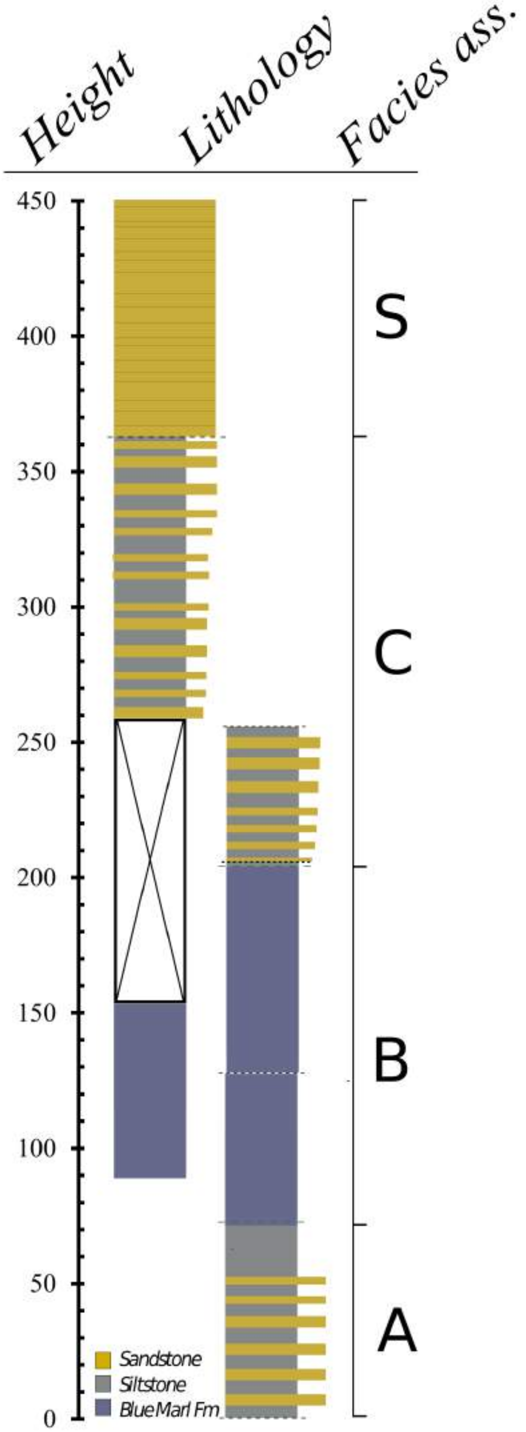

Figure 4.1: Overview of the facies associations with characteristic lithologies.

Figure 4.2: Facies association A was conducted in the gulley seen in the bottom of the image. It seems that the beds are continuous along the slope of the hill. However, due to faulting the extent of the lateral continuity remains uncertain.

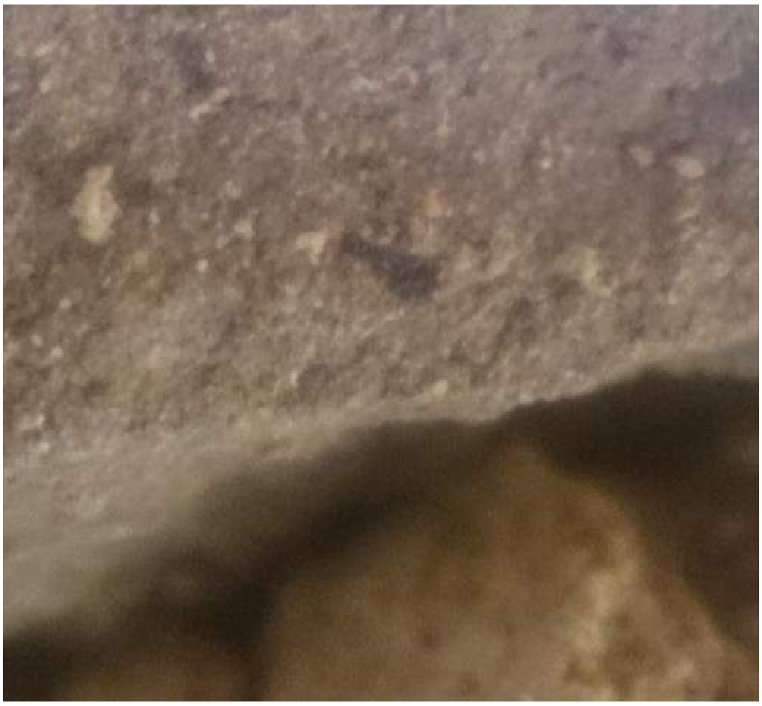

Figure 4.3: A flake of a black platy heavy mineral (± 1-2 mm).

Figure 4.4: White circular forms in the silt layers, the material within the circle corresponds to the silt.

Figure 4.5: An overview of the occurrence of the white circular forms (figure 4.4).

Figure 4.6: An ± 18 cm long tube with a diameter of ± 2 cm within the silt layer. The tube seems to be disconnected on both ends. The tube is coated with an orange/red, probably oxidized, layer of a few mm thick. Within this layer the material differs slightly from the surrounding silt in that it is finer. Clearly this is palaeo burrow, species unknown.

Figure 4.7: A purple circular accretion with a diameter of ± 4 cm with a hole in the middle. The accretion is situated in sandstone. Probably the accretion is the entrance of a burrow.

Figure 4.8: A indurated, purple to orange sandstone layer with a pocky surface. The indurated purple characteristics are probably originate from diagenisis; ferro-manganese concretions?. Some structures are visible near the bottom of the bed, the structures appear to be cross and horizontal lamination. The surface of the layer is probably marked by bioturbation. This also explains why sedimentary structures are only visible near the bottom.

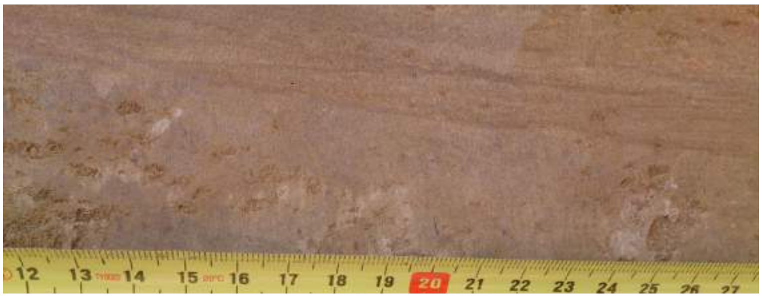

Figure 4.9: At some locations there are structures visible in the silt layers. They are cross-laminae.

Figure 4.10: One of the shells (Pectinidae, ± 4 cm) is deposited in a sandlayer. The shell is determined not to be insitu based on the orientation of the shell. The shell is, however, completely intact.

Figure 4.11: A indurated, purple to orange sandstone layer with at the surface clear markings of benthic dwellers. Possibly Rhizocorallium.

Figure 4.12: A a fairly intact shell fragment of ± 3 cm.

Figure 4.13: One side of a white bivalve. Around ± 1 cm in size and found in a vaguely finely laminated sandstone. The shell is not deposited insitu.

Figure 4.14: Unidentified features in the siltstones.

Figure 4.15: An unidentified feature in a sandstone.

Figure 4.16: Bryozoan.

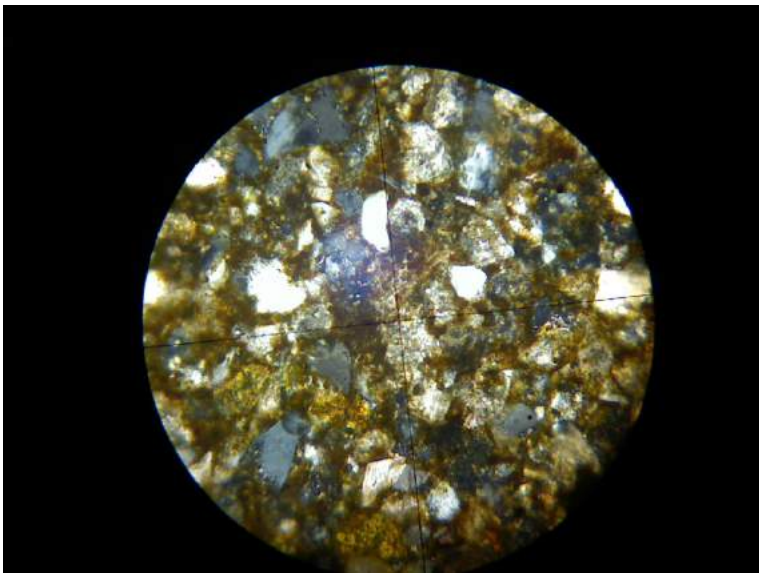

Figure 4.17: A microscopic photograph of a thin-section taken from a sample of a sandstone bed situated 13 m from the bottom of the section.

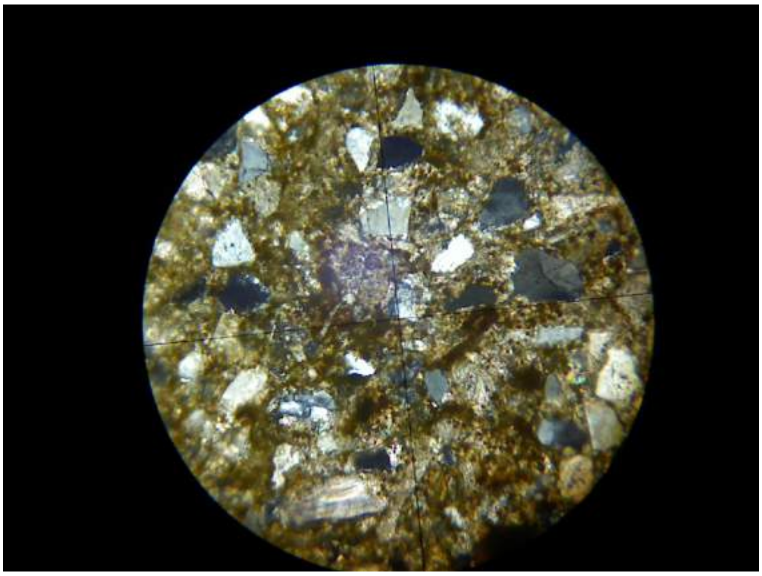

Figure 4.18: A microscopic photograph of a thin-section taken from a sample of a sandstone bed situated 61 m from the bottom of the section.

Facies association B

This facies association is represented by a thick package of blue/grayish marls. Weathering makes it difficult to distinguish individual layers. It appears that the layers are deposited in a constant angle similar to that of facies association A. The lower boundary of the facies association is a gradual transition. The top of the last clearly distinct sandstone bed is taken as the lower boundary for this facies association. Although the grain size remains fairly stable throughout the marls, there are intervals with increased grain sizes (figure **??**). The marls are poorly sorted. A near symmetrical skewness is observed except for the intervals with increased grain sizes, there the marls are positively skewed. Various fossils and imprints have been identified. Several bivalves have been observed: Lutraria/Tellinidae (figure 4.19), possibly Abra (figure 4.20) and Pectinidae (Amussium cristatum) (figure 4.22). An unidentified fragment was found near the top, possibly of echinoid or coral origin. Occurrence of a ± 10 cm tube hints toward biological activity, although weathering makes it impossible to indicate the rate of bioturbation.

Figure 4.19: Lutraria or Tellinidae indet. (marine)

Figure 4.20: Looks like Abra spec. (marine, in situ)

Figure 4.21: Unidentified fragment, possibly of echinoid or coral origin.

Figure 4.22: Pectinidae (marine)

Figure 4.23: Pectinidae(marine)

Figure 4.24: Sea urchin, unknown species

Facies association C

This facies association consists of a sequence of sandstones and siltstones. The sandstone/siltstone ratio increases towards the top, with some intervals with a decreased abundance of sandstone beds. All beds are deposited in a similar angle, the angle is identical to that of facies association A and B. The lower boundary of this facies association is marked by a sharp transition from a marlstone to a siltstone with on top of that siltstone a sandstone bed. The sandstone siltstone ratio increases towards the top. The beds can be traced over several kilometers (figure 3.3); all the layers seem to be continuous over a large area (figure 4.34). No hint of palaeo relief is observed.

The sandstones are coloured red, yellow and orange. The siltstones are light grey to dark and orange brown in colour. The bed thickness of the sandstones range between ± 20 and ± 30 cm, and have a slight thickening upward trend. The sandstone beds are organized. The upper beds of this facies association appear to be thicker, these are made up out of multiple thinner beds; composite beds. The bed thickness of the siltstones are much more variable ranging from ± 0.2 m to ± 8 m. The contact between the siltstone and sandstones appears to be sharp. However, there are some layers where the siltstone seems to be a continuous follow-up of the sandstone.

The overall average grainsize of the sandstones increases from ± 4.5 at the bottom to ± 3.5 phi near the top. Individual beds are clearly fining upwards. The siltstones also coarsen upwards in the sequence. It is unclear if individual siltstone beds contain grading. The sorting of the sandstone beds increases from poorly sorted towards approximately moderately well sorted towards the top. The siltstones are very poorly sorted. The siltstones are positively skewed. The skewness of the sandstones remains stable as strongly fined skewed.

Most of the sandstone grains exist of orange carbonate coated grains, the beds also contain black minerals (± 1-3%). Towards the top the ratio of black minerals decreases. An iron crust is formed on the top and bottom surface of most of the sandstone beds, bioturbation is visible through this iron crust. Near the bottom of the facies association some of the sandstone beds are completely eroded and are only visible as orange bands within the siltstones.

A sandstone layer near the bottom of the turbidite sequence is marked with an intact shell of the species Pectinidae. The shell is not in-situ. The sandstone layers contain shell fragments of unidentified species. Around sandstone layers near the bottom shell fragments are found, these not connected with the sand layer and could originate from sand layers uphill. The rate of bioturbation decreases towards the top. The surface of many sandstone beds are marked by horizontal burrows of the species Rhyzocorallium. The remains of a tunnel shaped vertical burrowers are found from the middle the section (diameter of ± 4 cm, figure 4.28).

Erosive features (figure 4.32) are observed at the bottom of the beds. The sandstone in figure 4.32 is one of the few layers with a well exposed bottom. Some tool marks are observed at the bottom of the lower sand beds. The wavy features in this sandstone layer have an average wave length of ± 18 cm. There are no further structures observed within the wavy features. They are not continuous and could be load casts. The classification of the contacts of these beds is arbitrary, some are clearly of erosive nature whilst others could also be marked as sharp contacts. The sandstone beds at the bottom of this succession have less features than the ones near the top. The sandstone beds contain parallel laminations (figure 4.31) and to lesser extent ripple cross-lamination (figure 4.33).

Figure 4.30: A vertical burrow of ± 11 cm in length an ± 1 cm in diameter.

Figure 4.25: The surface of second sand layer in the turbidite sequence. The surface is marked by horizontal burrows of the burrower Rhyzocorallium. A ± 0.5 cm thick iron has formed on the top the layer. The figure shows a shell fragment, which is not connected with the sand layer and could originate from sand layers uphill.

Figure 4.26: A ± 0.5 cm thick iron has formed on the top of many of the sand layers.

Figure 4.27: A sandstone layer near the bottom of the turbidite sequence. The middle of the figure is marked with an intact shell of the species Pectinidae. The shell is not insitu.

Figure 4.28: Side view on a sand layer with in the middle the remains of a vertical burrow.

Figure 4.29: A tunnel shaped burrow with a ± 5 cm diameter. The is disconnected at both sided and is found with a length of ± 9.5 cm. The original position is unknown.

Figure 4.31: One of the lower sand layers in the section with a thickness of ± 20 cm. Clearly, the layer has horizontal lamination. Some cross-bedding is observed, although vaguely.

Figure 4.32: There appear to be erosional features at the bottom of some of the sandstone layers. The sandstone in this figure is one of the few layers with a well exposed bottom. The wavy features in this sandstone layer have an average wave length of ± 18 cm. There are no further structures observed within the wavy features. They are not continuous and appear to be flute casts.

Figure 4.33: Cross section of a sand layer with wavy cross-lamination.

Figure 4.34: The sand layers are continuous over kilometers, approximately keeping the same thickness.

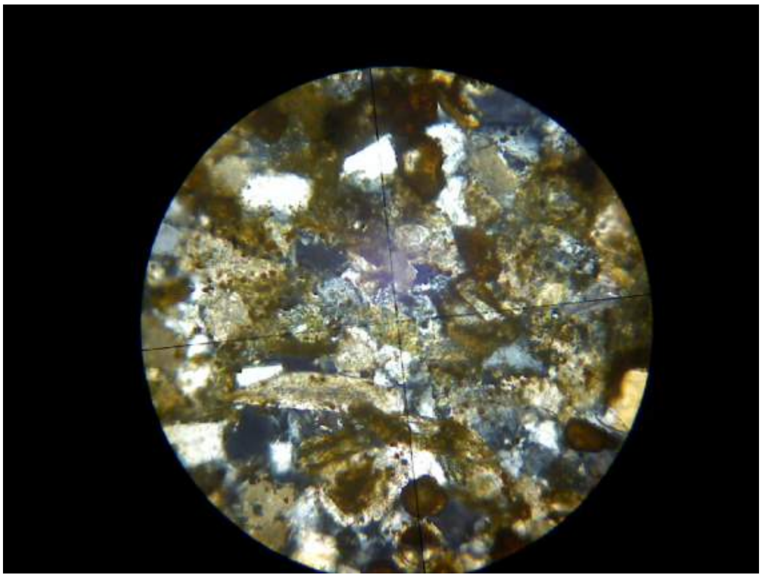

Figure 4.35: A microscopic photograph of a thin-section taken from a sample of a sandstone bed situated as one of the first clear sandstone beds emergent above the marl interval.

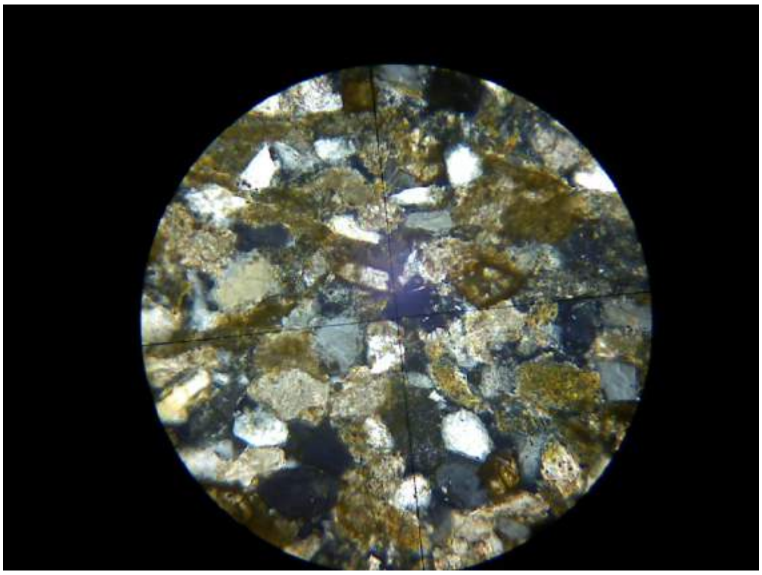

Figure 4.36: A microscopic photograph of a thin-section taken from a sample of a sandstone bed situated near the top of facies association C.

Facies association S

This facies association is represented mainly by well sorted orange to yellow sand beds with varying grainsizes with lags of mud clasts. There is no distinct boundary between the alternation of sandstone and siltstones underneath (facies association c) and this facies association. A fluctuating angle of deposition is observed, the layers are not deposited parallel. The maximum difference in angle is 35 degrees. The sandstone beds are regularly deposited. This facies association is, unlike the underlying facies association, not traceable over multiple kilometers. In fact the only outcrop observed is the one of this section; the road section.

The colour of the sandstone beds shifts from orange to a more yellowish colour towards the top. The lower boundary consists of gradually decreasing siltstone thickness from ± 1 meter in facies association C to ± 2 cm in this facies association. And increasing sandstone bed thickness from ± 0.3 m to ± 4 m. The thicknesses of the beds vary throughout this facies association ranging from approximately ± 1 to 4 m. The middle is marked by a shift in the thickness of the sandstone beds decreasing from averagely ± 4 to ± 1 m. The sandstone beds sometimes form composite beds. After ± 10 meters into the facies association erosive (wavy) features appear at the bottom of the sandstone beds. The bottom of the sandstone beds seem to evolve from wavy to straight.

The grain sizes of this facies association ranges between ±3 and 5.5 phi. There is no trend observed and thus it seems to be chaotically arranged. The sorting and the skewness do not change compared with the underlying facies associations C. Grainsizes appears to be stable along the succession (figure 4.56). Grainsize analysis verifies the observation of mostly fining upward grading in individual beds.

The first mud clast band appears at ± 10 m from the lower boundary of this facies association. They have an average diameter of a few centimeters. After ± 15 meters in this facies association the mud clasts also appear within the sand beds. Furthermore, in the middle of the facies association the bottoms of the sandstone layers become more indurated than the top, this coincides with the accumulation of purple crystalline material at the bottom of the individual sandstone beds. Near the top of the section not only the bottom part of individual layers is cemented with (secondary) crystalline material, but in some cases the crystalline material is observed up to the middle part.

Almost no fossils are observed in this part of the section.

This facies association is marked, besides the siltstones which are continuously present, by the occurrence of thin wavy silt layers which occur in lens shapes and contain sub-horizontal burrows in tube shapes. The overall silt content is strongly reduced towards the top of this facies association.

The facies association is marked by horizontal lamination and cross stratification, horizontal lamination is mostly situated below the cross-bedding. In some beds, fore and bottom sets can be recognized. The mud clasts are sometimes inter bedded in cross-stratification. These are low angled cross-stratifications. There seems to be some kind of order in which the sedimentological features are arranged. However, bad exposure makes it hard to recognize sedimentary structures. Some of the sandstone beds contain channel, lenses and/or wedge shapes.

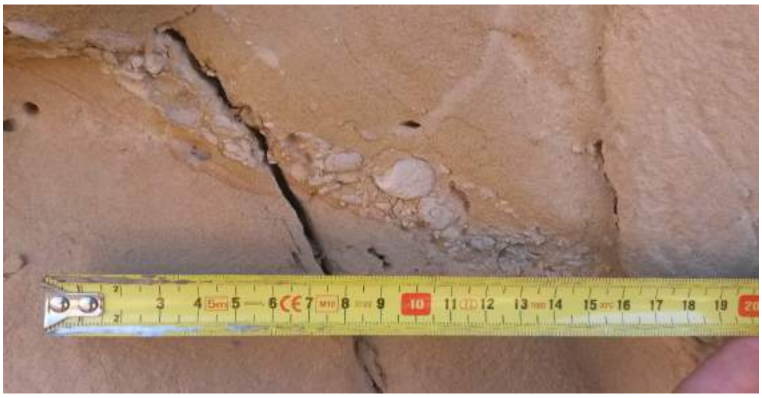

Figure 4.37: A thick sandstone layer with in the middle a band of ± 2 cm thick with mud clasts of varying size (max. ± 1 cm).

Figure 4.38: Thin laminated siltstone bed in between thick sandstone beds. The siltstone, especially at the top, is highly fragmented.

Figure 4.39: A chaotic alternation of sandstone beds.

Figure 4.40: An alternation of thick sandstone beds. In between thin beds of thinly laminate silts are visible.

Figure 4.41: Side view of a thick sandstone bed with clear horizontal lamination en cross-stratification on top.

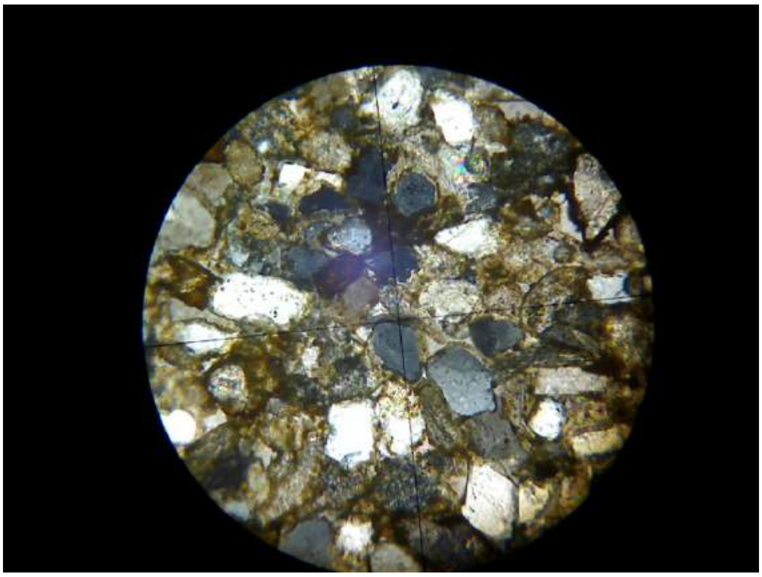

Figure 4.42: A microscopic photograph of a thin-section taken from a sample of a sandstone bed situated near the bottom of facies association S.

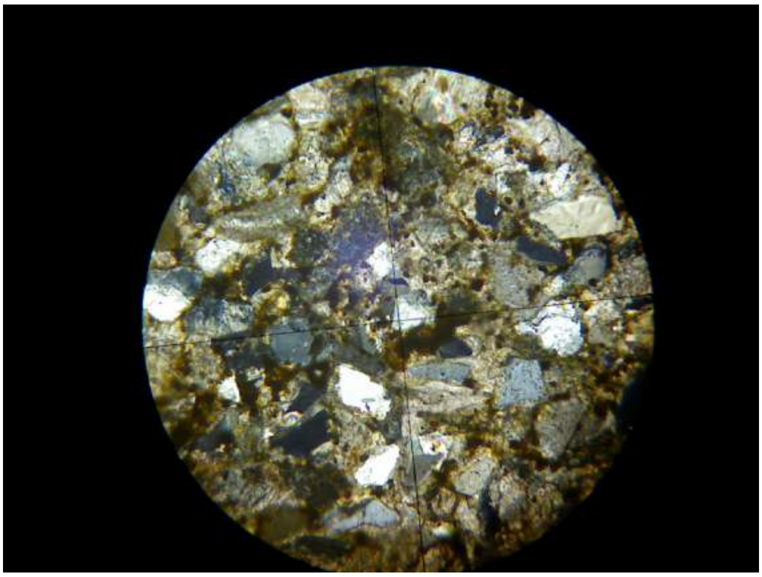

Figure 4.43: A microscopic photograph of a thin-section taken from a sample of a sandstone bed situated in the middle of facies association S.

Beyond the section boundaries

The bottom of facies association A is not the beginning in the succession, it continuous downwards for approximately ± 70 meters. The deposition looks similar to that of facies association A, but bad exposure and deformation made it impossible to make objective observations or even to recognize trends. The faulting in this part of the section has similarities with flower structure associated deformation. This part of the succession is underlaid by fine, white/blueish deposits. It seems that the colour is much lighter than the that of the marl interval (facies association B).

The top of facies association S is not the end of the section. On top lies, after ± 20 meters of badly exposed terrain, a conglomerate deposit. They consist of fine, brownish material as matrix with very rounded cobbles in it. As is shown in figure 4.44 the conglomerates have been subject to deformation. The figure shows an alternation of more gray and brown intervals within the conglomerates.

Figure 4.44: Conglomeratic unit on top of the Jebel Haricha section.

4.1.2 Section Oued Madhouma

Facies association X

This facies association is represented by a thick package of blue/greyish marls. The sequence transforms from a clean marl (figure 4.45) to a more silty marl to the top. The marls in the bottom of the sequence are homogeneous and no beds can be recognized, to the top beds become visible with in the silty part an alternation of more and less indurated layers. Around ± 60 cm below the unconformity with the lacustrine facies a ± 20 cm thick orange band and a heavily bioturbated siltstone of approximately ± 20 cm thick with oxidized tubes is visible within the silts.

Figure 4.45: Thick clean homogeneous marl packages near the bottom of the section.

The CM plots for this facies association (figure 4.76) shows a trend of pelagic deposits towards more deposits marked as being transported as uniform and graded suspension.

Facies association Y

This facies association consists of packstones and grainstones with dertrital and conglomeratic components. On top of the this main lithology the exposed outcrop contains ooidbeds, grainstones and conglomerates with grainstones as extra clasts. All layers are deposited in the same angle. The lower boundary of this facies association is a sharp, distinct transition from the marine siltstones to detrital limestones (figure 4.53, figure 4.46, number 2). There are erosive features observed at the transition. The facies association has total thickness of maximal ± 10 meters.

It is unclear what the lateral extent of this facies association is. It is, however, recognized in section 1, 2 3 and 5 (see figure 5.7). The exposure is not optimal in sections 2 and 3. The build-up of the layer is chaotic.

The main lithology of this facies association is described as chaotic reddish/orangish conglomeratic detrital limestones with ungraded rounded or angular extraclasts which consist mostly out of limestones (figure 4.53, upper part and figure 4.46, number 3).

The beds are chaotic, therefore, it is hard to distinguish and determine the thickness of the individual beds. The coarser conglomerates are estimated to have a bed thickness ranging between ± 20 and ± 200 cm. The complete package of these conglomeratic detrital limestones is approximately several meters thick.

The base of several layers have channel shaped incisions in the underlying layer(s), the channel shaped incisions are filled with the coarsest extraclasts accumulated at the base. The finer conglomeratic detrital limestones contain crossbedding near the base in which fining upward trends are recognized in individual crossbeds. The load, shape and size (± 2-10 cm) of the extraclasts varies per layer.

The petrology of the extraclasts is estimated to consists of approximatly 70% limestone, 20% sandstone/quartz and 10% pink coloured sandstone from below. The matrix is loose mud, bioclasts in the form of tubes (figure 4.47) and in lesser extend quartz grains. To the top in the sequence of conglomeratic detrital limestones the tube/mud ratio becomes higher.

The tube sizes vary in different and in the same layer from ± 0.1-10 cm, all the smaller tubes and clasts are carbonate covered. The carbonate tubes are thus overprinted by a carbonate layer (figure 4.47). In some layers no extraclasts are present resulting in units consisting of purely matrix. This facies association also contains some ooids and shell fragments (recognized species: Gastropoda). The facies association is also marked by the occurrence of microbial mats in the form of stromatolites (figure 4.55 and 4.51) and other forms of cyanobacteria development (figure 4.54).

Above the conglomeratic detrital limestones two conglomeratic layers are found with grainstones as extraclasts (figure 4.46, number 5), the grainstones vary greatly in size (± 20 cm) and have angular shapes. This facies, as well as the following two, have bed thicknesses ranging between ± 20 and ± 50 cm. The layers exist for 90% of these extraclasts, the rest is filled with consolidated carbonate mud.

The oncoid beds are packstones (see figure 4.50, 4.49 and 4.48). The oncoids are approximately ± 1 cm in diameter. The oolithic grainstone is made out of ooliths with transparent matrix in between. This facies also contain some oncoids and shell fragments (recognized species: Gastropoda).

In the sequence three possible palaeosols crop out as a soft badly consolidated white muddy consistence with clear organic content in the form of rootlets (figure 4.52, figure 4.46, number 4).

Points A and B (figure 3.7) are marked by coarse conglomerate units and the exposure of the unconformity which is lacking in points C, D and E (figure 3.7). In the most south-western point of the valley the outcrop is also, like in the east finer and marked by algae mats.Noteworthy are the lateral variations in this facies association. The sections in the east contains more grainstones, ooid layers and algae mats and finer extraclasts in the conglomerates than the sections in the north and in the west. The continuation of the eastern section in northern direction shows a coeval transformation of ooid and grainstone beds into conglomeratic detrital limestones.

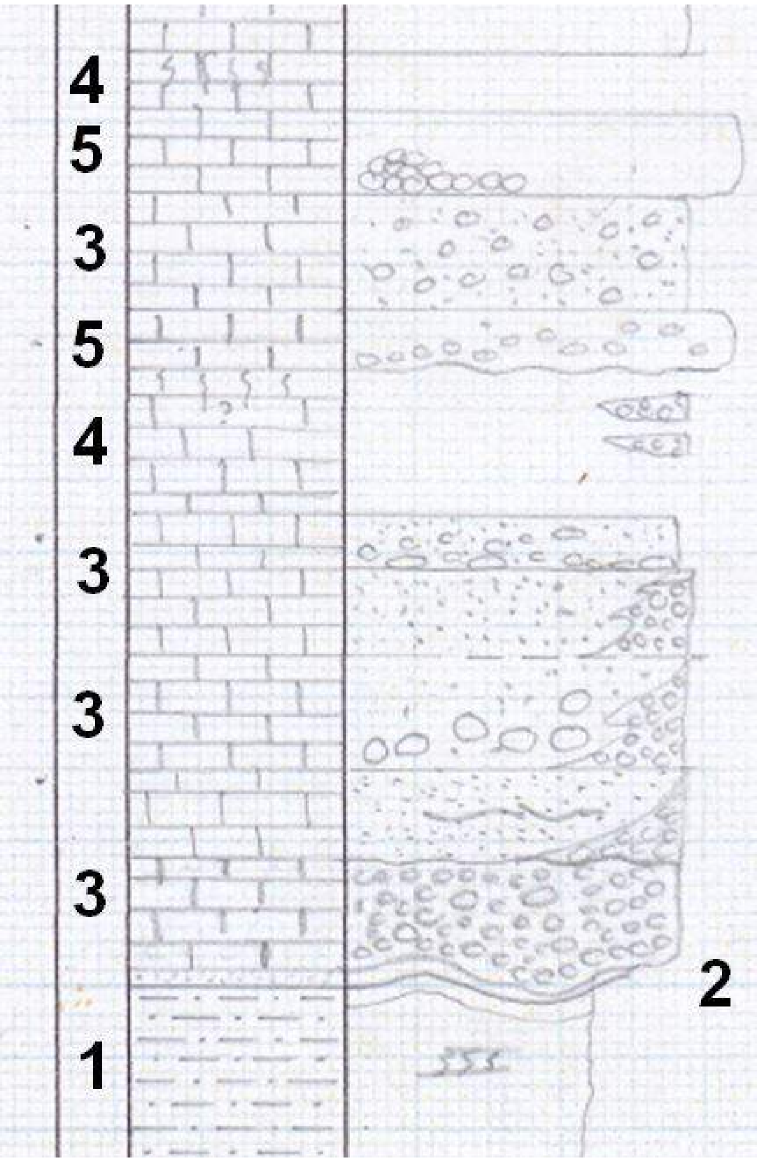

Figure 4.46: A representative sedimentary log of one of the sections in the Madhouma area.

Figure 4.47: An example of bioclast found as matrix, which is described as a tube. This sample is cut by half and the picture shows the inside of the tube.

Figure 4.48: An oolithic grainstones. The oolithic grainstone is made out of oncoids with transparent lime as matrix. The oncoids are approximately ± 1 cm in diameter.

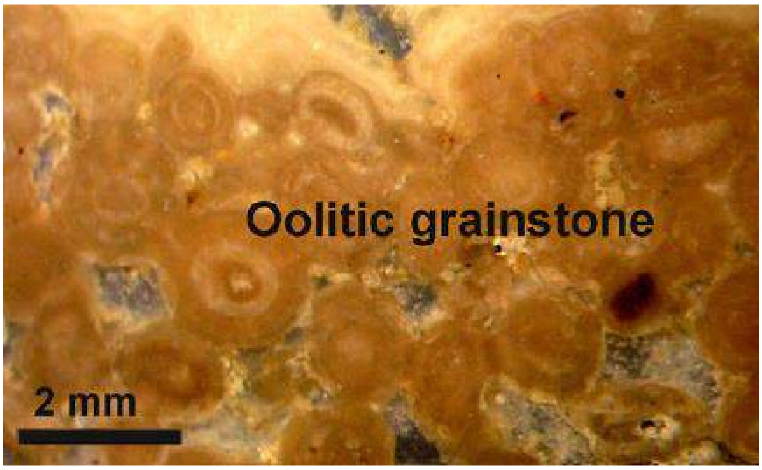

Figure 4.49: A thin-section of an oolithic limestone found in lake deposits Iraq (Khanaqa et al., 2013). It perfectly resembles a facies found in the Oued Madhouma section. There were no pictures taken of this facies.

Figure 4.50: An oncoid bed. The oncoid beds are packstones with limemud as matrix

Figure 4.51: Microbial mats in the form of the Stromatolites

Figure 4.52: A soft badly consolidated white muddy consistence with clear organic content in the form of rootlets. Could be a palaeo-sol deposit.

Figure 4.53: The sharp, distinct transition from the marine siltstones to detrital limestones. Erosional features are observed at the contact.

Figure 4.54: Micorbial mats, possibly the remains of cyanobacteria.

Figure 4.55: Extensive thick packages of microbial mats.

4.2 Particle analysis

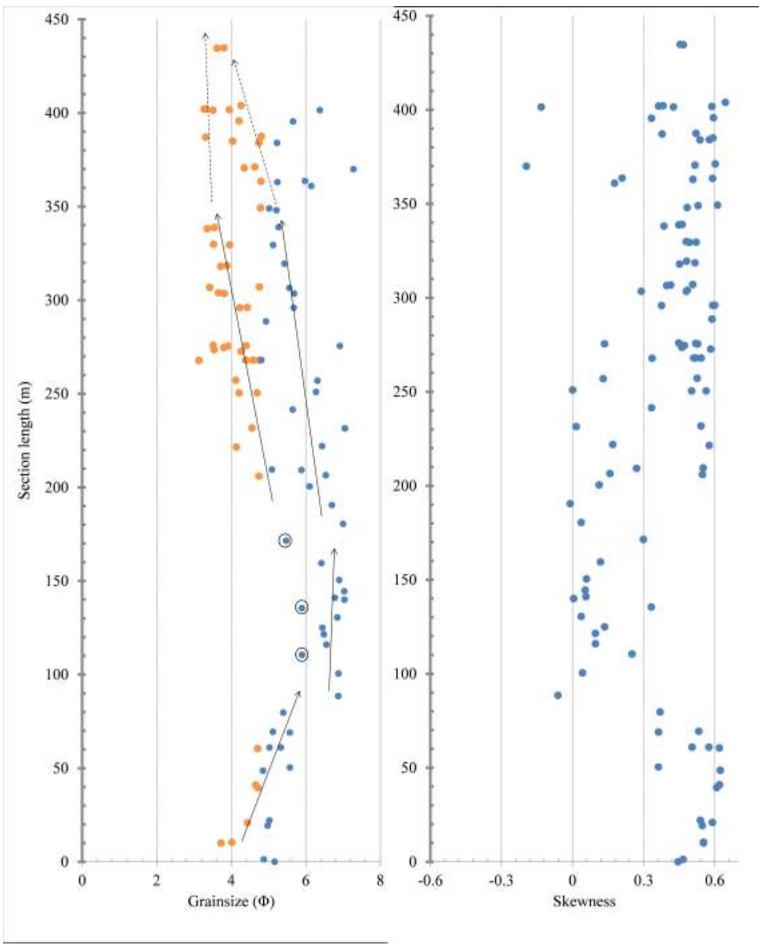

Figure 4.56: The grainsize and skewness are plotted over the section length. Samples taken from indurated orange sandstone beds are marked orange and samples taken from soft gray siltstone beds are marked as blue. Grainsize trends are indicated by arrows. Unclear trends are marked as dashed arrows. The black circles represent coarser intervals in the marl interval.

To identify grain size patterns along the stratigraphy hand-lenses were not sufficient. First, grain sizes were simply too fine. Second, grain sizes differences were too small to observe.

In figures 4.56 and 4.57 the mean grain size is plotted over the length of the section. Facies association A shows a fining upward trend in both the sandstones and the siltstones. Most samples in the marl interval (facies association B) are continuously of the same size. However, three samples in the marl interval show coarser grain sizes (indicated with circles, figure 4.56). The grain sizes in the marl interval are on average finer than the grains of the siltstones in between the sandstones. The sandstones (facies association C) on top of the marl interval is marked by a coarsening upward trend, this applies to both the siltstone and the sandstone beds. The sandstone beds of Facies association S seems to have no clear trend. Whilst the siltstone beds coarsen upwards. Note that, because lateral shifts were made whilst sampling due to inhospitable terrain, lateral variations can not be ruled out as a cause of grain size shifts, especially in facies association C.

As for grading in single beds the sandstone beds from facies association A and C show minimal fining upwards trends. The sandstone beds from the upper part of the section have exceptions to this fining upwards trend; some beds are coarsening upwards (figure 4.57). Only a few grain size samples were taken to identify grading in single beds, this implies large inaccuracies in the previous statement. The more indurated parts of the sandstone units are not always the coarsest layers.

Grain size distribution curves are plotted for all the representative beds of the different facies associations A, B, C and S. The sandstone beds of facies association A contain relatively finer coarse material than the sandstone beds of facies association C. Furthermore, the top of facies association S contains more coarse material and has a more variable distribution of the curves than the sandstones of lower part of the section. All the sandstone beds in both the Jebel Haricha and the Oued Madhouma sections show a fine material mode. Remarkable is the peak concentrations of grains with a size of 130 um in all sandstone sections.

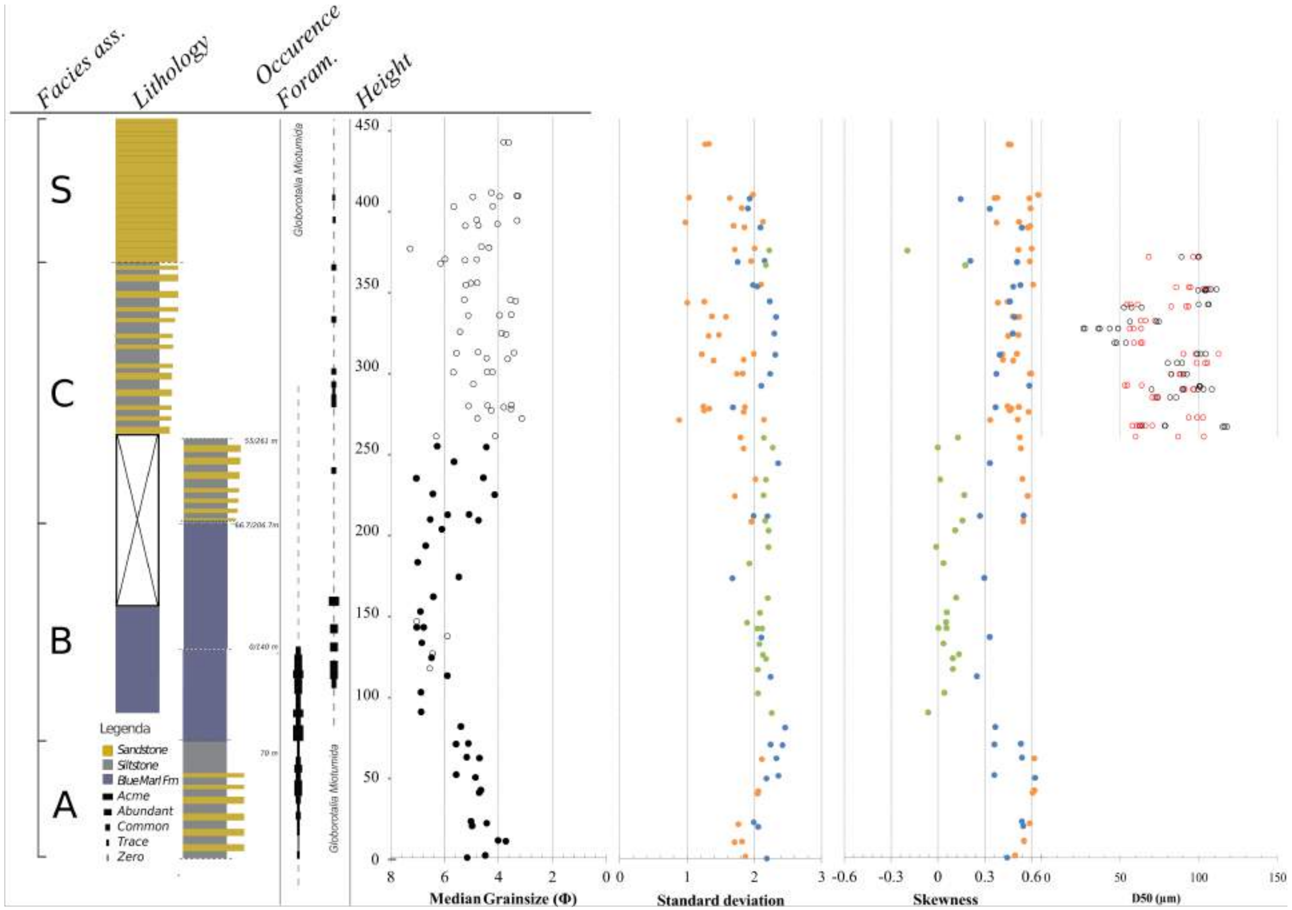

Figure 4.57: An overview in which the grain size (dots are samples from the gulley section and circles from the road section), standard deviation, skewness and top/bottom analysis are plotted relative to the lithologies of the section. In the graphs of the standard deviation and skewness the green, blue and orange dots represent respectively fine silts, medium to coarse silts and sands. Also, the bio-stratigraphic analysis is plotted.

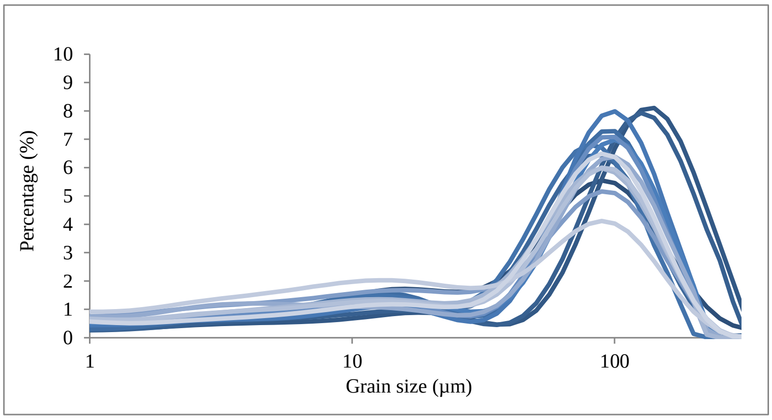

Figure 4.58: Grain size distribution curve of facies association A. Al the sampled sediments seem to be bimodal; a fine and a sand mode.

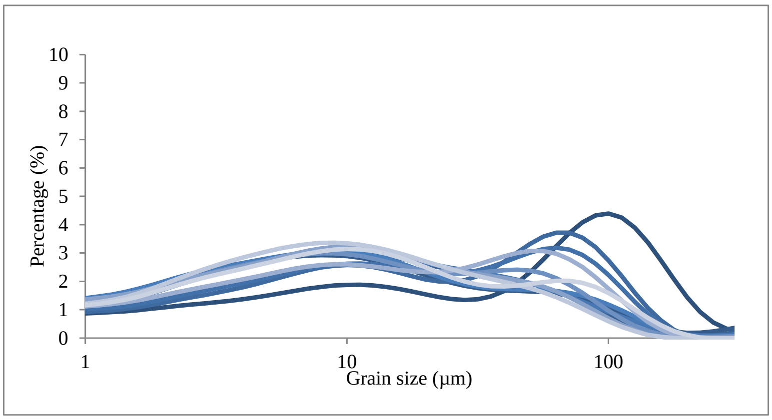

Figure 4.59: Grain size distribution curve of the marl interval (facies assocation B). Noteworthy is the that also the deposits in the marl interval are marked as bimodal. Striking are the coarser samples in the marl sequence.

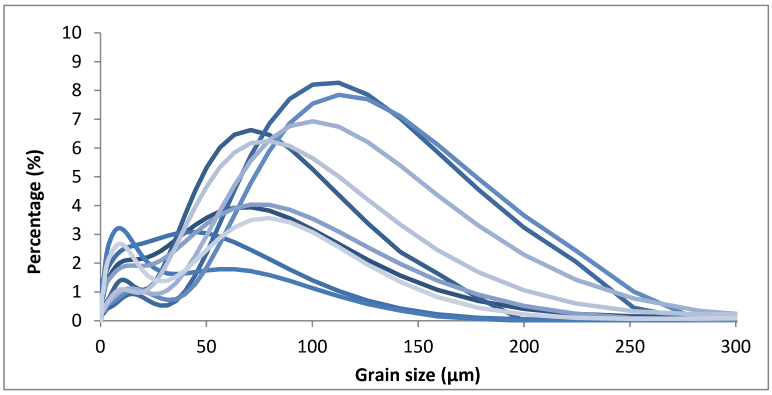

Figure 4.60: Grain size distribution of facies association C. The focus of the grain sizes seems to be larger than in facies association A.

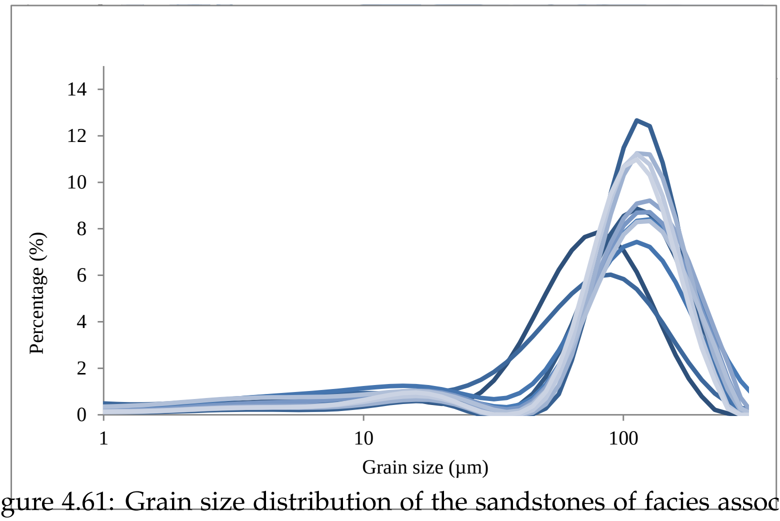

Figure 4.61: Grain size distribution of the sandstones of facies association S. One can observe an increase in grain sizes, better sorting and a more uniform distribution compared with facies associations A and C.

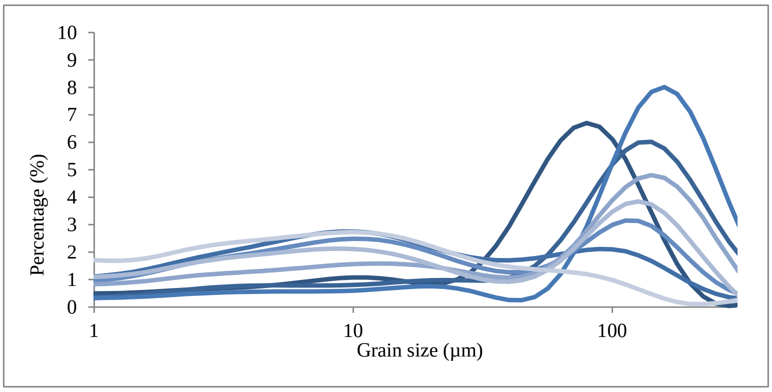

Figure 4.62: Grain size distribution plot of deposits of section 1 in the Oued Madhouma section.

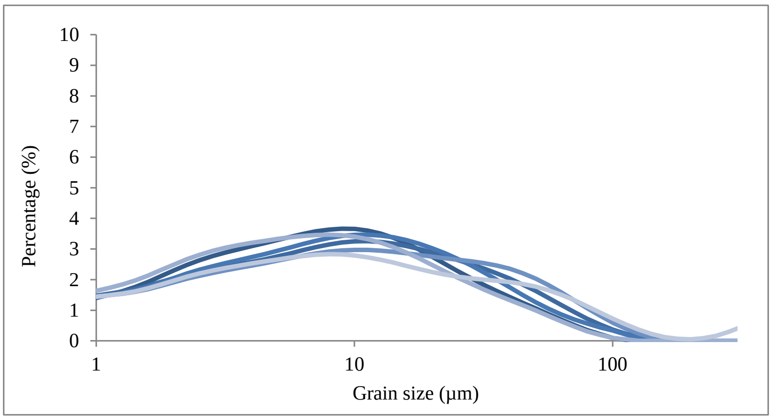

Figure 4.63: Grain size distribution plot of deposits of section 2 in the Oued Madhouma section.

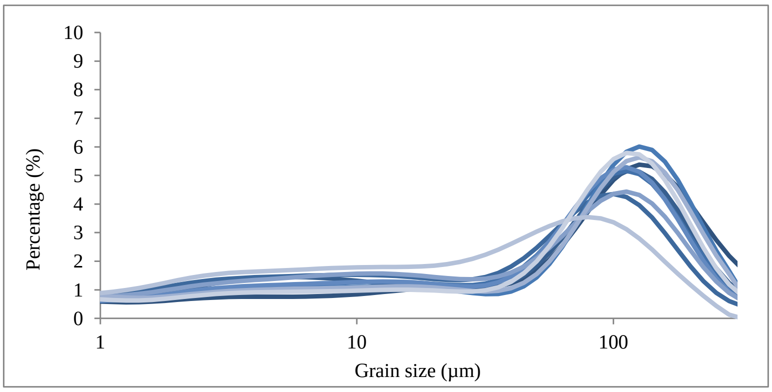

Figure 4.64: Grain size distribution plot of deposits of section 4 in the Oued Madhouma section.

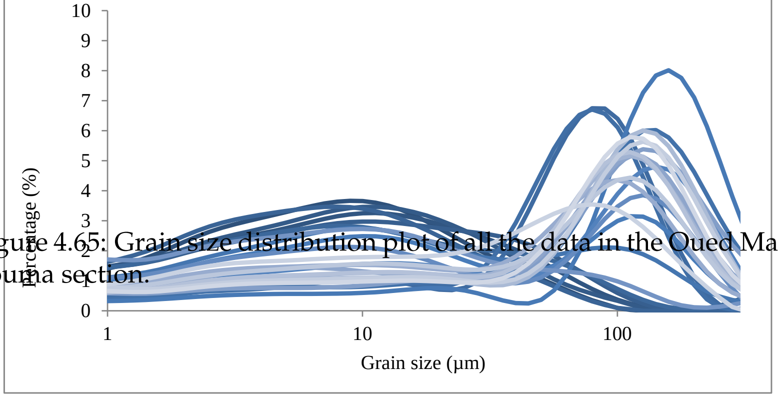

Figure 4.65: Grain size distribution plot of all the data in the Oued Madhouma section.

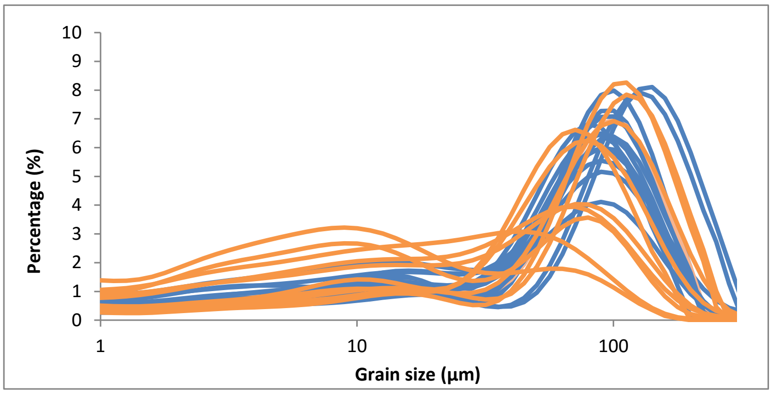

Figure 4.66: A grain size distribution plots comparing the data of facies associations A (blue) and C (orange) of the Jebel Haricha section.

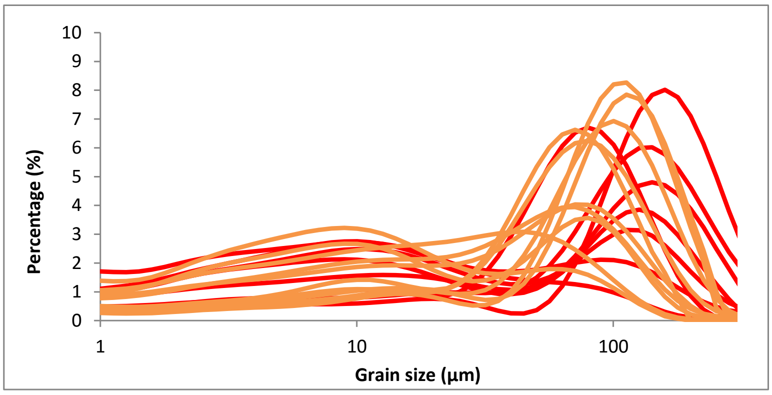

Figure 4.67: A grain size distribution plots comparing the data of section 1 of the Oued Madhouma section (red) and the data of facies association C of the Jebel Haricha section (orange).

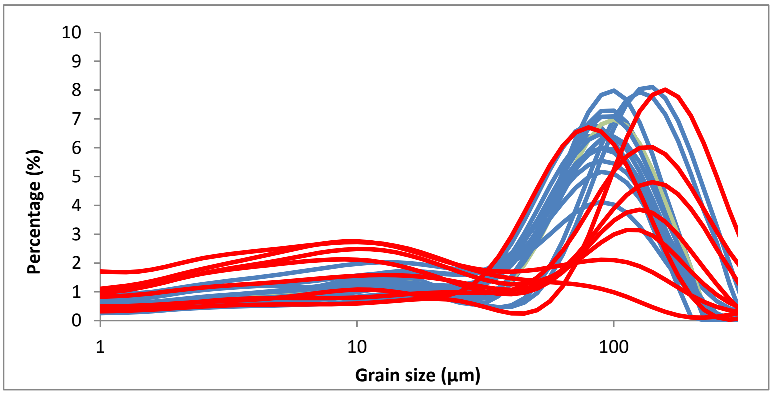

Figure 4.68: A grain size distribution plots comparing the data of section 1 of the Oued Madhouma section (red) and the data of facies association A of the Jebel Haricha section (blue).

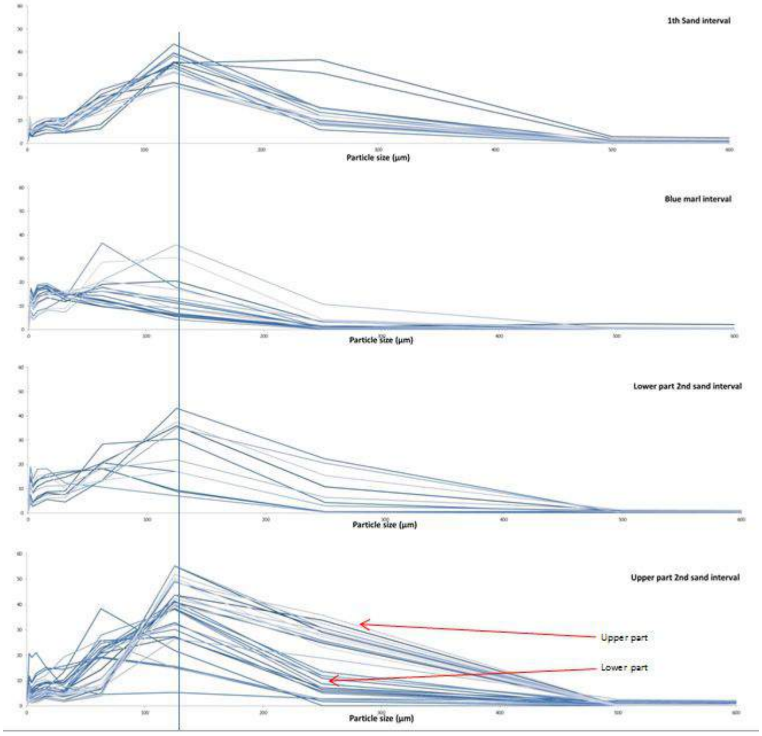

Figure 4.69: Grain size distribution curves are plotted for all the samples in the four sections (A, B, C and S). The first sand interval seems to contain finer ”coarse” material than the second sand interval. Furthermore, the top the second sand interval seems to contain more coarse material and has a more variable distribution of the curves than the sandstones of lower part of the section. All the sand sections show a fine material mode. Remarkable is the peak concentrations of grains with a size of 130 um in all sandstone sections.

The sorting parameter of Folk and Ward (1957) was used plus the simple sorting measure by Friedman (1979) to value the grade of sorting in the sandstones. The calculated sorting shows a difference between facies associations A and C; and the upper part of the section (facies association S). The upper part has better sorted sandstone beds (figure 4.57).

Next to the standard deviation the skewness is calculated to see the symmetry of the grain size distribution. Again the formulas of Folk and Ward (1957) were used to calculate the inclusive graphic skewness. The Haricha samples are positively skewed and most of them are bimodal. Medium to coarse silt is more skewed than fine silt (figure 4.57), the sandstone beds become less skewed with better sorting and has, at one point, the same value as coarse silt. The fact that fine silt has lower skewness values can be explained by the lack of the coarse mode. A scatter-plot is used to plot the process-sensitive standard deviation and skewness to get more insight in the geological processes (Friedman, 1979).

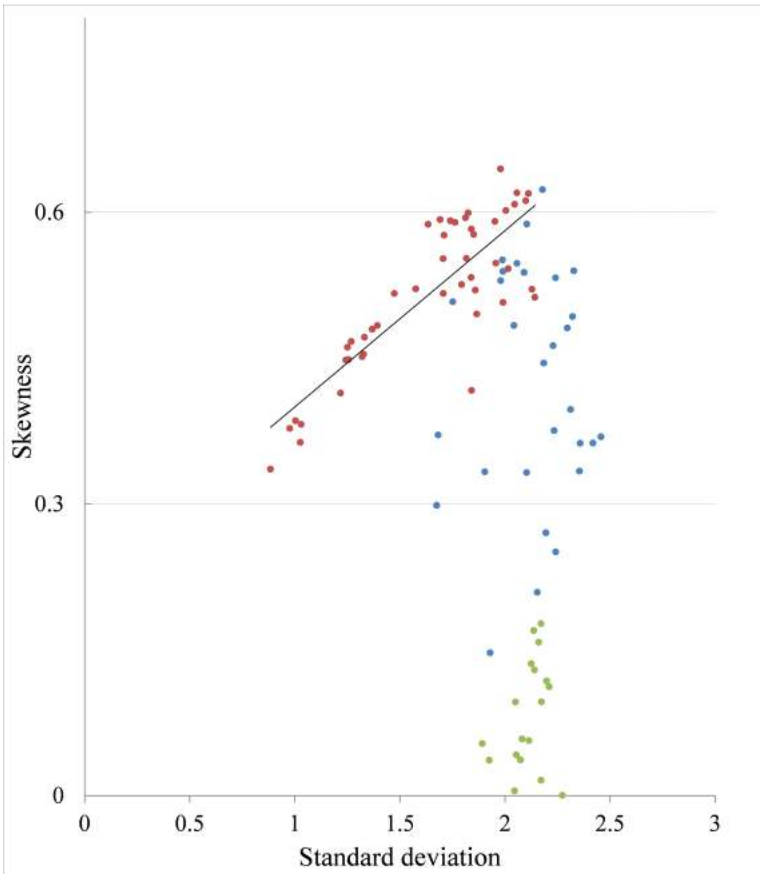

Figure 4.70: The skewness plotted against the standard deviation. Sandstone (red), coarse and medium siltstone (blue) and fine siltstone (green) samples are used. The sandstones show a logical linear trend, the more fines in the sandstone the poorer the sorting.

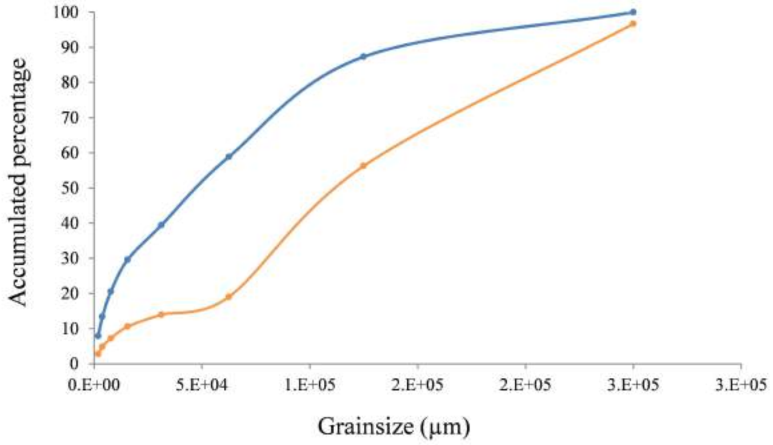

(a)

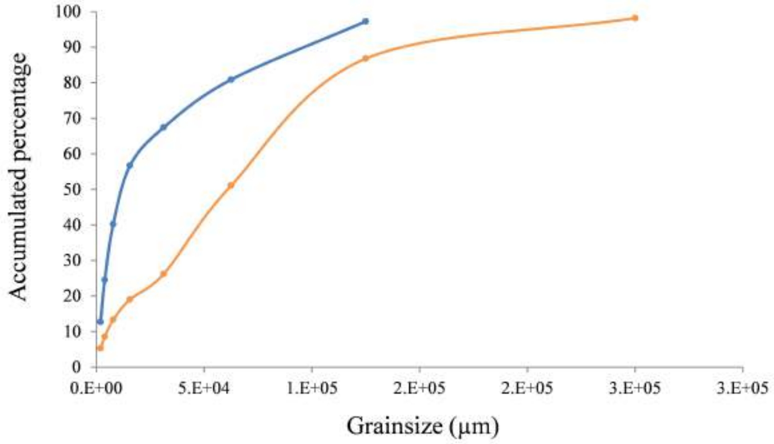

(b)

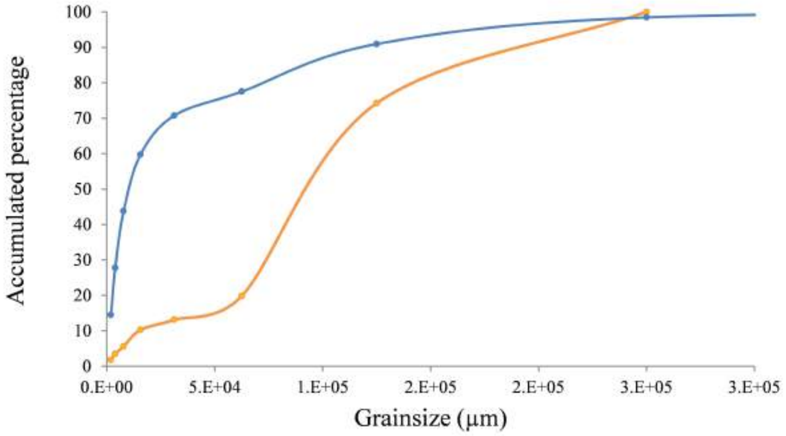

(c)

Figure 4.71: Accumulated grain size distribution curves of a representative sandstone (orange) and siltstone (blue) sample from the lower, middle and upper sandstone intervals of the Jebel Haricha section. All the sandstones seem to be bimodal.

In this section grain size data is processed in the CM plots of Passega (1964). The one percentile is plotted against the median grain size. Because the samples were measured in threefold, the data is also plotted in threefold. Sample 107, the first measured sample, seems to be subject to measuring errors.

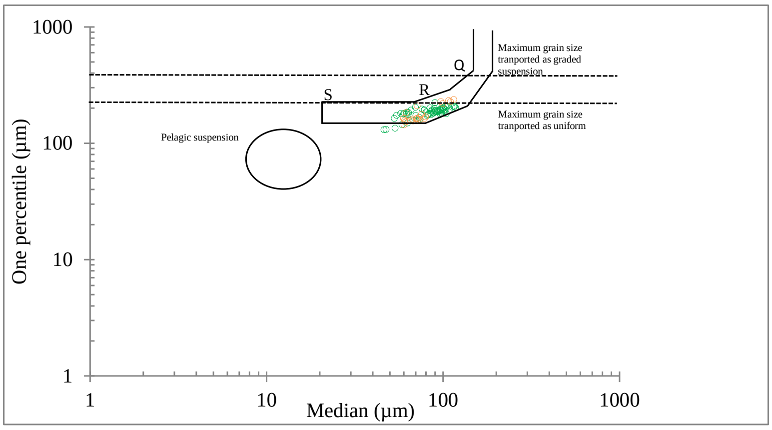

Figure 4.72: CM plot in which the grain size data of the sandstone beds of both facies association A (orange) and C (green) are plotted. The four samples from facies association A which are marked as graded suspension are all from the same sandstone bed at 10 m from the bottom of section A. It seems that the there is a trend of a decreasing one percentile and median grain size towards the top in the sandstone layers. Vice versa occurs in facies association C. They data of both facies associations are very alike.

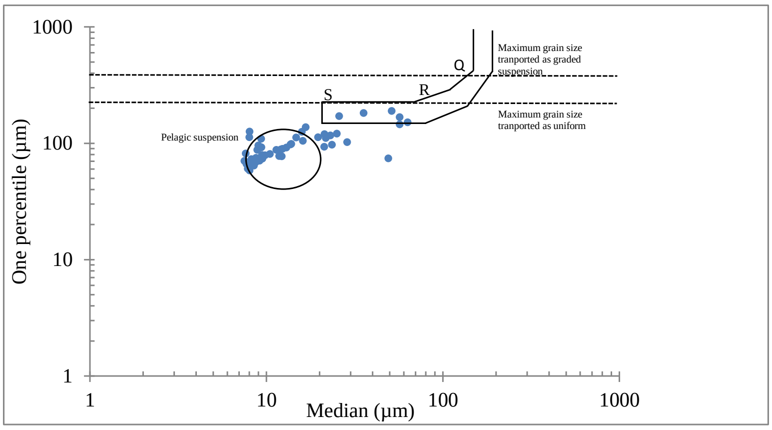

Figure 4.73: The grain size data of the marl interval is plotted in a CM plot. Some of the samples are marked as being transported in a uniform suspension. Most of the samples are plotted within the pelagic suspension section. The lower right off-trended sample seems to be a measuring error. The two other measurements of this sample are plotted in between the pelagic suspension and uniform suspension sections.

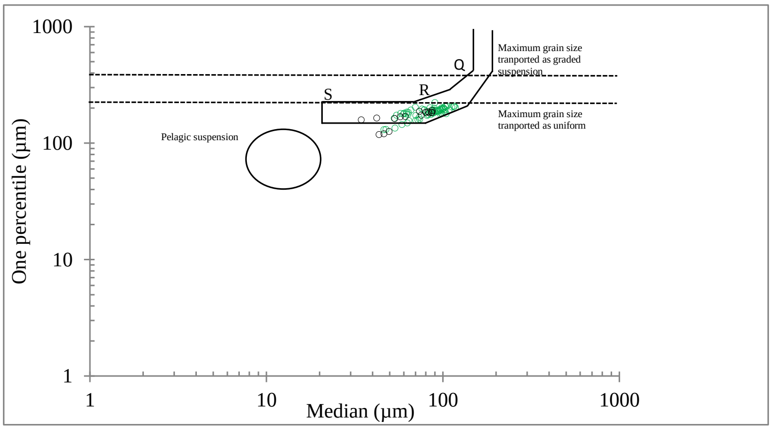

Figure 4.74: A CM plot comparing the sandstone beds of facies association C of the gulley (black) and of the roadsection (green). The data is very similar.

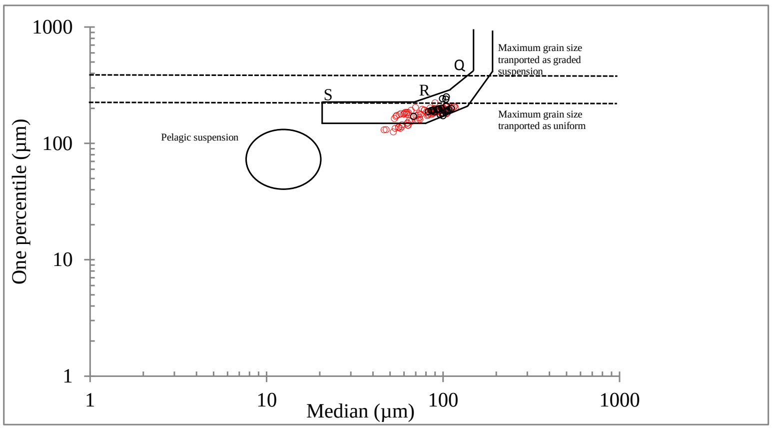

Figure 4.75: Facies assocation C is plotted with facies association S in a CM plot. The sandstone bed of the S are, in average, more orientated towards transportation in graded suspension than facies association C. S mostly overlaps samples of C.

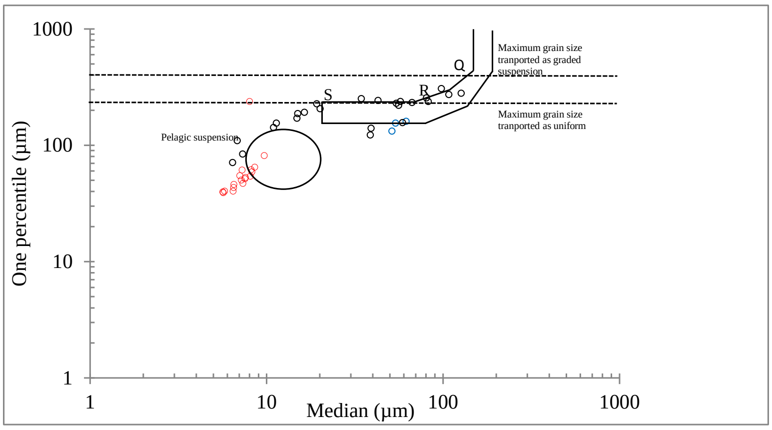

Figure 4.76: The marine facies assocation of the Madhouma section is plotted in a CM plot. The deposits of section 1 are represented by the black circles, the bottom part of section 2 is represented by the red circles and the top part of section two by the blue circles.

4.3 Facies interpretations

4.3.1 Section Jebel Haricha

Facies association A and C

This facies association is interpreted as a flysch consisting of distal turbidite deposits. Facies association A and C are interpreted, although there are differences, as one and the same facies association. Both are thus interpreted as turbiditic deposits.

The angle of deposition remained the same during the entire succession. There was no change in slope during the deposition of the Jebel Haricha section. The section was tilted after deposition. The lack of a palaeo relief and the sheet-like features (figure 5.7) point out that the turbidites are unchanneled and thus can be distinguished as lower fan (Normark, 1978) or as overbank deposits of the channelled mid and upper fan. However, because of the high sand/shale ratio and the lateral continuity, the sandbeds tend to be lower fan deposits (Ciro et al., 1988). The sheet-like deposits and lack of levees and channels are often seen in basinal turbidite fills in fore-deep settings (Mutti et al., 2003). The extent of the deposits also exclude contourites as possible deposition mechanism. It cannot be proven that the first sand interval has the same lateral continuity, but we assume that it is more or less deposited in the same setting. The thickening upward trend of facies association C could indicate the prograding of a turbidite fan (Mutti and Ricci Lucchi, 1972), sea level fluctuations or tectonic uplift. The latter two, as will be discussed in the discussion, can be excluded. Also, the sedimentation rate and thickness of the succession is presumably too high for contourite deposits.

The beds are well defined, continuous, thin bedded and regular. A characteristic of turbidites and in contrast with the often poorly defined, irregular contourites (Stow and Faugeres, 2008).

Most of the individual units have the for turbidites characteristic fining upwards grain size pattern, including the sandstone and siltstone interval (Bouma et al., 1962; Mutti and Ricci Lucchi, 1978). Generally, these fine intervals in between the sandstone beds are of a regular thickness, what corresponds to most turbiditic successions (Stow, 1985; Stow and Tabrez, 1998; Stow and Faugeres, 2008). It is unclear which part of the fines are hemipelagic and which part of turbiditic origin. However, the presence of crossbedding to at least the middle of the fine intervals point to a significant turbiditic origin of the fines.

The lower sand beds in this unit have sharper contacts, this is often seen, together with thin horizontal lamination covered with rare cross beds, in fine grained turbiditic settings (Stow and Shanmugam, 1980), the section consists of fine grained turbidites. The first sandstone interval (facies association A, underlying the marls) shows no clear erosional features like in the upper sandstone interval of this facies association (C). This could be explained by the fact that the sandstone beds of facies association C are uphill and better exposed. Both tool marks and flute casts are observed in the sandstone beds, characteristic for respectively thinner and thicker turbidite beds. The flute casts are indeed observed in the thicker beds (figure 4.32). In the upper part of the facies association the sandstone beds begin to show extensive parallel lamination and wavy features. The undisturbed horizontal lamination is a characteristic of sandy turbidites. Furthermore, the sandstone beds in the upper part of the succession have more similarities with the Bouma sequence (Bouma et al., 1962). It can be concluded that the turbidites become more mature/developed towards the top of the succession. The palaeocurrent direction in fore-deep setting is mostly oriented parallel to the axis of the basin (Mutti et al., 1999, 2003). The palaeocurrent indicaters in the sandstone beds, which point to a SW palaeo-current direction, support this idea.

The extensive bioturbation in this facies association is in line with turbidite or turbidite-like deposits. The concentration of bioturbation near the top of the individual sandstone beds is a specific turbiditic feature (Stow, 1985; Stow and Tabrez, 1998; Stow and Faugeres, 2008). This feature is present throughout the entire succession of this facies association.

The decreasing average grain size in section A of this facies association is coeval with the fading of the sandstone deposits into marls.

Until, the sandstones of this facies association emerge again in section C, where the grain size gradually increases again. The fact that A and C have similar depositional mechanisms indicate that the waning of the sandstone units could be explained by one or a combination of the following mechanisms:

- Gradual decrease followed by a gradual increase of sedimentation
- Deepening of the basin followed by infill and/or uplift of the basin
- Decrease and increase of bottom current strength

The distribution curves of the first (A) and the second (C) sandstone interval of this facies association are, as well as the grain size, similar. This supports the idea that they are of similar origin.

The positively skewed fines and sands are characteristic for the sandstone beds in the Jebel Haricha section indicating high fine content in the beds. Mutti et al. (2003) indicated that turbiditic systems in foredeep basins are marked, firstly, with an high percentage of fines mixed in the turbidites. These fines are accumulated due to the erosive power of the turbidites, which moved at high velocities through their conduits. Contourites are rather marked by negatively skewed sandstone units due to the waning effect of the continuous currents (Stow, 1985; Stow and Tabrez, 1998; Stow and Faugeres, 2008). Secondly, large amounts of highly efficient currents are needed to create the lateral continuous deposits as seen in the Jebel Haricha section. The similarities of the petrography of the first and second sandstone interval shows that the provenance area is probably the same.

As indicated before, the benthic assemblage shows a deepening upward trend throughout this facies association. This means that probably the start of the second sand interval (c) is not triggered by sea level fluctuations but by the onset of tectonic activity in the hinterland. This supports the theory of a prograding turbidite system. Note that the input of cold bottom waters could have influenced the palaeo-depth interpretation (see discussion).

CM plots point out that the sediments were transported in an uniform suspension. Whilst average turbidites are mostly transported in graded suspension. Sediments located under the Cu line are too fine to be transported as a graded suspension or rolled. In present seas graded suspension are rare. This is due the fact that sediments are mainly fed by rivers, supplying fines. These are than transported in uniform flows (Passega, 1964). It must be said that sediments transported in uniform suspension are not likely to be influenced by gravitation due to their low concentration. I suggest that the outermost deposits of turbidites behave as sediments in uniform suspension. Although the density is low, some of the initial inertia is kept by the sediments when most of the coarser fraction of the sediment is already deposited. These remaining sediments might behave as in uniform suspension.

Facies association B

The fine, somewhat concave organized marls are interpreted as a low energetic deep water environment deposits. This idea is supported by, firstly, the grain size, which shows an average larger than 6 phi, there are however some outliers with coarser grain sizes. The average grain size drastically decreases from the sandstone/silt interval underlying this facies association (facies association S). Secondly, the fossils found in this section indicate a deepening and/or decrease of depositional energy. The analysis of the micro-biostratigraphy supports this idea, and shows a deepening trend from the sandstone/silt interval (A) towards the marls. The skewness, which is just above zero, shows that the influence of the turbidites is is much lower than in facies association A and C. The fact that the coarser intervals in this section are also positively skewed possibly indicate persistent influence of the turbiditic currents. In figures 5.7 and 5.7 the distribution curves of the coarser intervals in the marls can be compared with the distribution curves of the sandstone beds of section A and C. The similarities support the idea that the turbiditic system never came to a halt during the marl interval, but only diminished. Not enough data was obtained to link these intervals to specific events.

Facies association S

This facies association is interpreted as a more proximal continuation of the underlying basinal turbidite sheets. Turbidite lobe deposits which are influenced by an undetermined amount of bottom currents. Due to the similarities between fine grained turbidites and its reworked contourite deposits, the influence of bottom currents cannot determined.

It is possible that this facies association is eroded or covered with soil at other locations. However, the highly indurated sandstone deposits hint to less extensive lateral deposition compared to the sheet deposits of the underlying facies association. This due to the fact that they are indurated and the sequence is too thick to be completely buried over multiple kilometers. The gradual transition from the underlying facies association to thicker sandstone beds and thinner fines could indicate the logical follow-up of higher energetic lobe deposits of the turbiditic fan. In contrary, the onset of contourites would be marked as an abrupt shift in facies, cutting into the turbidite sequence.

The gradually thinning of the fine deposits in between the sandstone units can be caused by removal and/or non-deposition. Together with the coeval thickening of the sandstone beds, it supports the idea of a higher energetic environment. A logical follow-up of the underlying more distal turbidite deposits.

The fact that the bottoms of the sandstone beds are not exposed in this part of the succession could explain the lack of observed flute and load casts, which are often used to distinguish contourites and turbidites (Stow and Faugeres, 2008). Only a 2-D vision across the beds is allowed.

Mud clasts are formed by cohesive clays which are ripped up and transported as a cohesive ball as bed load. The front of a high energetic current is capable in creating mud clasts, both contourite and turbiditic currents are thus capable of forming mud clasts.

The observed small-scale horizontal lamination and cross-bedding are both recognized as divisions of the Bouma sequence (Bouma et al., 1962), and could, in addition to turbidites, also occur in contourites (Stow and Faugeres, 2008; Shanmugam et al., 1993). Channel features are common in the sandy lobes of turbidites (Stow, 1985). The straight sharp bottom contacts of the sandstone beds could hint to either rapid sedimentation or minimal grain size differences. Shanmugam et al. (1993) notes that a distinction between turbidites and contourites can possibly be made by the comparing the organization within the individual units. He states that contourites have no organized vertical sequence within individual beds whilst turbidites are marked by the organized Bouma sequence. Most of the beds in this part of the section show relatively organized build-up. Note that in this part of the section the outcrops are not great and that sedimentary structures were hardly or not recognized (figure 5.7). Besides, cross-lamination is only rarely present in silts and fine sands, and slightly more common in medium to coarse-grained sands (Stow and Faugeres, 2008). The straight or wavy bottoms often with mud clasts are followed by horizontal lamination. The cross bedding is often seen next or above the horizontal lamination.

The more energetic depositional nature of the lobe deposits explains the decrease in biological activity throughout the sediments. The decrease in the rate of bioturbation is explained by the increased deposition of sand. Bioturbation in turbidites is mostly described as episodic, concentrated near the tops of beds, small scale, sometimes absent, rarely destroys all structures. In contrary, bioturbation in contourites is often described as continuous and intensive throughout the sequence and often destroys primary structures (Stow, 1985; Stow and Tabrez, 1998; Stow and Faugeres, 2008). Comparing this with the characteristics of this facies association, one can conclude that the former is most applicable. Nonetheless, Shanmugam et al. (1993) state that the rate of bioturbation is no distinguishing factor by showing bioturbation free contourites.

Bi-directional palaeo-current indicators can occur in contourite settings, and not in uni-directional gravitional flows as in turbidites (Stow and Faugeres, 2008). The occurrence of bi-directional palaeo-currents in this section is, however, limited to a single, uncertain observation. Furthermore, the beds were badly exposed in this part of the section which permitted a 2D view on palaeo-current indicators. Conclusion based on palaeo-currents indicators in this part of the section must, therefore, be factored with caution. Additionally, lack of of clear tidal related structures makes tidal influences unlikely.

One characteristic of pro-grading lobe deposits is the shift in the angle of deposition observed in the field. This facies association complies to this. A sandy lobe complex represents a stacking of nested sedimentary bodies, in which flows evolve in a complex manner. Numerous onlap, toplap and downlap surfaces are observed inside the lobe deposit. The lobe deposit is built by numerous individual events (Gervais et al., 2006). This also explains some of the top-, fore- and bottom sets observed in the field.

The influence of contourite driven depositional mechanisms can not be entirely excluded. Figure 4.57 shows that a part of this facies association is marked by a coarsening upward trend within a single bed. This is not likely formed by gravitational driven currents, but is rather formed under the influence of bottom currents (Stow, 1985; Stow and Tabrez, 1998; Stow and Faugeres, 2008). As an alternative explanation: according to (Mulder et al., 2001) there are turbidites with coarsening upwards grading patterns. They originate from hyperpycnal flows with fine sediments coming from rivers during floods.

The grainsize analysis shows that the skewness of the sandstone beds is similar as in the sandstone beds of the underlying facies association. The positive skewness is a feature commonly seen in turbiditic settings as is explained in interpretation section of facies association AC. It is thus unlikely that these sandstone beds are entirely formed by a contourite system. The effect of marine gateway driven bottom currents must be observable in the form of coarse lag deposits (Stow and Faugeres, 2008). This facies association does not have this feature. In fact it shows positively skewed sediments with a high fine content.

The CM plots of this facies association shows similar results as the underlying facies associations, if the distribution curves and the CM plots of this facies association are compared with the distribution curves and the CM plots of the underlying facies association they seem to be similar. This is logical if it were deposited in a similar turbiditic setting.

If bottom currents have deposited or influenced the deposition of the sandstones, they had no influence on grain size distributions. This is unlikely.

Not only can the coarsening upward trend in the section be explained by a prograding system, but also by tectonic uplift. Tectonic uplift increases the slope into the basin. It is known that the angle of deposition remained constant throughout the deposition of the section and thus it is known that tectonic uplift did not have a direct influence on grain size. However, an increased slope can also drastically increase the energy potential of gravity driven currents. Thus increased slopes near the origin of the turbidite system could potentially cause a grain size increase throughout the succession.

Since, as discussed, both fine grained turbidites and contourites have very similar features, must we rely on the sequence, grain size trend and the grading in the individual beds to suggest that this facies association is deposited by means of gravitational driven currents.

A prograding turbiditic model is verified by (Flinch, 1993), in which is stated that the Rifian corridor is subject to prograding deltaic systems. As mentioned before, river systems are necessary to produce the large volume highly efficient gravity driven deposits seen in facies association AC. The progradation explains the coarsening upward trend and eventually the depositional environment of facies association S. Also it supports the idea of hyperpycnal flows originating from rivers. This idea is also supported by the CM plots (see interpretation facies association a/c).

East to west bottom currents prevailed during Messinian times. An event with enhanced flow velocities occurred from ± 6.3 ma, possibly driving the oceanic psychosphere into the (southern) marine corridor (Benson et al., 1991). One possibillity is that the onset of this increase in flow velocity was coeval with the depostion of this facies association. However, although the observed palaeo-current indicators are not exactly recorded, a southern trend is recognized. The location of the section makes it unlikely that gateway driven bottom currents have caused the deposition of this facies association.

However, it must be said that influences of currents can not be ruled out. Small tidal and bottom currents could definitely have influenced deposition, observed in the form of bi-directional palaoe-current indicators and coarsening upward grading of individual beds. It can be concluded that a major depositional mechanism in the form of bottom currents driven through the marine gateway are unlikely. And therefore I would suggest a turbiditic system with only minor influences of bottom currents.

Conglomerates on top of section

It looks as if the deposits did not entirely lithify when becoming subject to deformation. This is a characteristic of the Villa franche formation (Flinch 1993). That is found in the area: an alluvial continental deposit. This confirms that there was an area of none or continental deposition after the emplacement of the rides prerifaine.

4.3.2 Section Oued Madhouma

Facies association X

This marly to silty facies association is interpreted as a deep marine deposit. This is mainly based on the fine grain sizes and the thickness of the complete package of deposits. The coarser intervals could indicate a similar turbiditic system as is seen in the Jebel Haricha section. The similar bimodal grain size distribution curves support this idea. This is in agreement with the fact that there is no clear grain size trend in this facies association; an alternation of coarser and finer material is probably caused by a turbiditic sequence.

Facies association Y

This facies association interpreted as lacustrine deposits. A mixture of insitu formed bioclasts and extraclasts, which are transported from the Atlas or Rifian mountain range and deposited in the lake during mass-flow events.

The bottom layer of the conglomerates contains mainly angular limestone extraclasts. Because it is known that limestones erode easily, one can conclude that the source area was nearby. To be more specific: the Jurassic limestone sequence in the Atlas mountain chain. The extraclasts settled on the bottom of a sink, in this case a lake, together with fine lime sands. Apparently, the transportation energy lowered from transporting ± 20 cm clasts to an energy in which sand settles. This indicates deposition in the form of events.

The carbonate tubes have been interpreted by Tucker and Wright (1990); Platt and Wright (1992); Garcia and Chivas (2006) as Charophytes. Specifically, in this case their family branch Characae; genus Chara, which are both macroscopic green algae. They take-up an important role in the littoral zone flora of carbonate rich, fresh or brackish water, lakes. They live up to 12 meter depth and their stems can reach 2 meters in length and they easily calcify through extra-cellular coating (Anadon et al., 2000). Thus, they easily fossilize due to the biomineralization by calcium carbonate (Anadon et al., 2000; Martin-Closas and Dieguez, 1998).

Normally charaphyte fossil assembleges contain gyrogonites and thallus (Kropelin and Soulie-Marsche, 1991). The lack of gyrogonites in the matrix and the lack of texture on the surface of the stems in this facies association correspond to the lime sand found in present lakes (e.g. Lake Ganau, Khanaqa et al. (2013)). Figure 4.77 shows newly formed lime sand and older more weathered sand from lake Ganau. The latter corresponds to the lime sand we found in the (conglomeratic) detrital limestones. The lime sand must have been trapped in between the incoming extraclasts from the Atlas mountains or the rides prerifaine.

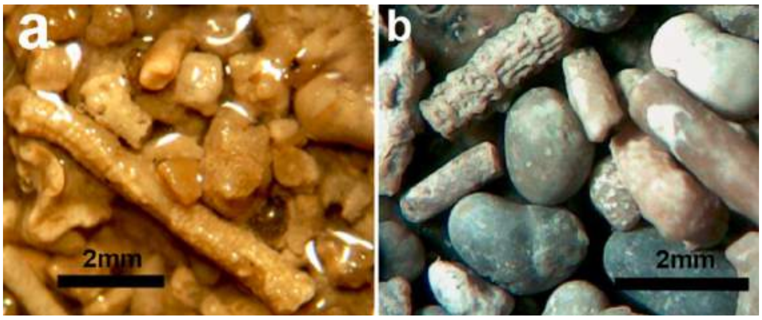

Figure 4.77: A. Freshly formed bioclasts. B. A mixture of fresh and weathered bioclasts. Both found in present day lake Ganau, Irak. Image modified after Khanaqa et al. (2013).

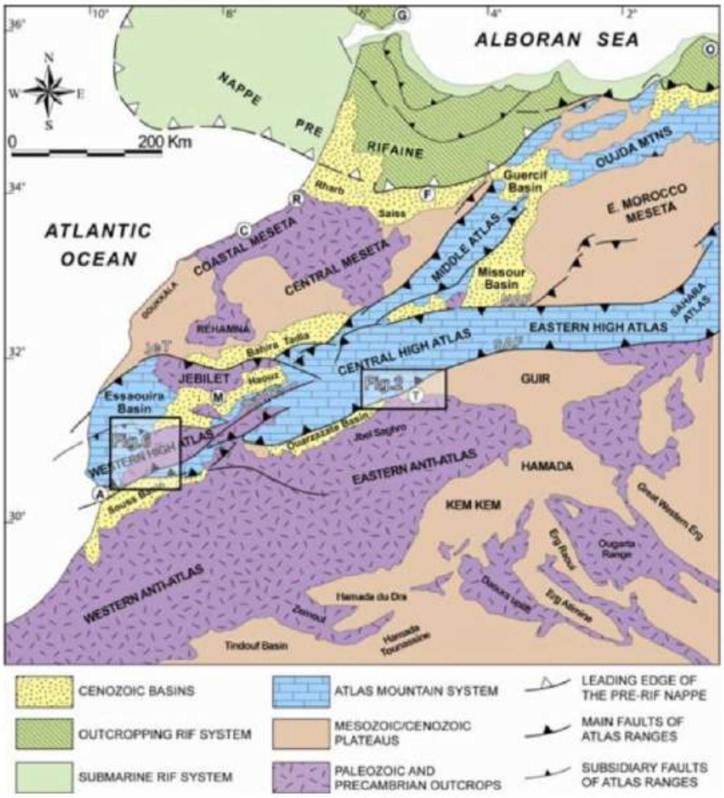

Figure 4.78: Geologic map indicating the locations of the limestone formations of the atlas mountain range.

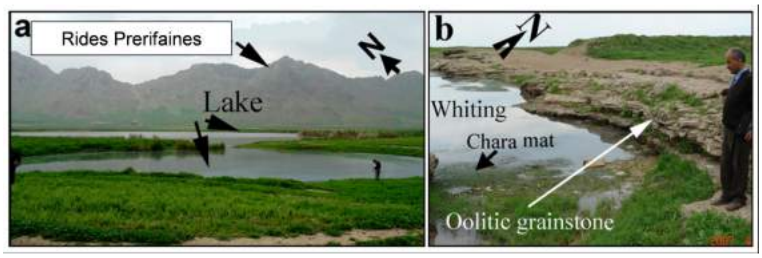

Figure 4.79: Representation of how the lacustrine environment at the Oued Jedida section could look like. With oolithic grainstones and chara mats in shallower water and conglomeretic units, originating from the Rifian or Atlas mountains, in the middle of the lake. Image modified after Khanaqa et al. (2013)

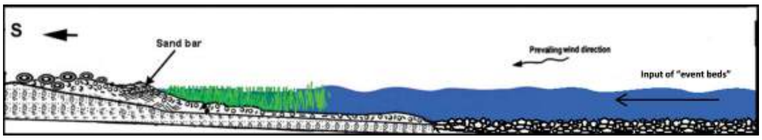

Figure 4.80: A cross-section of the possible lacustrine environment of the Oued Jedida section. The cross-section is composed of cross bedded ooilites; characea in shallow-waters (green), oncolites as top unit onshore and, bioclasts and ooids throughout all the deposits. The deeper parts of the lake are filled with conglomeratic units. Image modified after Khanaqa et al. (2013)

Because ± 70% of the extraclasts consist out of limestone, one can assume that the water load was (super)saturated with CaCO3 via the dissolution of calcium carbonate in the source area. This fits with the idea that the source area is located in the Jurassic limestone sequences of the Atlas mountain range or the rides Prerifaine. The lake is feeded by the Mesozoic-Cenozoic succession, which is 700 m thick. A part of this succession comprises of conglomerates composed of Jurassic limestone clasts ((Ellero et al., 2012), figure 4.78).

The occurrence Characae does not only indicate calcium carbonate rich water, they are mainly present in carbonate rich freshwaters (Khanaqa et al., 2013). Together with the cyanobacteria they positively influence precipitation of carbonate via photosynthesis (Merz-Preiss, 2000; Riding, 2000). This high level of carbonate content results in the carbonate coating of clasts as is seen in the field today.

The ooid beds and the oolithic grainstone beds resemble the microfacies found in present-day lake Ganau (Khanaqa et al., 2013), in high energy environments the ooids can accumulate to form a near shore bench (Swirydczuk et al., 1979, 1980). Although the succession is not entirely clear, it seems that these grainstone and ooid beds are succeeded by stromatolite features (Figure 34, Figure 37 and Figure 39). These stromatolites have been interpreted as being formed in a similar process of the originally microbial ooids. Figure 4.80 shows the possible sequence of the Mahdouma section with in the deeper parts of the lake the mixture between extraclasts and lime sand, this is followed by the shallow lake/lake edge deposits of ooids and grainstones.

Besides the Chara's lake Ganau also contains Ostracods and Gastropoda shell remains, this is also in agreement with the deposits of the Mahdouma section. Crossbedding and the combination if ooids and algal ooids indicate high energy environment with basinward progradation. The deposits must be close to the source area due to angularity limestones, limestones tend to erode relatively fast.

4.4 Bio-stratigraphy

4.4.1 Planktonic foraminifera

The presence of Gl. Miotumida group, whose first regular occurrence is at 7.24 Ma, throughout the entire section shows that the sedimentary succession belongs to the Messinian stage. The Gl. Miotumida group is continuously present throughout all the section, but its abundance varies in the subsections. In the bottom part of the Jebel Haricha section the occurrence is in traces, it becomes common after 44 m of stratigraphic thickness, and abundant by the base of facies association C. However, the abundance start decreasing at the top of the section, 30 m below the top of facies association S. Neogloboquadrinids coiling direction is dominantly sinistral (sinistrally coiled), but a high number of dextrally coiled was found too. This pattern of sinistral to dextral oscillations was previously described by Sierro et al., 1993 and it is common for assemblages of the Guadalquivir basin. Usually it occurs prior to event PF5, which is characterized by a sharp decrease in Miotumida group. Gl. Scitula is very rare or absent throughout the section. However, the few specimens found showed both dextral and sinistral coiling direction. The overall assemblage found in the section Haricha indicates that the sediments are early Messinian in age. The neogloboquadrinids sinistral coiling direction suggests that the sedimentation at Haricha occurs before the change of coiling pattern PF5, dated at 6.29 in the Atlantic sections (e.g. Sierro et al., 1993). Regarding the maximum age of the section, we refer to Ain el Beida section in the adjacent Rharb (Krijgsman et al 2004), where between cycles AEB6 and AEB 9 you have dextral and sinistral neogloboquadrinids, G. scitula dominantly sinistral and G. miotumida. The age of this interval based on the astronomical tuning showed in Krijgsman et al., 2004 is between cycles AEB 6 and AEB 9, approximately 6.37 and 6.29 Ma. The assemblage of planktonic foraminifera indicates an age interval of 6.37 - 6.29 Ma. The oldest one (6.37) is more uncertain but still probable. This correspond well to a small reversed magnetic interval.

4.4.2 Benthonic foraminifera

Benthonic foraminifera assemblage from Haricha section (HA, HR, HS) is composed by deepwater species (Oridorsalis stellatus, Cibicides kullenbergi, Eggerella bradyi, Cibicides wuellerstorfi, Uvigerina peregrina, Valvuneria complanata, Cassidulina spid, Globobulimina) Presence of deeper infaunal Nonion bethealum only in the HS samples indicates a deepening up of the Haricha succession. This assemblage is characteristic of upper slope deposits (300 to 500 m) with a possible deepening by the base of HS. Error bars These results are obtained from a limited number of samples. The interpretation of age and paleoenvironments are therefore preliminary.

Chapter 5

Discussion

According to the bio-stratigraphy and magnetostratigraphy, the Jebel haricha section was deposited approximately between 6.37 and 6.29 Ma during the middle of the Messinian. It is known that the locations of both the Jebel Haricha and the Madhouma sections are located in the fore-deep basin formed by the Rif mountain range (see geologic setting) during this time.

Figures 5.1 and 5.2 Flinch (1993) give an overview of the depositional environments during respectively the Late Tortonian and the Messinian in the fore-deep. According to Flinch (1993) the Jebel Haricha and the Oued Madhouma sections were located in a deeper part of the fore-deep basin during the Late Tortonian.

Although factual data about the palaeo-current direction is lacking, a south-western palaeo-current direction is recognized in facies association A/C. Figure 5.1 shows the depositional environments until the emplacement of the 'Rides Prerifaine'. This figure supports the idea of a source area located in the north east. Note that in this figure the northern gateway in not incorporated. However, based on paleontologic data by Wernli (1988) collected in multiple intra-montane basins, it seems that there was a northern connection between the Mediteranean sea and the Atlantic ocean. Nonetheless, it had probably no influence on the Jebel Haricha and the Madhouma sections.

The author also mentions the occurrence of prograding deltaic systems into the fore-deep. These system can provide the high amounts of sediments needed to feed the fine grained, highly efficient and large volume turbidite systems observed in the fore-deep (Flinch, 1993; Mutti et al., 2003) and which can also be verified by our field observations. A prograding turbiditc model is verified by (Flinch, 1993), in which is stated that the Rifian corridor is subject to prograding deltaic systems. As mentioned before, river systems are necessary to produce the large volume highly efficient gravity driven deposits seen in facies association AC. The progradation explains the coarsening upward trend and eventually the depositional environment of facies association S (Jebel Haricha section). Also it supports the idea of hyperpycnal flows originating from rivers. This idea is also supported by the CM plots, which show a trend from uniform transported sediments in facies association A/C to sediments transported as graded suspension in facies association S.

Deposition of the prograding turbidite systems stops with the emplacement of the 'Rides Prerifaine', as is visualized in figure 5.2. After the emplacement of the 'Rides Prerifaine' the location at Jebel Haricha became one of non-deposition. And the Oued Madhouma section became a shallow marine environment. This is stated by Flinch (1993) (figure 5.2) and is verified by our field data.

At the location of the Madhouma section, a deep marine sequence with possibly increasing turbiditc influences towards the top is succeeded by continental lake deposits. An angular unconformity separates the two facies associations. The distribution curves of the deep marine deposits show similarities with the turbiditic deposits of the Jebel Haricha section (figures 4.68 and 4.67). Also, the thin sections of both systems seem to have identical features. It is unlikely that both sections are part of the same depositional system, the two sections are separated by ± 50 km. Nonetheless, it is possible that these parts of both sections are deposited in a similar way. It is probable that there were multiple feeding deltaic systems. No data is available concerning the age of deposition of the Madhouma section, this makes it impossible to link the Jebel Haricha and the Madhouma sections.

After the hiatus, continental deposition in the form of a lake envi-

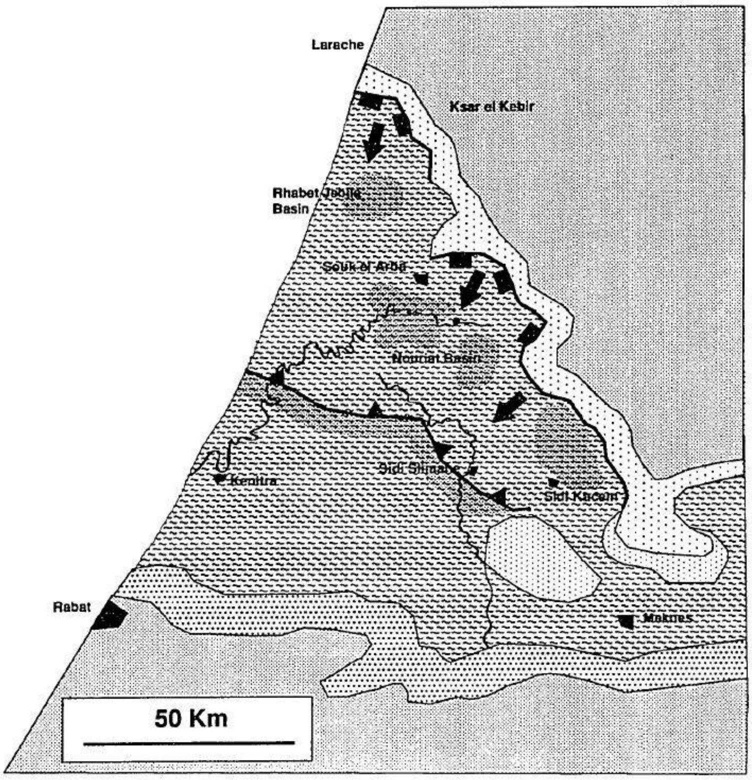

Figure 5.1: An overview of the fore-deep system during the Upper Tortonian by Flinch (1993). The black arrow indicate the direction of tectonic movement of the thrust front. The thrusting in the accretionary wedge is causing subsidence in the fore-deep. The areas north and south of the fore-deep are marked by exposure and non-deposition (gray). Dunes are deposited at the southern shoreline. A shallow water environment is present at the northern shore in the peripheral region of the Gharb basin. Excluding some sandy patches, deep pelagic facies develop, mainly marls are deposited in the fore-deep. According to Flinch (1993) the area of the Jebel Haricha section is located in a deep basin (marked with a darker colour in the marls).

ronment occurred filling up the lows of the basin. The age of the continental lake deposits on top of the deep water succession is determined. Hence, it is unknown of how much time the hiatus consists. The lake cut into the underlying layers. The resulting lateral variations explain why the sandstone deposits in the south-east are located at the same elevation as the lake deposits.

Facies in a fore-deep turbiditic system are not as straight forward as one might think. Velocity variations of turbidity currents, mainly controlled by highs and lows of the extensional system, can cause significant facies changes over short distances (Kneller and McCaffrey, 1999). Turbidite facies are marked by a decrease in grain size down stream as is also seen in the facies described by (Lowe, 1982; Mutti et al., 1999). One can therefore say that the distance to the source increased at the bottom of the Jebel Haricha section and later increased. Also, it is clear that tectonic activity enhances sediment influx and is possibly even needed to create a turbidite system with the characteristics seen in the Jebel Haricha section (e.g. turbidite traceable over multiple kilometers without significant thickness changes and the formation of lobe deposits).

The reason of the fluctuating presence of the tubiditic systems in both the Jebel Haricha and the Oued Madhouma section is discussed in the following section. First, varying supply of sediment by rivers could influence the amount of sediments transported down the basin floor. In this situation, a fore-deep basin, it is likely that the sediment influx by rivers is controlled by tectonic activity. Although more tectonic activity will enhance exhumation and thus sediment supply, it will not directly effect the travel distances of the turbiditic flows over the basin floor; only the frequency of the turbidites. Another possibility is replacements of the depocentre of the turbiditic lobe. This is unlikely because of the gradual nature of the transition, lobe replacement would be marked as an abrupt transition. Another factor are bottom currents. Bottom current intensity can have great influence on the reach of turbidites, there are however no direct signs of reworked deposits. Nonetheless, the influence of currents can not be ruled out. It seems that sea level fluctuations are the most logical control on the extent of the basin floor turbidites.

In the interval of 6.37 to 6.29 ma there is an overall gradual rise of the eustatic sea level. The latter means that the environmental shallowing in the upper part of the section must be caused by other mechanisms (figure 2.5). It is thus plausible, knowing that eustatic sea level shifts were irrelevant, that the shifts in relative sea level are most likely caused by subsidence and prograding infill of the fore-deep basin.

The use of grain size statistics for the prediction of palao-environments is still subject of debate. It is shown that there are many exceptions to these empirical predictive models (e.g. Seminar (1981). Although these predictive models can not be used on their own to predict palaeo-environments, they can be used to point in the right direction. The fact that the grain size distribution results in the Jebel Haricha section (figure 4.70 and 5.4) are marked as being river deposits is not strange. Beside the fact that turbidite and fluvial systems have similar characteristics (Miall, 1989), are turbidite systems erosive and can take up great amounts of fines. Turbidite deposits could thus very well be positively skewed and poorly sorted.

Krijgsman et al. (1999) pointed out that the southern Rifian corridor at Taza Guercif, which was the main Rifian corridor, completely closed off at 6 ma and was almost closed at time of deposition in the Jebel Haricha section. It is generally agreed that the corridor closed from east to west. Age control, in the form of bio-stratigraphy, pointed out that the middle of the Jebel Haricha section was deposited around ± 6.37 to 6.29 ma. From Krijgsman et al. (1999) it can now be concluded that the corridor was almost closed in the east and that corridor was still an open marine environment in the west (figure 1.1).

East to west bottom currents prevailed during Messinian times. An event with enhanced flow velocities occurred from ± 6.3 ma, possibly driving the oceanic psychosphere into the (southern) marine corridor (Benson et al., 1991). As is mentioned in the interpretation section of facies association S; the enhanced flow velocities could have influenced the deposition of the turbidites. Besides, the influx of cold deep sea waters can have influence on the biotic fauna on the sea bottom. It is therefore possible that the paleao-depth interpretation is not correct, and that the environment was in fact much shallower.

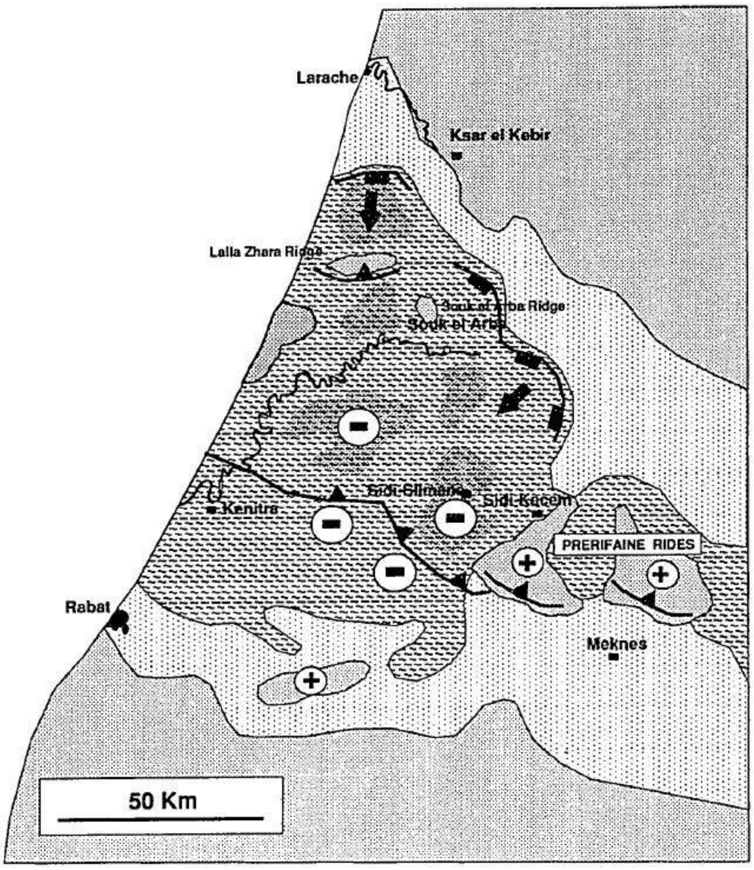

Figure 5.2: An overview of the foredeep system during the Messinian by Flinch (1993). The (+) represent uplift whilst (-) represents subsidence. The black arrow indicate the direction of tectonic movement of the thrust front. The areas north and south of the foredeep are marked by exposure and non-deposition (gray). Dunes are deposited at the southern shoreline. A shallow water environment is present at the northern shore in the peripheral region of the Gharb basin. Excluding some sandy patches, deep pelagic facies develop, mainly marls ( ), are deposited in the foredeep. The relief in the basin is caused and controlled by extensional faults. Emplacement of the Rides Prerifaine occured during the Upper Tortonian. The southern area of the Gharb basin was also lifted upwards during this time.

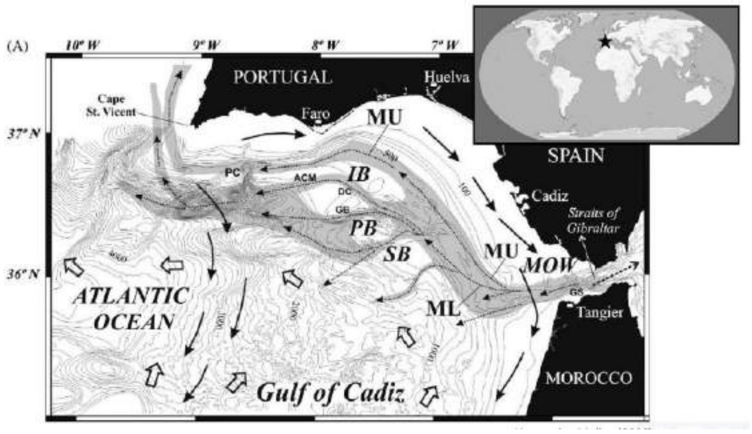

Figure 5.3: Present-day situation of contourite currents in the direction of the Gulf of Cadiz (Llave et al., 2006).

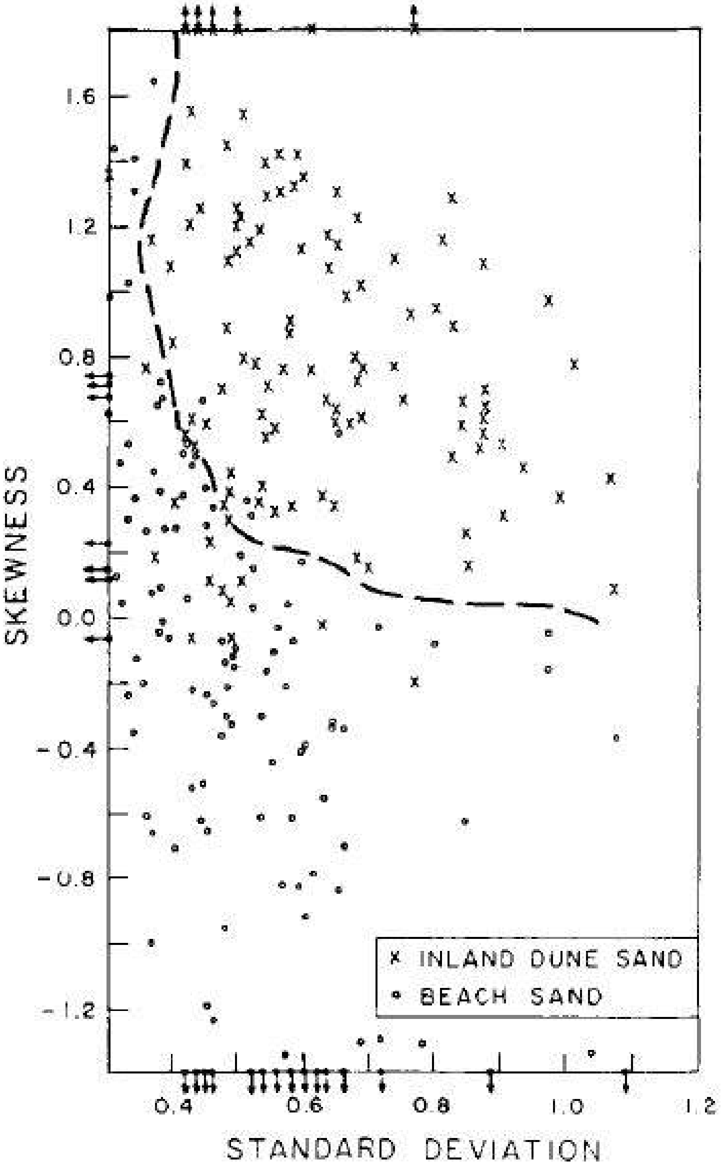

Figure 5.4: In this plot the empirical boundary between river sands and beach sands are displayed. The image from Friedman (1979). The grain size distribution results of the Jebel Haricha section (figure 4.70) can be marked as being river deposits according to this plot.

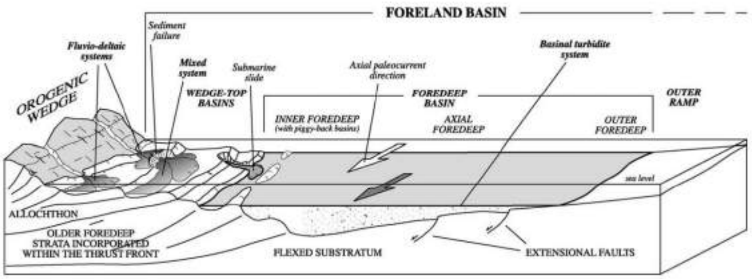

Figure 5.5: A typical foreland basin setting in which the fore-deep is filled with a basinal turbidite system. Image by Mutti et al. (2003).

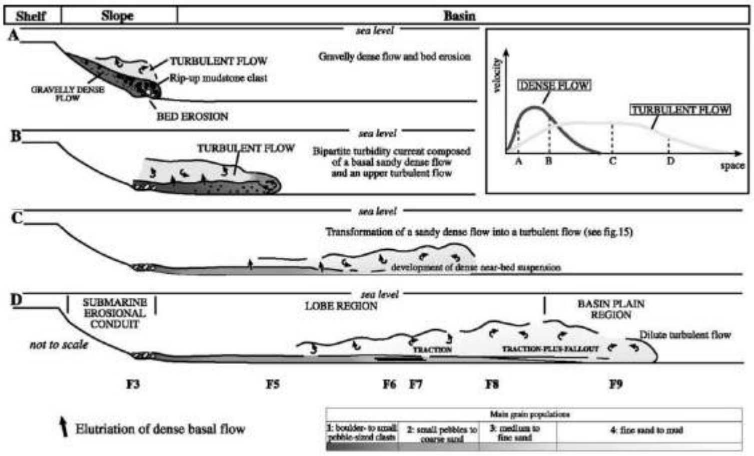

Figure 5.6

Figure 5.7

Chapter 6

Conclusion

Overall

- Deposition of the prograding turbidite systems are dominant, the influence of bottom currents are minor.
- Deposition of these prograding systems stops with the emplacement of the 'Rides Prerifaine' at the Jebel Haricha section. And that between 6.37 and 6.29 ma, that the corridor was almost closed in the east and that corridor was still an open marine environment in the west.
- It is possible that the two sections were deposited in the same marine domain, before the emplacement of the 'Nappe Perifaine'.
- Tectonic activity related to loading occurred around 6.37 ma.
- These sections do not give more insight in the closure of the marine corridor, they give no indication whether the corridor was open or closed.
- The Jebel Haricha section shows, however, that just before or during closure of the corridor in the east the western area of the corridor was marked by active sedimentation in an open marine environment. Which is dominated by flysch deposits and not particularly bottom currents.

Jebel Haricha section

- The Jebel Haricha consists entirely of turbidite deposits.
- Fluctuation in the depositional regime are caused by both tectonics and progradation.
- The assemblage of planktonic foraminifera indicates an age interval of 6.37 - 6.29 Ma for the Jebel Haricha section.
- Near the top of the section, in facies association S, there are parts that were subject to increased bottom currents. Which is in correspondence with enhanced bottom flows through the marine corridor.
- After the emplacement of the 'Nappe Prerifaine' the area was subject to non-deposition.

Oued Madhouma section

- The Oued Madhouma section is marked by the deposition of deep marine deposits, followed by increasing influences of turbidite systems.
- The marine deposits are followed, after an angular unconformity, by continental lacustrine deposits. Because this section was not dated it remains unclear if there is a hiatus in between. And if there is a hiatus: what the extent of the hiatus is.

Bibliography

Anadon, P., Utrilla, R., and Vazquez, A. (2000). Use of charophyte carbonates as proxy indicators of subtle hydrological and chemical changes in marl lakes: example from the miocene bicorb basin, eastern spain. *Sedimentary Geology*, 133(3):325–347.

Andrieux, J. (1971). *La structure du Rif central: etude des relations entre la tectonique de compression et les nappes de glissement dans un troncon de la chaine alpine*, volume 235. Editions du Service geologique du Maroc.

Author, U. (2015). Unknown title. *Unknown Journal*.

Balanya, J. and Garcia-Duenas, V. (1987). Les directions structurales dans le domaine d'alboran de part et d'autre du detroit de gibraltar. *Comptes rendus de l'Academie des sciences. Serie 2, Mecanique, Physique, Chimie, Sciences de l'univers, Sciences de la Terre*, 304(15):929–932.

Benson, R. H., Bied, R.-E., Bonaduce, G., et al. (1991). An important current reversal (influx) in the rifian corridor (morocco) at the tortonian-messinian boundary: The end of tethys ocean. *Paleoceanography*, 6(1):165–192.

Bouma, A. H., Kuenen, P. H., and Shepard, F. P. (1962). *Sedimentology of some flysch deposits: a graphic approach to facies interpretation*, volume 168. Elsevier Amsterdam.

Brahim, L. A. and Chotin, P. (1984). Mise en evidence d'un changement de direction de compression dans l'avant-pays rifain (maroc) au cours du tertiaire et du quaternaire. *Bulletin de la Société Géologique de France*, (4):681–691.

Comas, M., Platt, J., Soto, J., and Watts, A. (1999). 44. the origin and tectonic history of the alboran basin: insights from leg 161 results. In *Proceedings of the Ocean Drilling Program Scientific Results*, volume 161, pages 555–580.

Covey, M. (1986). The evolution of foreland basins to steady state: evidence from the western taiwan foreland basin. *Foreland basins*, pages 77–90.

Ellero, A., Ottria, G., Ouanaimi, H., and Malusà, M. G. (2012). *Structural geological analysis of the High Atlas (Morocco): evidences of a transpressional fold-thrust belt*. INTECH Open Access Publisher.

Faugeres, J.-C. (1978). *Les Rides sud-rifaines: Evolution sedimentaire et structurale d'un bassin atlantico-mesogeen de la marge africaine*. PhD thesis.

Flecker, R., Krijgsman, W., Capella, W., de Castro Martíns, C., Dmitrieva, E., Mayser, J. P., Marzocchi, A., Modestu, S., Ochoa, D., Simon, D., et al. (2015). Evolution of the late miocene mediterranean–atlantic gateways and their impact on regional and global environmental change. *Earth-Science Reviews*, 150:365–392.

Flinch, J. and Bally, A. (1991). Extensional collapse in an accretionary complex: Gibraltar arc (western mediterranean). In *Geological Society of America Abstracts with Programs*, volume 23, page A130.

Flinch, J. F. (1993). Tectonic evolution of the gibraltar arc. *Rice University, Houston, Texas*, 381.

Flinch, J. F., Bally, A. W., and Wu, S. (1996). Emplacement of a passive-margin evaporitic allochthon in the betic cordillera of spain. *Geology*, 24(1):67–70.

Folk, R. L. and Ward, W. C. (1957). Brazos river bar: a study in the significance of grain size parameters. *Journal of Sedimentary Research*, 27(1).

Friedman, G. M. (1979). Address of the retiring president of the international association of sedimentologists: Differences in size distributions of populations of particles among sands of various origins. *Sedimentology*, 26(1):3–32.

Garcia, A. and Chivas, A. R. (2006). Diversity and ecology of extant and quaternary australian charophytes (charales). *Cryptogamie. Algologie*, 27(4):323–340.

Gervais, A., Savoye, B., Mulder, T., and Gonthier, E. (2006). Sandy modern turbidite lobes: a new insight from high resolution seismic data. *Marine and Petroleum Geology*, 23(4):485–502.

Hodell, D. A., Benson, R. H., Kent, D. V., Boersma, A., Bied, R.-E., et al. (1994). Magnetostratigraphic, biostratigraphic, and stable isotope stratigraphy of an upper miocene drill core from the sale briqueterie (northwestern morocco): A high-resolution chronology for the messinian stage. *Paleoceanography*, 9(6):835–855.

Khanaqa, P. A., Karim, K. H., and Thiel, V. (2013). Characeae-derived carbonate deposits in lake ganau, kurdistan region, iraq. *Facies*, 59(4):653–662.

Kneller, B. and McCaffrey, W. (1999). Depositional effects of flow nonuniformity and stratification within turbidity currents approaching a bounding slope: deflection, reflection, and facies variation. *Journal of Sedimentary Research*, 69(5).

Krijgsman, W., Langereis, C., Zachariasse, W., Boccaletti, M., Moratti, G., Gelati, R., Iaccarino, S., Papani, G., and Villa, G. (1999). Late neogene evolution of the taza–guercif basin (rifian corridor, morocco) and implications for the messinian salinity crisis. *Marine Geology*, 153(1):147–160.

Kropelin, S. and Soulie-Marsche, I. (1991). Charophyte remains from wadi howar as evidence for deep mid-holocene freshwater lakes in the eastern sahara of northwest sudan. *Quaternary Research*, 36(2):210–223.

Llave, E., Schonfeld, J., Hernandez-Molina, F., Mulder, T., Somoza, L., Del Rio, V. D., and Sanchez-Almazo, I. (2006). High-resolution stratigraphy of the mediterranean outflow contourite system in the gulf of cadiz during the late pleistocene: the impact of heinrich events. *Marine Geology*, 227(3):241–262.

Lowe, D. R. (1982). Sediment gravity flows: Ii depositional models with special reference to the deposits of high-density turbidity currents. *Journal of Sedimentary Research*, 52(1).

Martin-Closas, C. and Dieguez, C. (1998). Charophytes from the lower cretaceous of the iberian ranges (spain). *Palaeontology*, 41:1133–1152.

Merz-Preiss, M. (2000). Calcification in cyanobacteria. In *Microbial sediments*, pages 50–56. Springer.

Miall, A. D. (1989). Architectural elements and bounding surfaces in channelized clastic deposits: Notes on comparisons between fluvial and turbidite systems. *Sedimentary Facies in the Active Plate Margin. Edited by A. Taira and F. Masuda. TERRAPUB, Tokyo*, pages 3–15.

Michard, A. (1976). *Elements de geologie marocaine*, volume 252. Editions du Service geologique du Maroc.

Monie, P., De Lamotte, D. F., and Leikine, M. (1984). Etude geochronologique preliminaire par la methode 39ar/40ar du metamorphisme alpin dans le rif externe (maroc). precisions sur le calendrier tectonique tertiaire. *Rev. geol. dyn. Geogr. phys.*, 25:307–317.

Morel, J., Gonord, H., and Cailleux, Y. (1983). Le glacis de taguelmane: un temoin du soulevement neogene de la meseta septentrionale (maroc): Comptes rendus de le academie des sciences de paris, v. 296. *Serie*, 2:477–480.

Mulder, T., Migeon, S., Savoye, B., and Faugères, J.-C. (2001). Inversely graded turbidite sequences in the deep mediterranean: a record of deposits from flood-generated turbidity currents? *Geo-Marine Letters*, 21(2):86–93.

Mutti, E. et al. (1999). *An Introduction to the Analysis of Ancient Turbidite Basins from an Outcrop Perspective: AAPG Continuing Education Course Note, No. 39*. Number 39. AAPG.

Mutti, E. and Ricci Lucchi, F. (1978). Turbidites of the northern apennines: introduction to facies analysis. *International geology review*, 20(2):125–166.

Mutti, E., Tinterri, R., Benevelli, G., di Biase, D., and Cavanna, G. (2003). Deltaic, mixed and turbidite sedimentation of ancient foreland basins. *Marine and Petroleum Geology*, 20(6):733–755.

Normark, W. R. (1978). Fan valleys, channels, and depositional lobes on modern submarine fans: characters for recognition of sandy turbidite environments. *AAPG Bulletin*, 62(6):912–931.

Passega, R. (1964). Grain size representation by cm patterns as a geological tool. *Journal of Sedimentary Research*, 34(4).

Platt, J. and Vissers, R. (1989). Extensional collapse of thickened continental lithosphere: a working hypothesis for the alboran sea and gibraltar arc. *Geology*, 17(6):540–543.

Platt, N. H. and Wright, V. P. (1992). Palustrine carbonates and the florida everglades: towards an exposure index for the fresh-water environment? *Journal of Sedimentary Research*, 62(6).

Riding, R. (2000). Microbial carbonates: the geological record of calcified bacterial–algal mats and biofilms. *Sedimentology*, 47(s1):179–214.

Roest, W. and Srivastava, S. (1991). Kinematics of the plate boundaries between eurasia, iberia, and africa in the north atlantic from the late cretaceous to the present. *Geology*, 19(6):613–616.

Rosenbaum, G., Lister, G. S., and Duboz, C. (2002a). Reconstruction of the tectonic evolution of the western mediterranean since the oligocene. *Journal of the Virtual Explorer*, 8:107–130.

Rosenbaum, G., Lister, G. S., and Duboz, C. (2002b). Relative motions of africa, iberia and europe during alpine orogeny. *Tectonophysics*, 359(1):117–129.

Sani, F., Del Ventisette, C., Montanari, D., Bendkik, A., and Chenakeb, M. (2007). Structural evolution of the rides prerifaines (morocco):

structural and seismic interpretation and analogue modelling experiments. *International Journal of Earth Sciences*, 96(4):685–706.

Seminar, S. (1981). Comparison of methods of size analysis for sands of the amazon-solimões rivers, brazil and peru. *Sedimentology*, 28(1):123–128.

Shanmugam, G., Spalding, T., and Rofheart, D. (1993). Process sedimentology and reservoir quality of deep-marine bottom-current reworked sands (sandy contourites): an example from the gulf of mexico. *AAPG Bulletin*, 77(7):1241–1259.

SINGH, G. (1988). History of aridland vegetation and climate: a global perspective. *Biological Reviews*, 63(2):159–195.

Sissingh, W. (2008). Punctuated neogene tectonics and stratigraphy of the african-iberian plate-boundary zone: concurrent development of betic-rif basins (southern spain, northern morocco). *Netherlands Journal of Geosciences/Geologie en Mijnbouw*, 87(4):241–289.

Srivastava, S., Roest, W., Kovacs, L., Oakey, G., Levesque, S., Verhoef, J., and Macnab, R. (1990). Motion of iberia since the late jurassic: results from detailed aeromagnetic measurements in the newfoundland basin. *Tectonophysics*, 184(3):229–260.

Stow, D. and Faugeres, J.-C. (2008). Contourite facies and the facies model. *Developments in Sedimentology*, 60:223–256.

Stow, D. A. (1985). Fine-grained sediments in deep water: An overview of processes and facies models. *Geo-Marine Letters*, 5(1):17–23.

Stow, D. A. and Shanmugam, G. (1980). Sequence of structures in fine-grained turbidites: comparison of recent deep-sea and ancient flysch sediments. *Sedimentary Geology*, 25(1):23–42.

Stow, D. A. and Tabrez, A. R. (1998). Hemipelagites: processes, facies and model. *Geological Society, London, Special Publications*, 129(1):317–337.

Swirydczuk, K., Wilkinson, B. H., and Smith, G. R. (1979). The pliocene glenns ferry oolite: Lake-margin carbonate deposition in the southwestern snake river plain. *Journal of Sedimentary Research*, 49(3).

Swirydczuk, K., Wilkinson, B. H., and Smith, G. R. (1980). The pliocene glenns ferry oolite-ii: Sedimentology of oolitic lacustrine terrace deposits. *Journal of Sedimentary Research*, 50(4).

Tucker, M. E. and Wright, V. P. (1990). Carbonate mineralogy and chemistry. *Carbonate Sedimentology*, pages 284–313.

Wernli, R. (1988). *Micropaleontologie du Neogene post-nappes du Maroc septentrional et description systematique des foraminiferes planctoniques*. Editions du Service geologique du Maroc.

Appendices

Appendix A

Sedimentary logs Jebel Haricha

HA

21-09-2014 22-09

1:100

Macroscopic Description

Stratigraphic Units	Photographs	Outcrop Data & Samples	Relief	Columnar Section: Compos. Texture	Structures: Trans-port Direct.	Structures: Sedimentary/ Diagenetic Structures	Bio-turb.	Additional Description	Fossil Cont.

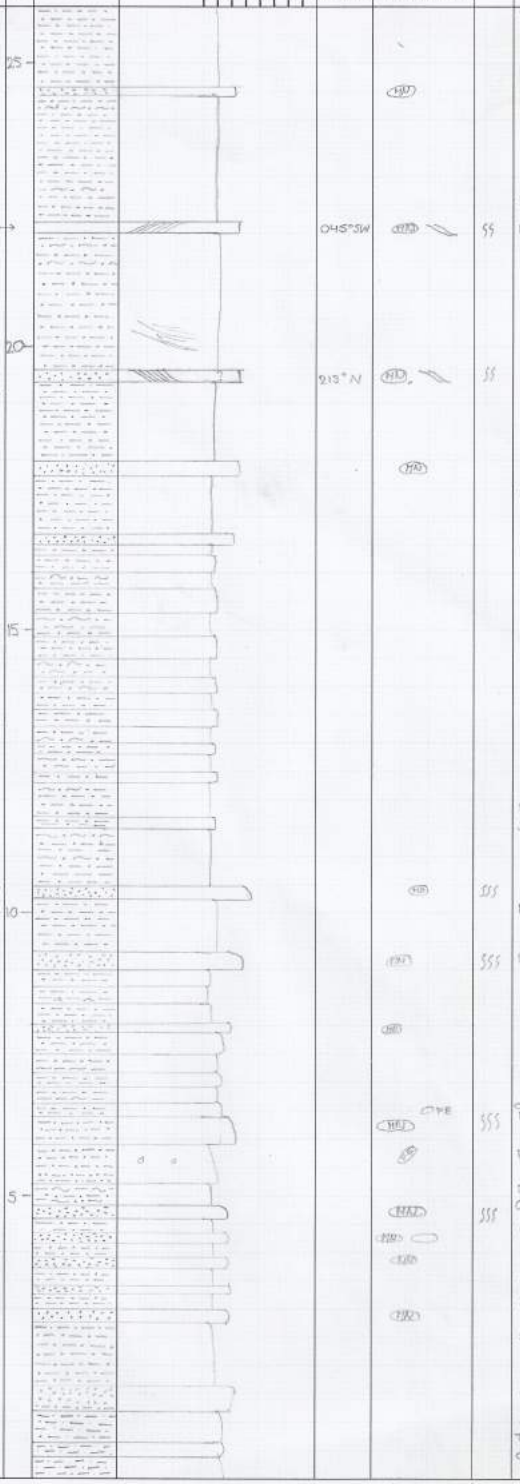

H-AB27 -

W2109 -4 H-AT22.1 AG22.1 →

BLACK STUFF GETS LARGER + MORE

↑ MORE SANDY UPWARD BROWNISH MARLS

LESS FEATURES IN TOP + SMALL BLACK LAYER IN GREYING UPWARD

045°SW — SS — MN SAME + CROSSBEDS BOTTOM SILTSTONE, GREY AND DARKER ON LAYERS. AGAIN BUT MORE BLACK OH? STAINS? • W2109-3 LAMINATED → PICT M

M14.30

38° → 290 NW

M14.25

213°N — SS

H-AB19.3 • AG19.3

LIGHT GREY, QUITE A LOT OF IRON SURROUNDED ○

APPEARS SAME AS ± 7 M

DARKER SILT LAYER, LESS ○ WITH IRON COATING

H-AB16

H-AB13.3 •

V

FINER INTERVALS ARE DARKER, ORG? MORE SILICICLASTIC UPWARD, ALSO SLIGHTLY COARSER + AGAIN ROUNDED WITH Fe COATINGS BIOTURB? HORIZONTAL

H-AG10.4 N •

SSS

H-AG10 -AB10 •

MORE WHITISH AFTER EXPOSURE IRON STAINS IN THE BOTTOM

SSS — VERTICAL BIOTURB, QUARTZ + BLACK 5%

M12.11

○ 4CM COARSER INSIDE IRON OUTSIDE BIOTURB? MIDDLE LAYER DARK + MORE CLAY ORG?

H-AB7.5 •

ALTERNATION GREY AND DARK GREY DARK GREY MORE CLAY UP TO 1CM ○ IRON OUTSIDE

M11.49 M11.51 — W2109 -2

SSS — ORANGE NODULES BIOTURBATED TOP POORLY SORTED PLANKTON + BIVALVE SHELL

M10.48

ROUNDED QUARTZ DOMINANT, RUST + 2% HEAVY BLACK

DARK CLAY + ORG?

M10.02

SSS — ORANGE + PURPLE SHELL WHITE ± mm 1 BLACK

QUITE POORLY EXPOSED ↓ M10.16

H-AB4 •

ALL Mn ACCRETION IN VF SAND.

WELL SORTED, BLACK CLASTS BIGGEST SUBANGULAR, SPHERIC.

SAME AS BELOW.

W2109 -01

38° → 310 NW ■? SAND

TA1.3 AG1.3 •

Mn BAND, POSSIBLE CROSSBEDS

H-AB1 • AG1

MORE HEAVY MINERALS TOWARDS TOP ± 4-10% BROWN MATRIX CLAY FLAKES 1% QUARTZ

MORE S1. MORE /M10. MENNO → 22-09 1 p.v. 21

HA

22-09 / 23-09
24-09

2

Macroscopic Description

Stratigraphic Units	Photographs	Outcrop Data & Samples	Relief / Columnar Section (Compos. Texture, Φ, Mud-stone, Wacke-stone, Pack-stone, Grain-stone, Bound-stone, >4 … <-1)	Trans-port Direct.	Sedimentary/ Diagenetic Structures	Bio-turb.	Additional Description	Fossil Cont.
							ALTERNATION OF LIGHT GREY SILTST. AND DARKER, SOFTER CLAY RICH SILTSTONE UP TO 53.0m	
		H-AB50,4 • AG 50.4	50					
	M16,20	H-AG48.7 •				ʃ+	LESS PUDDLE + PYRITE RASP	
		H-AB47.7 •						
						ʃ	BIOTURBATION ± 2 0.5m PERPENDICULAR TO THE BED.	
			45					
		H-AB44.5 •					MORE SANDY LOTS OF RASPBERRYS	
		H-AB43.8 •				ʃ	DARK GREY	
	M15.47 13:09				(RP)	ʃ	39° → 299 NW → MAX GRAINSIZE 1mm INDURATED LESS WELL SORTED BLACK SPOTS STILL ELONGATE, CLAY MATRIX INCREASE BLACK + MINERALS - BIOTITE 5% 1 TINY SHELL FRAGMENT, LOW CLAY CONT CARB. COATING AROUND GRAINS	± 0.5cm GLOSSY PURPLE CRUST DOTS
		H-AG41 •			(HN)		SILT → VF WELL SORTED PYRITE RASD - LESS BLACK HEAVY DARK GREY, MORE CLAY PYRITE RASPBERRY + BIOTITE	
		H-AB39.5 • AG 39.5	40			ʃ	LIGHT GREY LAYERS MIGHT BE GETTING SLIGHTLY COARSER → NOT	
					(RP)			
							HARDER LAYERS	
		H-AB37.1 •					0,5CM BIVALVE INSITU? AS USUAL, COARSER LIGHTER GREY SAME SIZE, LESS CLAY CONTENT	
			35	23° → 300 N.	28° → 270N 34° → 268N	ʃʃ ʃ	ANGULAR VF → F SAND NORMAL BIOTUB AS WELL BLACKENING UPWARD + TOWARDS FE BIOTURB WITH FINE SAND	
		H-AB34 •		350° S	(HN)	ʃʃ	AGAIN POORLY SORTED VF → F - 28° → 310 NW BLACK GRAINS MICAS AGAIN	
							POSSIBLY FAULTED AREA, SMALL OFFSETS POSSIBLY CONTINUOUS SILTSTONES. → FOR SURE ↳ APPARENT USUAL SILT.	
		H-AG29.9 •	30		(RP)	ʃ	BIOTURB ± 4CM DIAMETER	
	M16.21 M16.23	H-AB 29 • AG 29					◯ 5X5CM BLACK INSIDE IRON OUTS LOT OF IRON CONCRETIONS "HOLLOW" BROWNISH GREYISH, LESS SILICA ↓ MORE CLAY 1CM	
		H-AB26 •			(HN)	ʃ	FINING UPWARD CROSSED? MORE SANDY SILT POSSIBLE INSITU BIVALVE CLUSTER	

HA

Macroscopic Description

24-09 3

25-09

Stratigraphic Units	Photographs	Outcrop Data & Samples	Columnar Section: Relief	Columnar Section: Compos. Texture	Structures: Trans-port Direct.	Structures: Sedimentary/ Diagenetic Structures	Structures: Bio-turb.	Additional Description	Fossil Cont.

W2509 -01 M17.05 2609

H-AB76.7

BROWNISH SILTSTONE, ORGANIC COLOUR, SHELL REMAINS + FORAMS 3% SEE PICTURE.

MM IRON COATING

HIGH CLAY CONT, >1% BLACK MINERALS SOME CARB. COATED GRAINS? DARK SILTSTONE/ MARL CONCAVE FRACTURING

H-AB73.8

SHELL FRAG >5%, >5MM DARKER GREY. MORE CLAY MATRIX SOME CARB COATED GRAINS, OR FORAM.

POSSIBLY TINY >1MM SHELL FRAGMENTS LIGHT GREY SILTSTONE, SOME HEAVY MINERALS

M12.05

1,5 MM + REMAINS.

INTERVAL LESS WELL EXPOSED, SOME BEDS MIGHT BE OVERLOOKED

H-AG69.4

H-AB69

AG69

40° → 312 NW

POSSIBLE ALTERNATION IN CLAY CONT

WELL SORTED, MICAS → SMALL & UP, BLACK PYRITE RASP, BIOTURB UP TO 2 CM

→ POORLY SORTED & WHITE BLACK CONCAVE, ORANGE → PYRITE RASPB

H-AB65.7

BIOTUBE DIAMETER >1CM DARK BROWN OUTSIDE ORANGE SILTSTONE

LIGHT GREY SILTSTONE

MORE BLACK MINERALS BROWNISH ORANGE WHITE MINERALS LAMINATED?

H-AB63.4

MOST MARLY SO FAR, DARK GREY UNIFORM LAYER.

>1% BLACK MINERALS

MB

M13.07

NEW? MB

PURPLE + SHELLS → PICT

MICAS + 0,5 MM BLACK PLATE, RASPB! → WHITE SILTSTONE

H-AT61

M13.17 26/9

H-AG61

?

LENSES WITH FINE GREY SAND, ORANGE COATING, NOT PURPLE

H-AB60.5 - AG60.5

BLACK HEAVY ROUNDED MINERALS, LESS WHITE YELLOWISH ORANGISH WELL SORTED

VERY FINE → SILT, WHITE CARB COAT + ELONGATED BLACK 2.5MM

LOW HEAVY MINERAL CONT SLIGHTLY MORE ORANGE

M12.12

MB

5% HEAVY MINERALS VERY SMALL + 1MM BLACK PLATE

DARKER, ROUND WITH IRON COVER → PICT BIOTURB 0,5CM

M12.03 2409

SHELL REMAINS UP TO 1.5 mm AND 1MM BLACK SLATY CLAST → PICT GREYISH ORANGISH POORLY SORTED SILT SLIGHTLY MORE HEAVY MINERALS + MICAS

H-AB56.7

H-AB54.5

DARK GREY

DECREASED LARGER HEAVY MINERAL CONT AND WHITE QUARTZ WELL SORTED

HA			**Macroscopic Description** 25-09 4							
			Columnar Section			**Structures**				
Stratigraphic Units	**Photographs**	**Outcrop Data & Samples**	**Relief**	**Compos. Texture**	Φ MUDSTONE WACKESTONE PACKSTONE GRAINSTONE BOUNDSTONE >4 <-1	**Trans-port Direct.**	**Sedimentary/ Diagenetic Structures**	**Bio-turb.**	**Additional Description** MARLS	**Fossil Cont.**
		H-AB103.5 •								
		H-AB100.5 • AG100.5	100							
		H-AB97.7 •								
			9.5							
		H-AB94.7 •								
		H-AB91.5 •								
			90							
		H-AB88.5 • AG88.5							BIVALVE SHELL SEMI IMPRINT 2 cm	
		HAB85.5 •								
			85							
		H-AB •								
		H-AB82.7 •								
		H-AB79.7 AG79.7								

DECREASING RESOLUTION → EVERY 5M.

HA

Macroscopic Description

26-09

5

Stratigraphic Units	Photographs	Outcrop Data & Samples	Relief	Compos. Texture	Φ MUD-STONE WACKE-STONE PACK-STONE GRAIN-STONE BOUND-STONE >4 <-1	Trans-port Direct.	Sedimentary/ Diagenetic Structures	Bio-turb.	Additional Description	Fossil Cont.
		H-AB130.5 AG130.5	130						H-AB 140 AG 140 ↑ 145m BIOTURB OF 10 CM	
									H-AB 137.4	
		H-AB127.5 ·								
									H-AB 134.5	
			125							
		H-AB 124.3 ·								
		H-AB 121.5 · AG 121.5								
			120							
		H-AB118.5 ·								
		H-AB115.7 ·								
			115							
		HAB 112.5 ·								
		H-AB110.5 AG110.5 ·								
			110							
		H-AB 106.5 ·								
			105							

HB

27.09 ADD FOSSILS

Stratigraphic Units	Photographs	Outcrop Data & Samples	Macroscopic Description							
			Columnar Section			Structures				
			Relief	Compos. Texture	Φ MUD-STONE WACKE-STONE PACK-STONE GRAIN-STONE BOUND-STONE >4 <-1	Trans-port Direct.	Sedimentary/ Diagenetic Structures	Bio-turb.	Additional Description	Fossil Cont.
			25							
		H-BB24.5								
		H-BB21.5								
			20							
		H-BB18.5 BG18.5								
		H-BB16								
			15							
		H-BB12.5								
			10							
		H-BB9.5 BG9.5								
		H-BB6.5								
			5							
		H-BB3.5								
		H-BB0 -BG0								

HB

Macroscopic Description

2

Stratigraphic Units	Photographs	Outcrop Data & Samples	Relief	Columnar Section: Compos. Texture	Columnar Section: Φ MUD-STONE WACKE-STONE PACK-STONE GRAIN-STONE BOUND-STONE >4 <-1	Structures: Trans-port Direct.	Structures: Sedimentary/ Diagenetic Structures	Structures: Bio-turb.	Additional Description	Fossil Cont.
			50							
		H-BB49.5 BG49.5								
		H-BB46.5								
			45							
		H-BB43.5								
			40							
		H-BB39.5 BG39.5								
	W2709 -01	H-BB36.5								
			35							
		H-BB33.5								
		H-BB30.5 BG30.5								
			30							
		H-BB27.5								

HB

27-09

3

Macroscopic Description

Stratigraphic Units	Photographs	Outcrop Data & Samples	Relief	Columnar Section: Compos. Texture	Columnar Section: Φ >4 <-1 (MUDSTONE, WACKESTONE, PACKSTONE, GRAINSTONE, BOUNDSTONE)	Structures: Transport Direct.	Structures: Sedimentary/ Diagenetic Structures	Structures: Bio-turb.	Additional Description	Fossil Cont.
			70							
									HC 0/	
			66							
		H-BB65.5 · BG65.5							1st HARD BED 3 SANDBEDS IN ± 1.5 M, THICKENING UPWARD UP TO 25CM.	
		H-BT65 · BG65	65				segmented mud lenses			
			64						sharp contact blue marls – silty marls (greyish) with red sand beds	
		H-BB62.5 ·								
			60							
		H-BB59.5 · BG59.5								
		HBB55.5 ·	55							
		HBB52.5 ·								

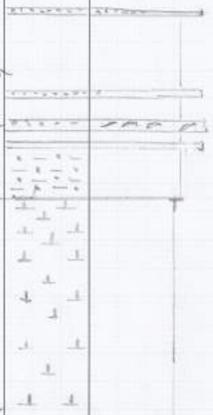

HC

28-09-2014

1

Macroscopic Description

Columnar Section

Structures

MUD-STONE WACKE-STONE PACK-STONE GRAIN-STONE BOUND-STONE

Stratigraphic Units	Photographs	Outcrop Data & Samples	Relief	Trans-port Direct.	Bio-turb.	Additional Description	Fossil Cont.
		HCG 25.3 HCG 25 HCB 24.5	25			→ 20CM UF-F SANDBED	
				015 S		WELL SORTED, CROSSBEDDED	
		H-CT		MARK	S	POSSIBLY COMPOSITE LAYER 3 a 5 WELL SORTED, FINE SAND BOTTOM IRONCRUST ON TOP. NOT MUCH BIOTURBATION. H-CT → LOW LATERAL	
	W2809-09				S		
		2X HCB 21.5					
					S	VERY THIN SANDBED WITHIN SILT SEG. POORLY EXPOSED BUT BIOTURBATED	
			20				
		HCB 18.5					
	W2809 09			085 SW	S	IRON CRUST ON TOP. THIN LAYER AT BOTTOM 3/1% BLACK CLASTS, WELL SORTED VERY LARGE BIOTURB. 4 CM DIAM NO CLEAR STRUCTURES LOW ANGLE	/1CM.
						GREY MARL → AGAIN SAME	
		HCG 15.5 HCB 15.5				STRAIGHT DOWN ↑	SHELL
	W2809 07	HCG 15	15		S	IRON CRUSTED 1.5 CM DIAMETER BIOTURB. BOTTOM + TOP IRON CRUST NO BLACK MINERALS FAUNA [illegible]	
						ALTERNATION OF MOSTLY GREY ORANGE / BROWNISH BEDS SLIGHTLY COARSER → H-CG	
		HCB 12.5					
			10			→ APPARENTLY ±20CM ORANGE FS LAYER	
		HCB 9.5					
		HCB 7.5				ALTERNATION OF VARYING MARLS/SILTS ~ GRAINSIZE CLAY → SILT ~ LIGHT GREY TO DARK AND ORANGE BROWN NOT CLEARLY EXPOSED APPARENTLY SAME AS BELOW	
			5				
		HCB 4.5					
						SEE URCHIN ACHINOIDS ↓	
	W2809 06	HCG 3 HCG 2.8		MARK	SS	TOP RED SEQUENCE ! 35° → 295 NW, IRON CRUST UF → F ORANGE LESS BIOTURB., 5 CM SHELL AT BOTTOM	?
	W2809 -01/02 /03/04 /05	H-CT HCB 1.5			SSS	WELL SORTED + 3% BLACK ± 0.5MM IRON CRUST, TOP + BOTTOM, ORANGE BIOTURBATED SURF. SPECIES, TOP SILT	?
		?				GREY SILTSTONE WITH FE, SHELL REMAINS AND BLACK MINERALS UP TO 1MM [illegible]	
				031 S		PARALLEL + CROSS LAMINATED VERY FINE LAMINATED ORANGE SAND CROSSBEDDED, POORLY EXPOSED	
		HB67 →	0			GREY SILTSTONE, MUD MATRIX	

HC

10.09 2

Macroscopic Description

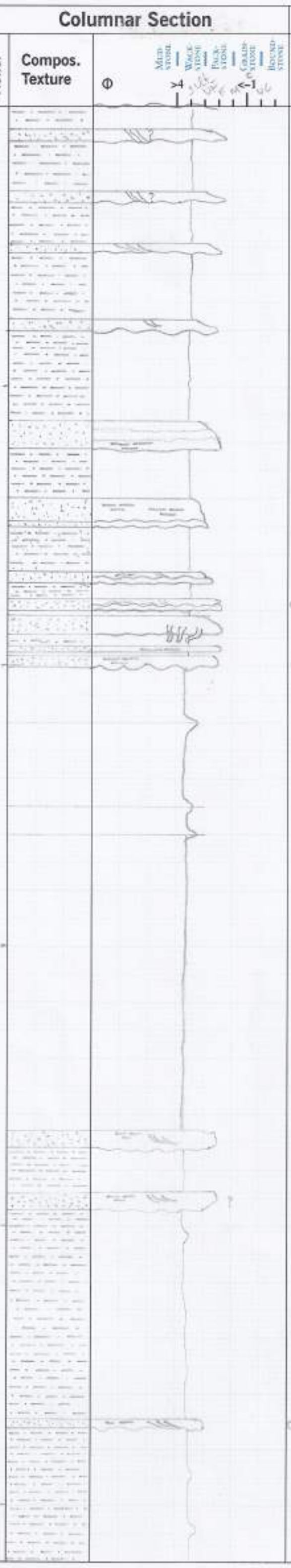

Stratigraphic Units	Photographs	Outcrop Data & Samples	Relief	Trans-port Direct.	Additional Description	Fossil Cont.
		HCB(?) HCG 47.7				
	W2909 05/06				LOW ANGLE CROSSBEDDING / PARRALEL LAM + BIOTURB	
				019 S	IRON CONCRETION TOP + BOTTEM 1→2MM, CROSSBEDDED - BIO AT TOP	
			45		GREY SILTSTONE	
		HCB 44.5 HCG 44.5 HCG 44 TOP+BOT			HORIZONTAL BIOTURB DIAM 1CM COMPOSITE LAYER, FINING UPWARD ORANGE SANDS STILL POORLY CEMENTED	
					IRON CONCRETION AT BOTTOM PARRALEL LAMINATION OR CROSSBEDS? IRON CONCRET ROUNDED INBETWEEN	
		HCB 41.5			SAME AS BELOW	
	W2909 -03/04			081 SW	LAYERING IN MARL/SILT FINING UPWARDS + COMPOSITE TINY SHELL FRAGMENTS, VERY ORANGE BIOTURB CONTINUES IN SILT - DIAM 3CM ALMOST NO BLACK MINERALS NO CROSSBEDS VISIBLE, PARRALLEL NO BIOTURB	
	W2909 -02		40	015 NW	FLOW DIRECTION MEASURED PERPENDICULAR TO PICTURE 015; DIP 30° → 287 NW	
		HCB 38				
					ALTERNATING SILTSTONES AND MARLS?	
		HCB 35 HCG 35	35			
		HCB 32			IRON OLLST, EROSIVE BOTTOM NOTCHES FINE ORANGE SANDSTONE, CARB COATED GRAINS!	
					COMPOSITE LAYER, MIDDLE LAYER SLIGHTLY COARSER CROSSBEDS + PARRALLEL, MULTIPLE 180° RANGE TOWARDS SOUTH	
	W2909 -01		30			1.5CM BIOTURB
		HCB 28.5				
		[illegible]				
				010 S	AGAIN COMPOSITE LAYER TURBIDITE/CONTOURITE/MARL LAMINATED TOP PARRALLEL - CROSSBEDS IRON CONCRETIONS ON TOP ROUNDED ORANGE, CROSSBEDS MULTIPLE DIRECTIONS	
			25		} 1M TO MUCH PROBABLY!	

HC

29-09 3

Stratigraphic Units	Photographs	Outcrop Data & Samples	Relief	Compos. Texture	Φ	Trans-port Direct.	Sedimentary/ Diagenetic Structures	Bio-turb.	Additional Description	Fossil Cont.
		HCB 53,5							TOP IRON WITH IRON MARBLES? ERODED. NO SIGNS OF STRUCTURES	
		HCB 50.5					?/ ?	5	TOP IRON CONCRETION. BIOTURB. LOWERMOST PART CONTAINS LARGE MICAS	

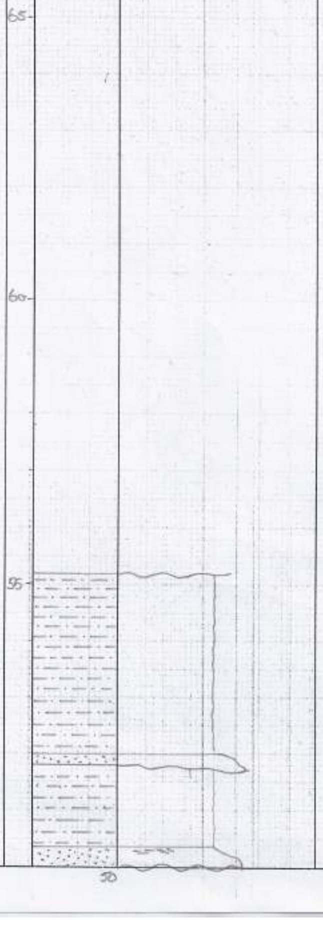

HR

30-09

Macroscopic Description

/

Stratigraphic Units	Photographs	Outcrop Data & Samples	Relief	Columnar Section: Compos. Texture	Columnar Section: Φ (Mud-stone, Wacke-stone, Pack-stone, Grain-stone, Bound-stone)	Structures: Trans-port Direct.	Structures: Sedimentary/ Diagenetic Structures	Bio-turb.	Additional Description	Fossil Cont.
			25							
		HRB23.5								SAME AS BEFORE 1CM
		HRB20.5 HRG20.5	20						VERY DARK GREY MARL	
		HRB17.5								
			15							
		HRB14.5								
		HRB10 HRG10	10						BLEUISH GREY MARL WITH SMALL BIVALVES & 0.5CM	
	W3009 -02	HRB 6.5							LIGHTER GREY, MORE SILTSTONE CLAY MATRIX FEW SHELL FRAGMENTS	
			5							
		HRB 3.7							DARK GREY BLEUISH MARLY SILT SOME SHELL REMAINS + BIVALVE SAME AS BELOW ↓	
	W3009 -01	HRB01 HRG01							BROWNISH GREY AND DARK BLUE MARLY SILTSTONE WITH LARGE FOSSILS, HIGH CONCENTRATION	

34.28587, -5 64159

HR

07-10

2

			Macroscopic Description							
			Columnar Section			Structures				
Stratigraphic Units	Photographs	Outcrop Data & Samples	Relief	Compos. Texture	Φ >4 <-1	Trans-port Direct.	Sedimentary/ Diagenetic Structures	Bio-turb.	Additional Description	Fossil Cont.
									R 150m ≃ 5-8 in S-section	
			45						HRB 99 102 107.5 ? 104.5 136 141 145.5 149.5	
			40							
		HRB 35.5								
			35							
		HRB 32.5								
			30							
		HRB 29.5 HRC 29.5								
		HRB 26.5							SEA URCHIN	

HS

Macroscopic Description

02-10

/

Stratigraphic Units	Photographs	Outcrop Data & Samples	Columnar Section: Relief	Compos. Texture	Φ	Structures: Trans-port Direct.	Sedimentary/ Diagenetic Structures	Bio-turb.	Additional Description	Fossil Cont.

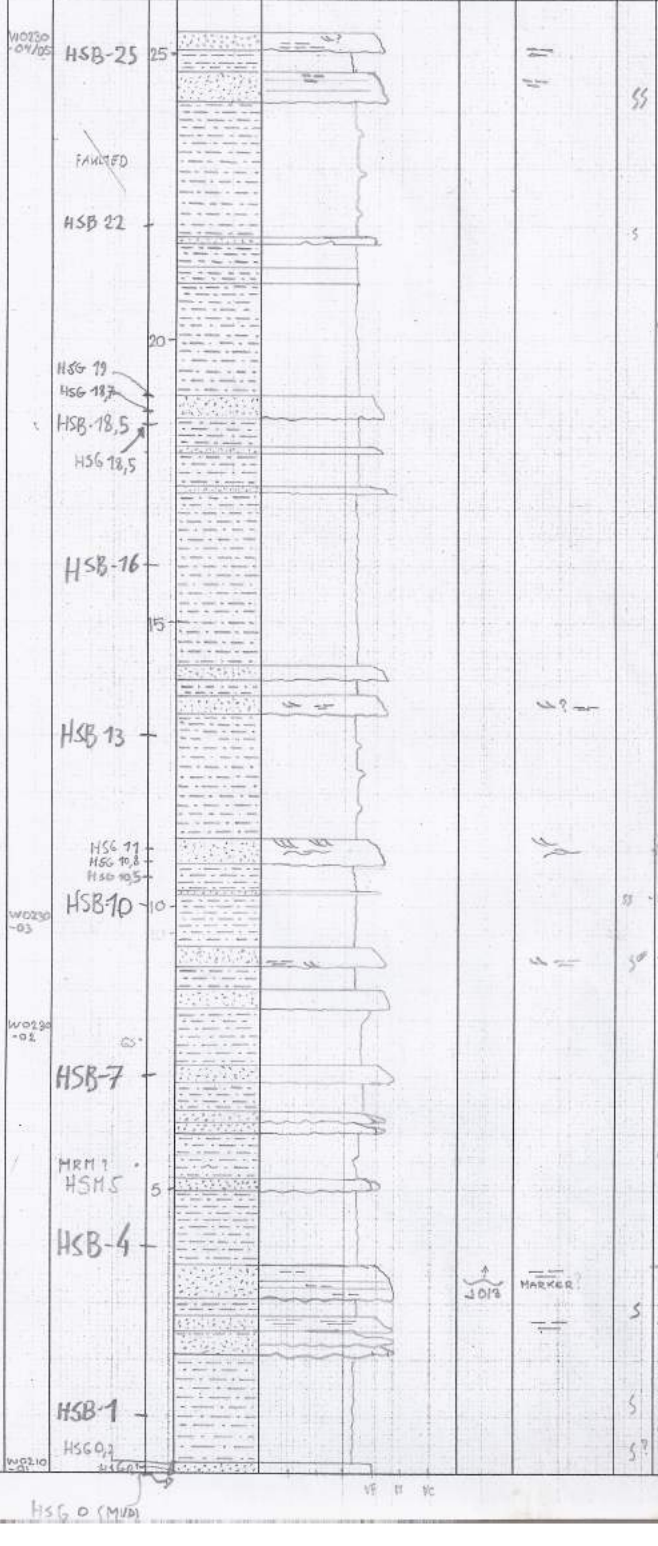

IRON CONCRET → PICT
VERY FINE CROSSB. ↗ APPARENT
BOTTOM FINELY PARALLEL LAMINATED
TOP MANY SHITTOWERS BLACK GRAINS 5% ≈
SUB 10° COMPOSITE
LARGE HORIZONTAL TUBE 4 CM DIAM
INDURATED CARB CEMENTATION
↓ BOTTOM 10 CM
LOTS OF SMALL MUSCOVITE

IRON TOP + BOTTOM, SHITBALLS

2. MORE INDURATED, MORE CARB CEMENTED GREY SILTSTONE, BIVALVES AND SHELL REMAIN 0,5 CM MAX

GREY SILTST, AS USUAL NOT INDURATED

SANDS HAVE NOT CHANGED MUCH
LACK OF CEMENTS MAKES CLASSIFICAT. HARD

4% BLACK CLASTS AND SHELL REMAINS
PROBABLY BIVALVE
LIGHT GREY SILTSTONE

TOP IRON CONCRETIONS

COMPOSITE? 3 LAYERS, BOTTOM THIN CROSSBEDS? 45 → 310 NW

+ THIN 2-5 · 8 CM SAND

LAMINATED
CRYSTALLINE 5 CM BOTTOM + IRON

SHITTOBBE + IRON LAYER ON TOP
STRANGE CONE OF IRONRICH AND BLACK CLAST SEE PICT

IRON CONCRETIONS ON TOP + SHITBALLS
HOMOGENEOUS LAYER BOTTOM 5 CM LAM
CROSS OR PARALLEL

WELL SORTED, GRAINS CARB COAT, NO BLACK CLASTS

5% BLACK CLASTS + FTOH. FOTO 4 MM

POSSIBLY LAMINATED, HARDLY VISIBLE DUE TO LOW CEMENTATION

FINE → SILT ALSO ORANGE LAMINATED? 1% TINY BLACK GRAINS

COMPOSITE SILT LAYER MARL + VF SAND

BOTTOM BADLY SORTED, LARGER QUARTZ

COMPOSITE, BOTTOM IRONCOLER + EROSIONAL FEAT LOW CEMENTATION
GREY SILT
↗ SLIGHTLY COARSER FINING UPWARD DOMINANT QUARTZ TO FINE
SILT BIOTURB
ORANGE + MUD AND QUARTZ RICH
COMPOSITE, 2 LAYERS + TOP SILT

BIOTURB, VERTICAL 0,5 CM
2% black clasts, GREY SILTST.
UP TO 0,5 CM SMALL BIVALVES!
POSSIBLY IN SITU

POSSIBLY BIOTURB. TOP
SLIGHTLY OXIDIZED TOP
PREDOMINANTLY ORANGE VF SS
MUD MATRIX, 21% black

34.28597, -5.64270

2

02-10/04-10.

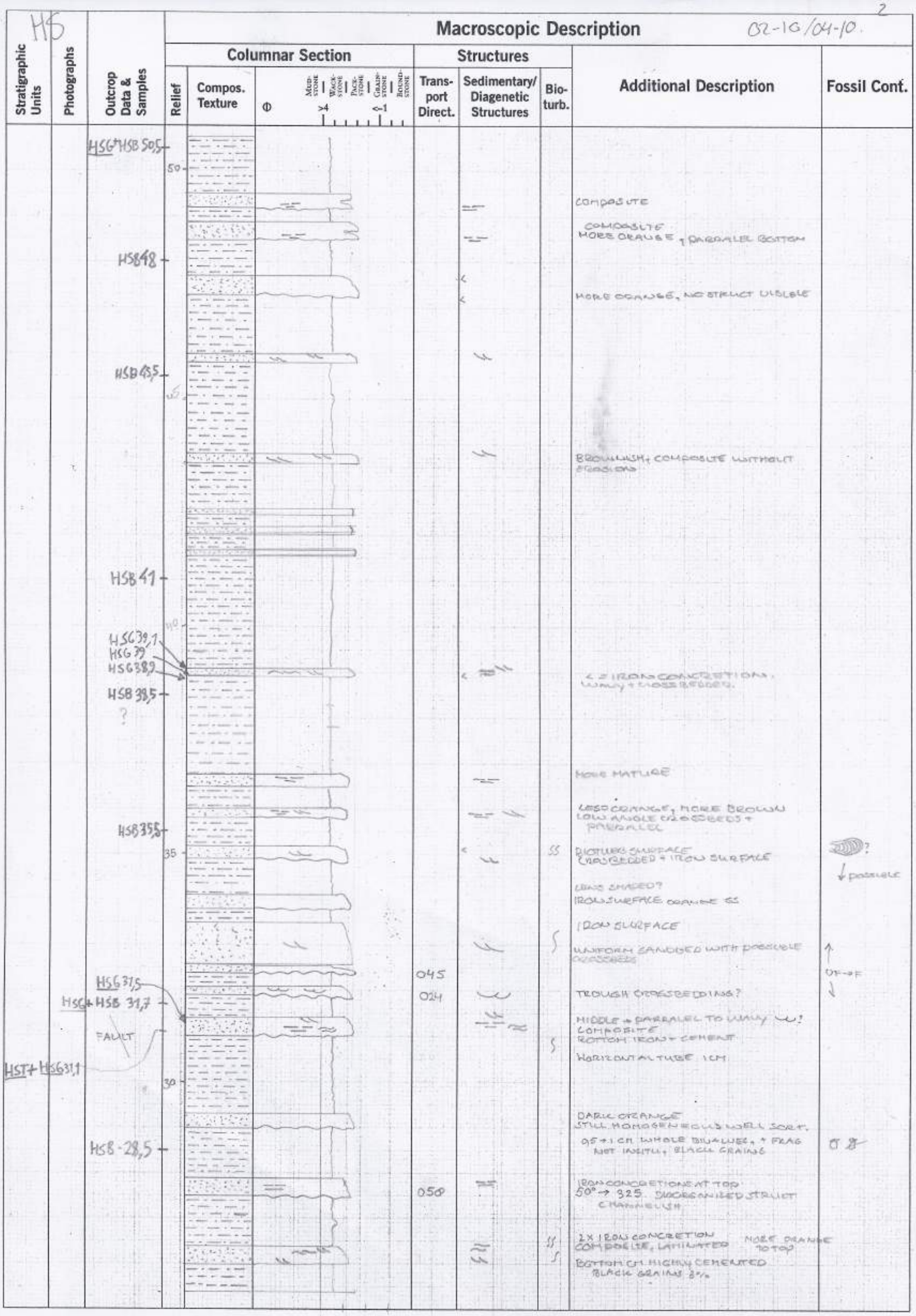

COMPOSITE

COMPOSITE
MORE ORANGE, PARALLEL BOTTOM

MORE ORANGE, NO STRUCT VISIBLE

BROWNISH, COMPOSITE WITHOUT EROSION

< 2 IRON CONCRETION.
WAVY + CROSSBEDDED.

MORE MATURE

LESS ORANGE, MORE BROWN
LOW ANGLE CROSSBEDS +
PARALLEL

BIOTURB SURFACE
CROSSBEDDED + IRON SURFACE

?
↓ POSSIBLE

LENS SHAPED?
IRON SURFACE ORANGE SS

IRON SURFACE

UNIFORM SANDBED WITH POSSIBLE CROSSBEDS

↑
UF→F
↓

TROUGH CROSSBEDDING?

MIDDLE → PARALLEL TO WAVY !
COMPOSITE
BOTTOM IRON + CEMENT

HORIZONTAL TUBE 1CM

DARK ORANGE
STILL HOMOGENEOUS WELL SORT.
0,5 → 1 CM WHOLE BIVALVES, + FRAG
NOT INSITU, BLACK GRAINS

IRON CONCRETIONS AT TOP
50° → 325 DISORGANIZED STRUCT
CHANNELISH

2 X IRON CONCRETION
COMPOSITE, LAMINATED
MORE ORANGE TO TOP

BOTTOM CM HIGHLY CEMENTED
BLACK GRAINS 3%

HS

Macroscopic Description 04-10

3

Stratigraphic Units	Photographs	Outcrop Data & Samples	Relief	Columnar Section: Compos. Texture	Columnar Section: Φ (Mudstone, Wackestone, Packstone, Grainstone, Boundstone; >4 … <-1)	Structures: Trans-port Direct.	Structures: Sedimentary/ Diagenetic Structures	Structures: Bio-turb.	Additional Description	Fossil Cont.

75

HSG 73,9 – sand top

HSG 73,6

HSG+HSB 73,5 – sand base

HSB 69,8 – 70

HSB 67

65

HSG+HSB 63,5

HSG 62,4 – sand top

HSG 62 – sand base

HSB 60 – 60

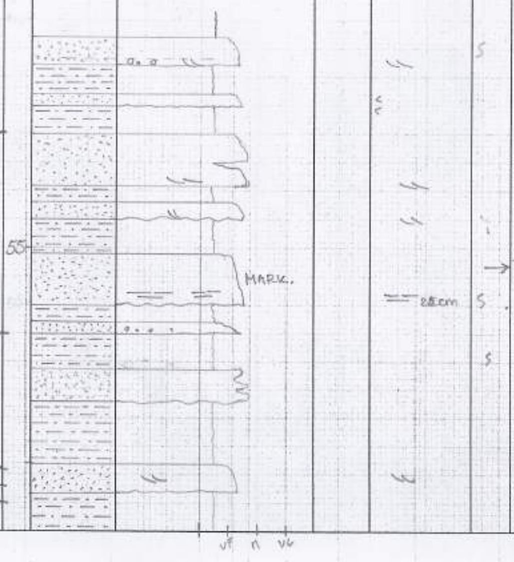

HSB 57

HSB 53,5

HSG 51,1

HSG 50,8

HSB+HSG 50,5

MIDDLE BIOTURBATED
BOTTOM, CROSSBEDS AND MUDCLASTS

TINY SILTLAYER IN BETWEEN.

VERY ORANGE

MASSIVE TOP
→ TAKE MULTIPLE SAMPLES
25CM PARALLEL
↗ BREAK UNIFORM
CARB RICH INDURATED CONCAVE SILT
ORANGE BOTTOM & CREMISH TOP
INVISIBLE STRUCTURES

BOTTOM BIOTURB., MUDCLAST MAX 1CM
COMPOSITE 50 CM LAYER
ORANGE, SLIGHTLY REDDISH/BROWN

ORANGE, SANDSTONE, STILL VERY UNIFORM

HS

06-10

Macroscopic Description

Stratigraphic Units	Photographs	Outcrop Data & Samples	Relief	Columnar Section: Compos. Texture	Columnar Section: Φ / Mud-stone, Wacke-stone, Pack-stone, Grain-stone, Bound-stone	Structures: Trans-port Direct.	Structures: Sedimentary/ Diagenetic Structures	Structures: Bio-turb.	Additional Description	Fossil Cont.

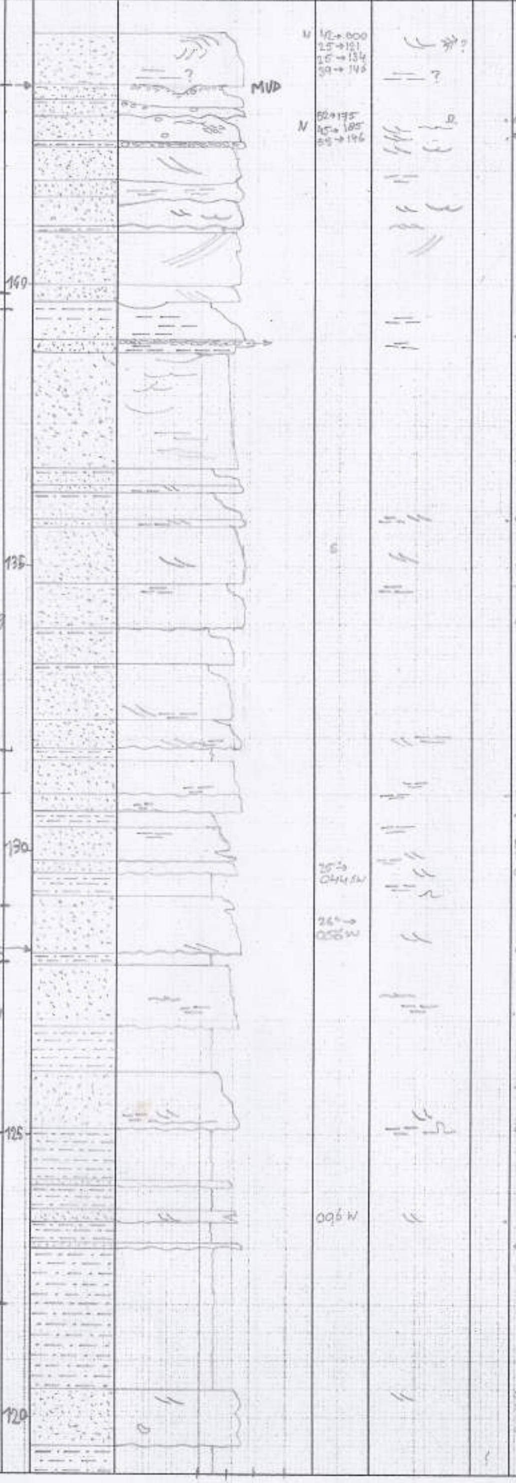

Photographs: W0610-09; W0610-07; W0610-06; W0610-05; W0610-04; W0610-03; W0610-02; W0610-01

Outcrop Data & Samples:
HSB 143,5
~~FAULTED~~
HSG 139,8
HSG 139,5
5/058→109
HSB 131,8
HSG 129
HSG 128,1
HSB + HSG 128
LISTRIC NORM 60→128 W
HST 127
HSB 125
HSB 122

Additional Description:

TOPSETS CLINOFORM

4M CROSSBEDS, MULTIPLE DIRECTIONS ?
CHANNEL OPPOSITE

MUD: Lagoonal deposit?

TOP, CRAZY MUDCLASTS → MORE GREY
· CONVOLUTE ! PICT 0610-00 → MUDCLAST

· MUDCLASTS UP TO 5
CHANNEL + LISTRIC CROSSBEDS
ORANGE, LOW CEMENT

HIGHLY INDURATED REDDISH LAYER
SLIGHTLY CHANNEL SHAPED. PURPLE

POSSIBLE LARGE BOTTOMSETS
LAMINATION YELLOW AND ORANGE
LARGER STRUCTURES, ENTIRE BED
ORANGE TOWARDS TOP, BLACK MIN 2 & 3 %

RED BOTTOM ORANGE TOP, STRANGE LAMINEA
ALL PARALLEL LAM.

↑ ±1CM
MUDCLASTS, CONVOLUTE STRUCT
↓

36°→ 303 NW
ORANGING UPWARD, COMPOSITION
OF THIN BEDS 2→10CM CONSISTING
OF LAMINATED ORANGE AND GREY
MAINLY WAVY, CROSS/PARALLEL AND
SMALL CHANNELS!
1.5CM BOUDIN LIKE LAYER TOWARDS TOP

· WAVY, PARALLEL, CROSSBEDS IN CUT
MADE UP OF THIN LAYERS ORANGE
CROSSBEDDED TOWARDS S. PURPLE SURFACE — CARB CEMENT

VERY YELLOW SANDSTONE, LOW CEMENT

TOP LAYER, MORE INDURATED, PURPLE
SLIGHTLY DARKER ORANGE PARALLEL
FINING UPWARDS LAM
47→ 123° NW

LIGHT ORANGE

MORE MASSIVE
STRUCTURES LARGER
SLIGHTLY MORE ORANGE TOWARDS TOP

MASSIVE TOP ? GREYISH BROWN
BOTTOM MORE INDURATED

- LAMINATED VFS / SILT

· RR BROWN TO GREY SILT
TOP 10 CM PARALLEL LAM SILT + VFSAND

BONLAG 5CM
PARALLEL BOTTOM, CROSSBED ON TOP — 2 CM MUD LENSES

CROSSBEDS SILT AND VF IRON SAND
PARALLELY LAMINATED SILT + SSD

DARK CREME → MORE ORANGE TOP
APPARENT MASSIVE TOP + SILT COMP !

CROSSBEDDED BOTTOM,
SUB HORIZONTAL

POSSIBLY COMPOSITE
AGAIN PARALLEL BEDS

· LAMINATED SILT BOTTOM
MORE CREME BOTTOM
ONLAP 15 CM !

TOWARDS TOP, BEDDED 5 → 10CM
MORE MASSIVE

CONVOLUTE BOTTOM SECOND LAYER

· SILTBED IN BETWEEN

< IRONSTONE, SHIT TOWARDS 44 → 295 NW
THIN SANDBAND

SILT GREY IN SANDBAD, POSSIBLE SORT
RED IN ORANGE
POORLY EXPOSED DUE TO ROCKS
COMPOSITE + CROSSBEDDED
PL → MUD PERCOLATION
BIOTURBATED COARSE SILT

Fossil Cont.:
?
32° → 300 NW

34.28628, -5.64517

H5

06-10/07-10

85 → 95 FOUTJE

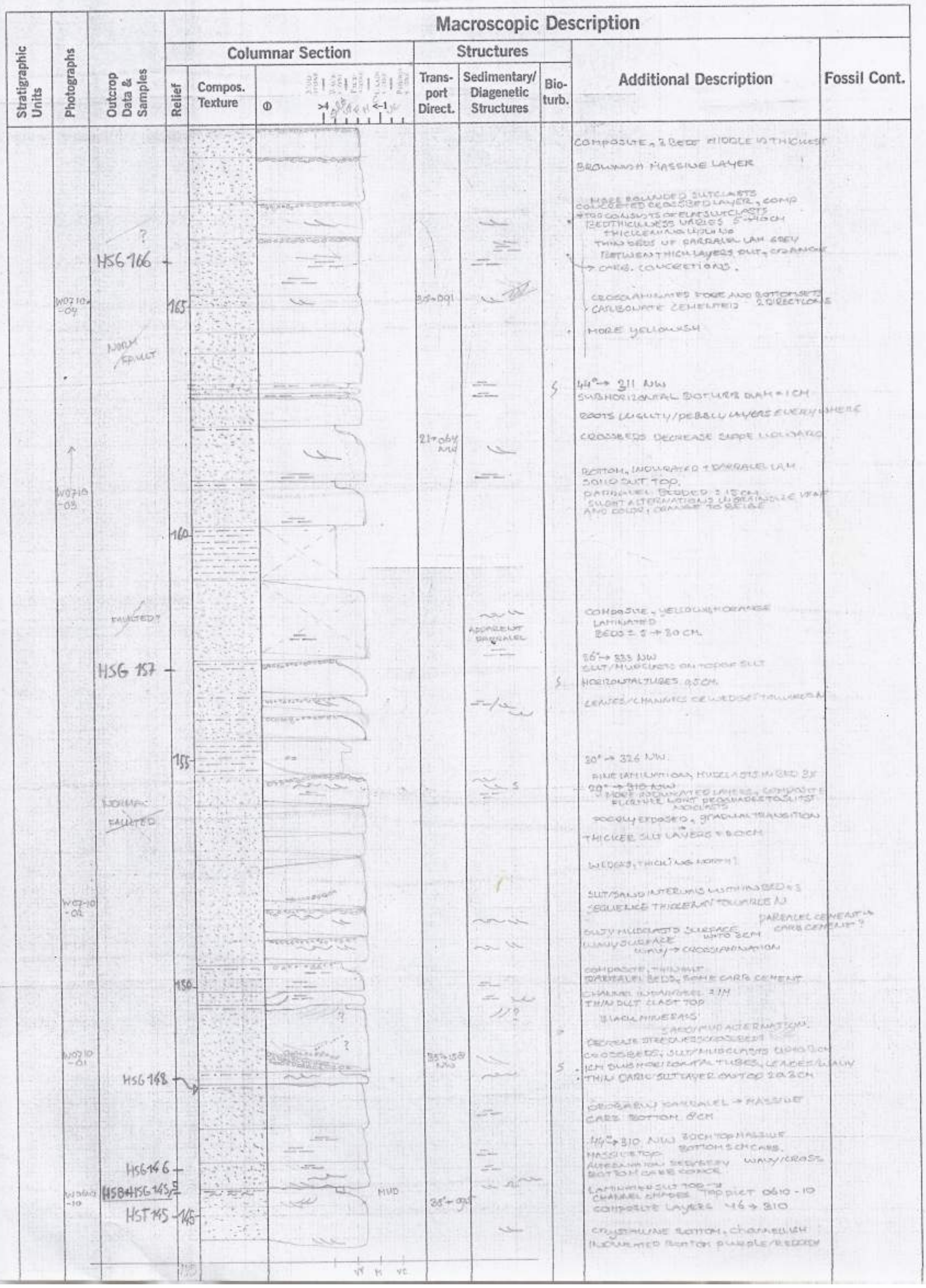

COMPOSITE, 2 BEDS MIDDLE IS THICKEST

BROWNISH MASSIVE LAYER

MORE ROUNDED SILTCLASTS
CONCRETED CROSSBED LAYER, COMP
TOP CONSISTS OF FLAT SILTCLASTS
BEDTHICKNESS VARIES 5-40 CM
THICKENING UPWARDS
THIN BEDS OF PARRALEL LAM GREY
BETWEEN THICK LAYERS SILT, ORANGE
→ CARB. CONCRETIONS.

CROSSLAMINATED FORE AND BOTTOMSETS 2 DIRECTIONS
CARBONATE CEMENTED

MORE YELLOWISH

44° → 211 NW
SUBHORIZONTAL BIOTURB DIAM ≈ 1 CM

ROOTS SILTY/PEBBLY LAYERS EVERYWHERE

CROSSBEDS DECREASE SIZE UPWARD

BOTTOM, INDURATED + PARRALEL LAM
SOLID SILT TOP.
PARRALEL BEDDED ± 15 CM
SLIGHT ALTERNATIONS IN GRAINSIZE [illegible]
AND COLOR, ORANGE TO BEIGE

COMPOSITE, YELLOWISH ORANGE
LAMINATED
BEDS ± 5 → 20 CM.

26° → 333 NW
SILT/MUDCLASTS ON TOP OF SILT
HORIZONTAL TUBES 0,5 CM.
LENSES/CHANNELS OR WEDGES THICKNESS [illegible]

30° → 326 NW
FINE LAMINATION, MUDCLASTS IN BED 3?
29° → 310 NW
MORE INDURATED LAYERS, COMPOSITE
FURTHER [illegible] GRADES TO SILTST
MUDCLASTS
POORLY EXPOSED, GRADUAL TRANSITION
THICKER SILT LAYERS ± 10 CM

WEDGES, THICKENING NORTH?

SILT/SAND INTERLAMINATED BEDS
SEQUENCE THICKENING UPWARDS
PARALLEL CEMENT → CARB CEMENT?
SILTY MUDCLASTS SURFACE UP TO 3 CM
WAVY SURFACE
WAVY → CROSSLAMINATION

COMPOSITE, THIN SILT
PARALLEL BEDS, SOME CARB CEMENT
CHANNEL INFILLING 3 M
THIN SILT CLAST TOP
BLACK MINERALS
SANDY/MUD ALTERNATION
DECREASE STEEPNESS CROSSBEDS
CROSSBEDS, SILT/MUDCLASTS UP TO 3 CM
1 CM SUBHORIZONTAL TUBES, LENSES/WAVY
THIN CARB SILT LAYER ON TOP 2 A 3 CM

CROSSBEDDING PARALLEL → MASSIVE
CARB BOTTOM 8 CM

46° → 310 NW 30 CM TOP MASSIVE
BOTTOM 5 CM CARB.
MASSIVE TOP
ALTERNATION SEQUENCE WAVY/CROSS
BOTTOM CARB CONC

LAMINATED SILT TOP →
CHANNEL SHAPES TOP SILT 0610 - 10
COMPOSITE LAYERS 46 → 310

CRYSTALLINE BOTTOM, CHANNELISH
INDURATED BOTTOM PURPLE/REDDISH

HS

09-10

Macroscopic Description

Stratigraphic Units | Photographs | Outcrop Data & Samples | Columnar Section: Relief, Compos. Texture, Φ >4 <-1 | Structures: Transport Direct., Sedimentary/Diagenetic Structures, Bioturb. | Additional Description | Fossil Cont.

HSG185 -185

0710-06

HSG177

0710-05

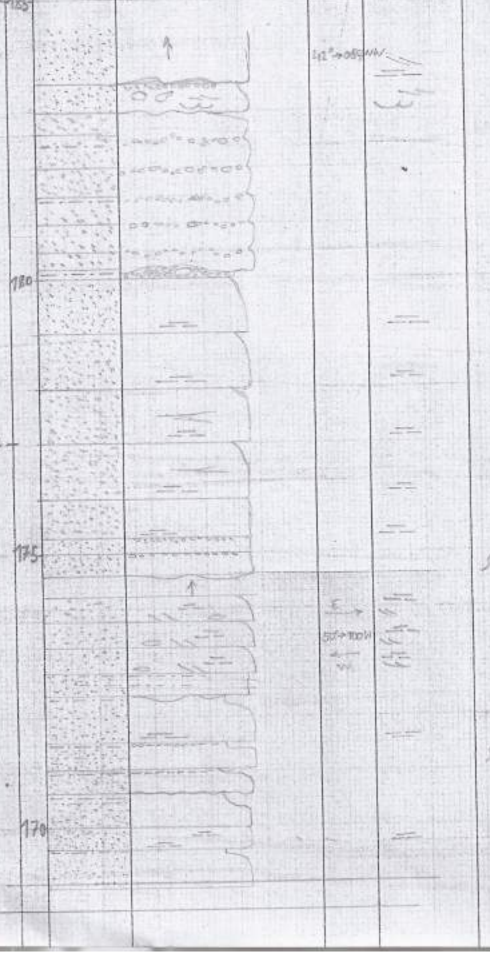

34.28628, -5.64618

45°→304 NW.

MASSIVE SAND, ORANGE/REDDISH

ROUND MUDCLASTS

W→ LOW ANGLE CROSSBEDS

MORE ORANGE UPWARD

WAVY INDURATED LAYERS

[illegible]

MORE SILTY TOWARDS THE TOP

CLASTS ARE CEMENTED, AND SILTCLASTS

OVERALL CREME COLORED FINE SAND

BOTTOM YELLOW.

± 15 CM, REST SAME (X2)

LITTLE BIT WAVY, ENTIRELY PARALLEL

COMP + IND 5 cm X 3

MORE REDDISH

COMPOSITE, MORE INDURATED 5cm

YELLOW

COMPOSITE

COMPOSITE, [illegible] CONCRETION [illegible]

BOTTOM PARALLEL

→ FADES EASTWARD

CHANNELS 1CM [illegible]

THIN CEMENT, ACROSS / PARALLEL

CROSSBEDS [illegible] DIRECT!, MULTIPLE

LENSES INDURATED

5X INDURATED PARALLEL LAMINATED

SLIGHTLY WAVY + LOW ANGLE CROSS

BOTTOM 20 CM → [illegible]

SOFT LAYERS YELLOW

LIGHTER, YELLOWISH THIN LAYERS

FINING UPWARD.

1.5CM BIOTURB, [illegible] ?

HIGHER OUTCROP, LIGHTER [illegible]

51°→ 310 NW, [illegible]

TOP FINING TOWARDS SILT

LESS ORANGE, LAMINATED

BOTTOM 10CM CEMENTED

POSSIBLE WEDGE, THICKENING NORTH

PARALLEL [illegible] MORE INDURATED

THIN SILT BED 20° ON BEDDING

LAMINATION NOT VISIBLE

BOTTOM [illegible]

Appendix B

Sedimentary logs Oued Mahdouma

VN

12-10

1

Macroscopic Description

Stratigraphic Units	Photographs	Outcrop Data & Samples	Relief	Columnar Section: Compos. Texture	Columnar Section	Structures: Trans-port Direct.	Structures: Sedimentary/ Diagenetic Structures	Structures: Bio-turb.	Additional Description	Fossil Cont.
			6							
			5						?Wackestone? oncoids ±2mm clusters, larger grains. Very fine grainstone with clusters of oncoids of ±1cm coarse grainstone To the north large channels and large angular pebbles full with oncoids(?)(repetitive) Possible wedge	
	(← 20mm N) 12-10/45 12-10/44					19+110 SW				
			4					5	[illegible] horizontal bioturbation long tubes 1cm diameter. Possible wedge only fine sand [illegible] random pebbles <5% carbonate coated clasts clasts up to 2cm. tubes, light [illegible]) carbonate coating. [illegible] tubes, [illegible] angular to rounded clasts max 17cm. fining upwards [illegible] clasts made of mudlimestone + [illegible], at bottom clasts up to 4cm carbonate coated. with [illegible] to the top tubes become dominant [illegible] [illegible] fining top clasts [illegible] to the right Paleosol (see sketch) continues to the [illegible] oncoids few	☒
						14+010N	5m to the S: Packstone [illegible] Paleosol algae mats			
	12-11/45		3				Paleosol – rootlets – white balls – [illegible] – highly organic			
	12-11/01	VN paleosol				? 20+237SW 20+04N	conglomerate		(16+307 S) fining up and thin beds) more orange to the top	☒<1%
			2							
		VNC 1.4							from this point overall becomes coarser	
			1			8+301S 8+306S			angular clusters of coarse extraclasts (tubes, mudclasts. coarse bioclasts fining upwards. up to 1cm	
									extraclasts: quartz [illegible], bioclasts [illegible] extraclasts 5% quartz fining upwards. Becomes more orange to the top. extraclasts: fine - pebbles, rounded, ungraded. Badly sorted	☒<1%
		VNC 0.2	0							

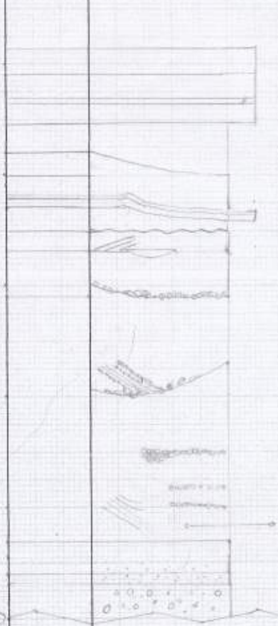

33.34970, -5.31254

VT

16-10
SOUTH VALLEY

Macroscopic Description

Stratigraphic Units	Photographs	Outcrop Data & Samples	Relief	Columnar Section: Compos. Texture	Columnar Section: Φ	Structures: Transport Direct.	Structures: Sedimentary/ Diagenetic Structures	Structures: Bio-turb.	Additional Description	Fossil Cont.

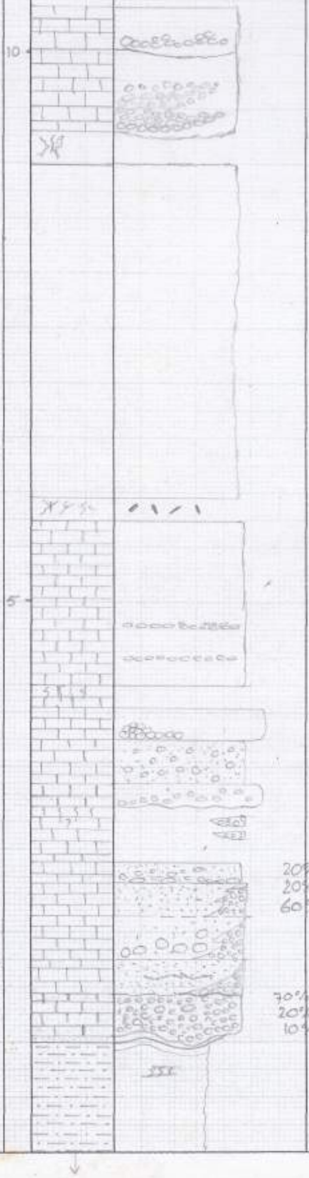

PETROLOGY
50% LIMEST - CHERT - OOLITE
30% QUARTS SAND IND.
20% REW. LAC CAR.

40 cm PEBBLE BAND
FINING UPWARD CLASTS.

CHANNELS WITH LARGE CLASTS
UP TO 15 cm

BEDS ARE CHAOTIC.

PALEOSOIL, INCUTTING CHANNELS OF UP TO 15 cm CLAST SUBANGULAR POORLY SORTED
3m VERY FINE LIME MATRIX WITH QUARTZ GRAINS COATED ↳ ANGULAR
ALSO BIOCLASTS TUBES
0,5 cm CLASTS, CLUSTERED LIMESTONE

ALTERNATING THIS AS MATRIX IN COARSE GRANULAR MEDIUM CARBONATE SAND

PALEOSOIL, VERRY RED WITH SMALL ORGANIC MATERIAL IN IT ROOTLETS

CONGLOMERATIC PACKSTONE, ROUNDED
SMALL PEBBLES UP TO FEW CM MAX 3
LAMINATED / BEDDED
PEBBLES PRIMARILY LAMINATED
FINING UPWARD SEQUENCES.

FINE CARB., PALEOSOIL / RECENT

PROBABLY FULL OF LARGE ~10 CM GRAINSTONE PEBBLES, [illegible] MATRIX

CHANNELS ? AND WEDGES
APPARENTLY GENERAL MOVE TO SOUTH

VERRY WELL ROUNDED ~ 5 CM UP TO 7 CM DETRITAL, MUD WITH BLACK SPOTS + SECUNDAIR FROM BASE

WAVY CHANNELS

GRAINST, THIN SECTION SPARITE MATRIX QUARTZ GRAINS, MUD GRAIN PEBBLES CRISTALLIZED
NEIGT NAAR PALEOSOIL, CARB GRAINS COATING
AVERAGE TOWARDS MIDDLE

VTT 3.2
H12:W 2X
VTC 3.0

VTC 2.6
20% IND SST QUARTZ
20% REW LAC. CARB
60% LIMEST ? W.

PEBBLES FATTER AND MORE ANGULAR, BIOCLASTIC MATRIX
FINE LAMINATION, FINE → MIDDLE CARB GRAINS → BIOCLASTIC AS WELL

PEBBLES 2 → 5 CM, MORE MATRIX, FINE CARB. MATRIX AND TUBES
DU CHARA, BIOCLAST

VTC 1.7

CARBONATE, MIDDLE TO CARSE LAMINATED TROUGH CROSSBEDS

CHAOTIC LAYERS
DETRITAL LIMESTONES

70% LIMEST - OO/CHRT
20% IND SST QUARTZ
10% PINKISH SAND FROM BELOW.

CONGLOMERATIC, CARBONATE MATRIX UP TO VERY COARSE → PEBBLE UP TO 10 CM.
→ OXIDATED BIOTITE VF SAND

VERY EROSIVE CONTACT !
CHANNEL SHAPED, INCISION APPROXIMATELLY 0,5 → 1,5 M
WIDTH MAX 5 M
BLEUISH SILTST
20 CM ORANGE BAND BENEATH CONT. 150M BELOW 20 CM HEAVILY BOTURBS, HORIZONTAL ROUNDED, OXIDISED 1 CM [illegible] + IRON OOLS
FLAT OVAL BIVALVE, RAD TO EDGE

WALTER PETROLOGY

33 94061, -5 32260

SCALE 1:50

VB 13-10 1

Macroscopic Description

Stratigraphic Units	Photographs	Outcrop Data & Samples	Relief	Compos. Texture	Φ >4 <-1	Trans-port Direct.	Sedimentary/ Diagenetic Structures	Bio-turb.	Additional Description	Fossil Cont.
			9							
		VBC 7.7	8	lime						
				sand?				∫	more carbonate in comparison with layer below Fuller micro tubes	
		VBC 6.9	7	Lime					no large clast lots of quartz grains. bioturbation tubes ±ascendia congle with very small bioclasts: -tubes	
			6						Crossbedding fining upwards	
	13-10/3		5	Lime					less carbonate? becomes better sorted but coarser clasts	
			4	lime					clast decrease in average size and are bit angular an increase in tubes to ±5% *small tubes and size? as matrix clasts exist of mudstones and oncoids bottom marked by cobbles up to ±30cm angular flakes	
				lime						
	13-10/01 13-10/01 13-10/02	VBC 2.9	3				to the S Sand became intruded by pebbles, tubes and crossbedding see VN	∫∫	organic rich layers on contact in between upper 20cm wavy lamination wavy onlap crossbedding to the rest ~~possible fossils~~ see 13 ± 270 W? [illegible]	clusters ±3%
			2			26±20 SW 17±050 SW		∫	Reddish coloured, white tubeholes, biofit, muscovit crossbedding up to ±1.5 cm possibly in other direction but can not be measured possible bioturbation tubes filled with grey silt	
			1	silt					grey coloured with orange bands of ±2 to 10 mm and not alligned bedding Possible crossbedding to SW up to ±1cm Forams, muscoviet up to ±.1 mm.	
			0							

GPS 23.94594, -5.31855